

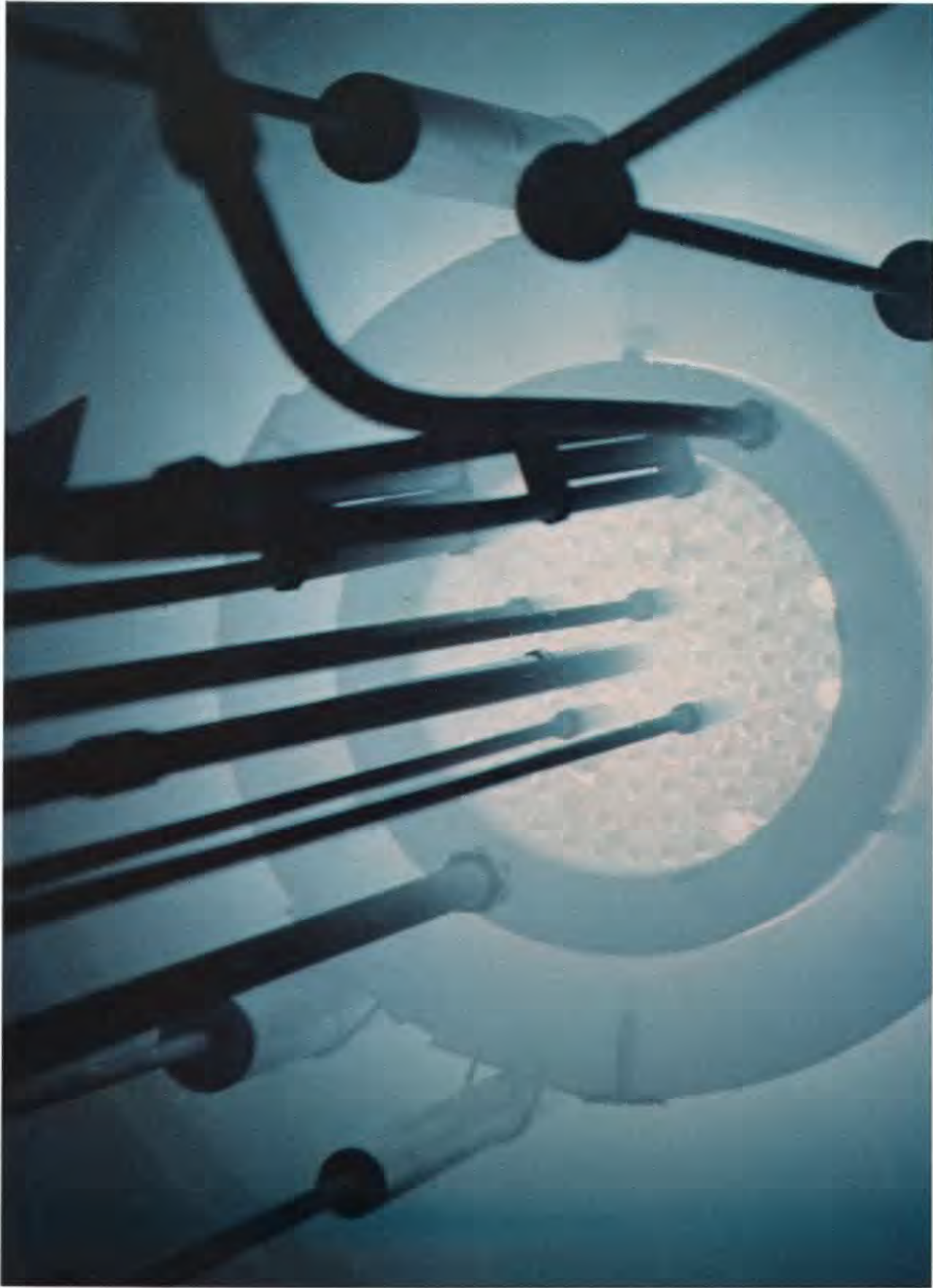
4.25
48

Irradiation of Samples for $^{40}\text{Ar}/^{39}\text{Ar}$ Dating Using the Geological Survey TRIGA Reactor

GEOLOGICAL SURVEY PROFESSIONAL PAPER 1176



**IRRADIATION OF SAMPLES FOR
 $^{40}\text{Ar} / ^{39}\text{Ar}$ DATING USING THE
GEOLOGICAL SURVEY TRIGA REACTOR**



Core of Geological Survey TRIGA reactor in operation. Central thimble tube, which is about 4 cm in outside diameter and surrounded by control and transient rods, is in center of core. Blue glow is Cerenkov radiation, emitted by charged particles traveling faster than the speed of light in reactor cooling water.

Irradiation of Samples for $^{40}\text{Ar}/^{39}\text{Ar}$ Dating Using the Geological Survey TRIGA Reactor

By G. BRENT DALRYMPLE, E. CALVIN ALEXANDER, JR.,
MARVIN A. LANPHERE, and G. PATRICK KRAKER

G E O L O G I C A L S U R V E Y P R O F E S S I O N A L P A P E R 1 1 7 6



UNITED STATES GOVERNMENT PRINTING OFFICE, WASHINGTON : 1981

UNITED STATES DEPARTMENT OF THE INTERIOR

JAMES G. WATT, *Secretary*

GEOLOGICAL SURVEY

Doyle G. Frederick, *Acting Director*

Irradiation of samples for $^{40}\text{Ar}/^{39}\text{Ar}$ dating using the Geological Survey
TRIGA reactor.

(Geological Survey professional paper ; 1176)
Bibliography: p. 26-29

Supt. of Docs. no.: I 19.16:1176

1. Argon--Isotopes. 2. Radioactive dating. 3. Nuclear reactors.
I. Dalrymple, G. Brent. II. Series: United States. Geological
Survey. Professional Paper 1176.

QE508.I77

551.7'01

80-607859

CONTENTS

	Page		Page
Abstract	1	Optimization of irradiation parameters — Continued	
Introduction	1	Minimization of $^{40}\text{K}(n, p)^{40}\text{Ar}$ interference	26
The $^{40}\text{Ar}/^{39}\text{Ar}$ technique	3	Minimization of $^{40}\text{Ca}(n, n\alpha)^{36}\text{Ar}$ interference	26
The GSTR facility	4	References cited	26
Sample encapsulation	4	Derivation of equations	32
Monitor minerals	8	$^{40}\text{Ar}/^{39}\text{Ar}$ age equation	32
Flux characteristics of the GSTR	10	Error formulae	33
Vertical gradients	12	^{37}Ar decay correction	33
Horizontal gradients	14	Effect of $^{40}\text{Ca}(n, n\alpha)^{36}\text{Ar}$ interference	35
Self-shielding	16	Computer programs	42
Activity predictions	16	NEUT2 — Activity prediction program for GSTR	42
Corrections for interfering argon isotopes	18	AR37 — ^{37}Ar decay correction program	51
Optimization of irradiation parameters	25	Selected bibliography	54
Production of sufficient ^{39}Ar	25		

ILLUSTRATIONS

	Page
FRONTISPIECE. Core of the Geological Survey TRIGA reactor in operation.	
FIGURE 1. Schematic cross section through U. S. Geological Survey TRIGA reactor	5
2. Diagram showing details of GSTR core	6
3. Photograph showing partly assembled aluminum sample holder and quartz sample vials	7
4-8. Diagrams showing:	
4. Cross section of a sealed 8-mm quartz sample vial with 10-mm high sample	7
5. Clamp for cooling quartz vials while they are being sealed	7
6. Aluminum sample holder	8
7. Aluminum sample holder plates showing four useful arrangements of quartz vials of various sizes within an irradiation level	9
8. Typical reactor tube for the central thimble	9
9. Graph of approximate $^{39}\text{Ar}_K$ productivity at centerline of central thimble as a function of K_2O content and irradiation time	13
10. Graph of $^{40}\text{Ar}_{\text{rad}}/^{39}\text{Ar}_K$ ratio as a function of K-Ar age and irradiation time in central thimble of GSTR	14
11. Schematic diagram of change in true thermal power level as a function of fueling and calibration	14
12. Graph showing vertical flux gradient in the central thimble of GSTR	14
13. Graph showing relative fluence in GSTR as measured with nickel wires and with the St. Severin monitor	15
14. Isometric drawing of sample locations in self-shielding experiment on diabase 8L691	16
15-22. Graphs showing:	
15. Results of self-shielding experiment on diabase 8L691	16
16. Activity resulting from various neutron reactions in GSTR as a function of irradiation time at 1 MW	20
17. Effect of reaction $^{40}\text{Ca}(n, n\alpha)^{36}\text{Ar}$ on calculated $^{40}\text{Ar}/^{39}\text{Ar}$ age	22
18. Approximate ranges of K/Ca atomic ratios for some common minerals and rocks	22
19. Effect of $^{42}\text{Ca}(n, \alpha)^{39}\text{Ar}$ reaction on calculated $^{40}\text{Ar}/^{39}\text{Ar}$ age	23
20. Effect of $^{40}\text{K}(n, p)^{40}\text{Ar}$ and $^{41}\text{K}(n, d)^{40}\text{Ar}$ reactions on calculated $^{40}\text{Ar}/^{39}\text{Ar}$ age	24
21. $^{39}\text{Ar}_K/^{37}\text{Ar}_{\text{Ca}}$ as a function of K/Ca atomic ratio in GSTR	25
22. Irradiation time in GSTR required to maximize the ^{39}Ar produced from ^{39}K while minimizing interferences from $^{40}\text{Ar}_K$ and $^{36}\text{Ar}_{\text{Ca}}$	25
23-35. Graphs showing effect of the reaction $^{40}\text{Ca}(n, n\alpha)^{36}\text{Ar}$ on calculated $^{40}\text{Ar}/^{39}\text{Ar}$ ages:	
23. K/Ca = 0.02	35
24. K/Ca = 0.05	36
25. K/Ca = 0.1	36
26. K/Ca = 0.2	37

	Page
FIGURES 23-35. Graphs showing effect of the reaction $^{40}\text{Ca}(n, n\alpha)^{36}\text{Ar}$ on calculated $^{40}\text{Ar}/^{39}\text{Ar}$ ages — Continued	
27. K/Ca = 0.5	37
28. K/Ca = 1	38
29. K/Ca = 2	38
30. K/Ca = 5	39
31. K/Ca = 10	39
32. K/Ca = 20	40
33. K/Ca = 50	40
34. K/Ca = 100	41
35. K/Ca = 200	41

TABLES

	Page
TABLE 1. Natural abundance and decay constants for selected isotopes of chlorine, argon, potassium, and calcium	2
2. Analytical data for monitor minerals	10
3. Results for mineral standards irradiated in GSTR	11
4. Neutron energy distribution on the centerline of the central thimble of the GSTR	11
5. Comparison of nuclear reactors used for $^{40}\text{Ar}/^{39}\text{Ar}$ irradiations	12
6. Data for activity calculations, TRIGA reactor	17
7. Principal neutron reactions leading to the production of argon isotopes	18
8. Correction factors for Ca- and K-derived Ar isotopes for the U. S. Geological Survey TRIGA reactor	19
9. Standard mineral and rock compositions used in BASIC program NEUT2	45
10. Selected bibliography of use of $^{40}\text{Ar}/^{39}\text{Ar}$ data in terrestrial, lunar, and cosmological studies	54

IRRADIATION OF SAMPLES FOR $^{40}\text{Ar}/^{39}\text{Ar}$ DATING USING THE GEOLOGICAL SURVEY TRIGA REACTOR

By G. BRENT DALRYMPLE, E. CALVIN ALEXANDER, JR.,¹MARVIN A. LANPHERE, and G. PATRICK KRAKER

ABSTRACT

The characteristics of the Geological Survey TRIGA Reactor (GSTR) as a source of fast neutrons for the $^{40}\text{Ar}/^{39}\text{Ar}$ technique of K-Ar dating have been determined using data from more than 45 irradiations in the central thimble (core) facility. The GSTR has a flux over the entire energy spectrum of 1.1×10^{17} n/cm²·MWH and a fast/thermal ratio on the centerline of the central thimble of 1.17 for fast neutron energies greater than 0.6 MeV. Production of ^{39}Ar is about 7×10^{-13} mole/gram-percent K₂O MWH, and the cross section for the reaction $^{39}\text{K}(n, p)^{39}\text{Ar}$ is 65 ± 4 millibarns for epithermal (> 0.6 MeV) neutrons. Most $^{40}\text{Ar}/^{39}\text{Ar}$ dating applications require about 10-40 hours of irradiation in the GSTR at the maximum continuous power level of 1 MW. The peak neutron flux in the central thimble is 4 cm above the physical centerline, and the vertical flux gradient in the centermost 20 centimeters varies from a small fraction of a percent to a maximum of about 3.5 percent per centimeter. The effect of this gradient can be effectively cancelled by suitable sample encapsulation and the use of a sample holder designed for the purpose. The horizontal flux gradient is less than 0.5 percent over the width of the central thimble. Self-shielding in a solid core of diabase 2.40 cm in diameter and 2.54 cm high is approximately 3 percent from the outside to the center, but self-shielding is probably negligible for the smaller samples usually irradiated for K-Ar dating.

Corrections for interfering Ar isotopes produced by neutron reactions with Ca are relatively reproducible with values of $2.64 \pm 0.017 \times 10^{-4}$ for $(^{36}\text{Ar}/^{37}\text{Ar})_{\text{Ca}}$ and $6.73 \pm 0.037 \times 10^{-4}$ for $(^{39}\text{Ar}/^{37}\text{Ar})_{\text{Ca}}$. The measured values for $(^{40}\text{Ar}/^{39}\text{Ar})_{\text{K}}$, however, vary by an order of magnitude. This variability, whose cause is unknown, has been reported from other reactors. The corrections for interfering Ar isotopes can be minimized by using optimization curves for the GSTR to choose the best sample size and irradiation time for a given material. Of more than 100 possible neutron reactions in common rocks and minerals, only 26 need be considered for purposes of radiological safety. The activity produced by these reactions upon irradiation of samples can be conveniently and accurately predicted either by a computer program or from graphs specifically devised for the GSTR.

INTRODUCTION

Since first proposed by Sigurgeirsson (1962) and Merrihue (1965), the $^{40}\text{Ar}/^{39}\text{Ar}$ technique of K-Ar dat-

ing has been investigated and utilized for geochronological studies by many laboratories throughout the world. Although most of the early studies involved meteorites and lunar rocks, it soon became apparent that the technique was a potentially powerful tool for the investigation of terrestrial chronology.

The U. S. Geological Survey's experiments on the $^{40}\text{Ar}/^{39}\text{Ar}$ technique began in 1970 at Menlo Park, Calif. (Dalrymple and Lanphere, 1971), using the Geological Survey TRIGA² reactor (GSTR), sited in Denver, Colo. Since then more than 700 samples have been irradiated for $^{40}\text{Ar}/^{39}\text{Ar}$ experiments in over 45 separate irradiations. In addition, the GSTR has been used extensively by several investigators pursuing $^{40}\text{Ar}/^{39}\text{Ar}$ research in academic institutions, principally the University of Minnesota and Ohio State University. During the course of the research at the Geological Survey in Menlo Park and at the University of Minnesota, we experienced many technical problems directly related to the reactor and its neutron flux. In pursuing solutions to these problems, we have collected much valuable technical information on the use of the GSTR for $^{40}\text{Ar}/^{39}\text{Ar}$ dating. The degree to which satisfactory solutions have been found has a direct effect on the validity and accuracy of the scientific results from $^{40}\text{Ar}/^{39}\text{Ar}$ dating experiments. Thus it is important that this information on the GSTR be made readily available to other scientists in the field. Some of this information has been published in the scientific media but most,

¹ Department of Geology and Geophysics, University of Minnesota. Supported by National Aeronautics and Space Administration under grant NGL 24-005-225. Publication No. 1029 from School of Earth Sciences, University of Minnesota.

² TRIGA (Training Research Isotope General Atomic) is a trademark of the General Dynamics Corp.

because of the technical nature of the material and the inevitable editorial pressures for brevity, has not.

Some of the information in this paper, such as data on flux gradients and appropriate constants for interference corrections, is directly concerned with the particular characteristics of the GSTR and some, such as the derivation of equations and the methods of predicting activities, is more generally applicable. Most research reactors, however, are similar in many respects, and information concerning the problems, characteristics, and techniques for the GSTR can be applied quite easily to other reactors, at least in principle if not in detail. In particular, this report will be valuable to those who contemplate starting a program of $^{40}\text{Ar}/^{39}\text{Ar}$ research, whether using the GSTR or some other research reactor.

This paper is concerned with the technical aspects of sample irradiation and not with the interpretation of $^{40}\text{Ar}/^{39}\text{Ar}$ age data. For the latter, we refer the interested reader to the section entitled "Selected Bibliography," a compilation of papers on the use and interpretation of the $^{40}\text{Ar}/^{39}\text{Ar}$ technique in terrestrial, lunar, and cosmologic problems.

Throughout this paper, we use the convention that the mass number of an isotope is indicated by a left-hand superscript, for example ^{40}Ar for argon-40. Right-hand subscripts indicate the origin of the isotope:

atm = atmospheric
rad = radiogenic
Ca = calcium derived
K = potassium derived

For example, $^{37}\text{Ar}_{\text{Ca}}$ denotes argon-37 formed by neutron reaction with calcium. For nuclear reactions we use the standard notation.

target (incoming particle, ejected particle) product

where n stands for neutron, p for proton, γ for gamma-ray, α for alpha particle (^4He nucleus), and d for np (^2H nucleus). For radioactive decay, β^- indicates the emission of an electron and ϵ indicates electron capture; λ is the decay constant. Power in the reactor is indicated in either megawatts (MW) or kilowatts (kW). The abbreviation MWH is used for megawatt-hour and is a convenient way to indicate irradiation "time": 1 MWH is an irradiation time of 1 hour at a power level of 1 megawatt, 10 hours at a power level of 100 kilowatts, and so on. We use the term neutron flux to represent the rate at which neutrons pass through the sample in units of neutrons per square centimeter per second ($\text{n}/\text{cm}^2\text{-s}$), and neutron fluence to represent the total time-integrated flux "experienced" by the samples in n/cm^2 . Other symbols are defined, as necessary, in the text.

Finally, the natural abundances, half-lives, and decay constants for selected isotopes of chlorine, argon, potassium, and calcium are listed in table 1. These data are required for many of the calculations relevant for $^{40}\text{Ar}/^{39}\text{Ar}$ experiments. The decay constants and isotopic abundances for potassium are those recently adopted by the International Union of Geological Sciences Subcommittee on Geochronology at the 1976 International Geological Congress in Sydney, Australia

TABLE 1.—Natural abundance and decay constants for selected isotopes of chlorine, argon, potassium, and calcium

[If no half life given, stable; y=years, d=days, and m=minutes. References: 1. Weast (1976); 2. Nier (1950); 3. Stoenner, Schaeffer, and Katcoff (1965); 4. Garner and others (1975); 5. Beckinsale and Gale (1969); and 6. Steiger and Jäger (1977)]

Element	Atomic weight	Isotope	Relative natural abundance	Half-life	Decay constant	References
Cl	35.453	^{35}Cl	0.7553			1
		^{36}Cl		3.1×10^5 y	$2.236 \times 10^{-6} \text{ y}^{-1}$	1
		^{37}Cl	.2447			1
		^{38}Cl		37.3 m	$1.858 \times 10^{-2} \text{ m}^{-1}$	1
		^{39}Cl		55.5 m	$1.249 \times 10^{-2} \text{ m}^{-1}$	1
Ar	39.948	^{36}Ar	.00337			1,2
		^{37}Ar		35.1 d	$1.975 \times 10^{-2} \text{ d}^{-1}$	3
		^{38}Ar	.00063			2
		^{39}Ar		259 y	$2.58 \times 10^{-3} \text{ y}^{-1}$	3
		^{40}Ar	.99600			2
K	39.098	^{39}K	.932581			4
		^{40}K	.0001167	1.250×10^9 y	$\lambda_{\epsilon} = 0.581 \times 10^{-10} \text{ y}^{-1}$ $\lambda_{\beta} = 4.963 \times 10^{-10} \text{ y}^{-1}$	4,5,6
		^{41}K	.067302			6
Ca	40.08	^{40}Ca	.96947			4
		^{42}Ca	.00646			1
		^{43}Ca	.00135			1
		^{44}Ca	.02083			1
		^{46}Ca	.00186			1
		^{48}Ca	.0018			1

(Steiger and Jäger, 1977). These values differ from those used in most of the earlier literature on $^{40}\text{Ar}/^{39}\text{Ar}$ dating, therefore, care should be taken when comparing K-Ar ages in this paper with those calculated using the earlier values. The effect of the new constants is nonlinear. For example, an age calculated with the new constants is 2.7 percent older than one calculated with the old constants at one million years but 1.7 percent younger at 4,500 m.y. Conversion tables and formulae are given by Dalrymple (1979).

THE $^{40}\text{Ar}/^{39}\text{Ar}$ TECHNIQUE

In the conventional K-Ar technique, the quantity of radiogenic ^{40}Ar in a rock or mineral is measured by isotope-dilution mass spectrometry. In this procedure, an aliquant of the sample is fused in vacuum and the reactive gasses removed. During fusion, a tracer of ^{38}Ar (which also contains some ^{40}Ar and ^{36}Ar) of known amount and composition is added to the gas released from the sample. The isotope ratios of this gas mixture are measured, and after correcting for atmospheric argon, which is present as a contaminant, the amount of $^{40}\text{Ar}_{\text{rad}}$ is determined by comparison with the ^{38}Ar from the tracer. The potassium is measured, most often by flame photometry, in a separate experiment on another aliquant of the sample. Once the potassium is known, the amount of ^{40}K can be calculated from the known abundance of the potassium isotopes (table 1). The potassium and argon data are then combined and an age is calculated with the K-Ar age equation

$$t = \frac{1}{\lambda} \ln \left[\frac{^{40}\text{Ar}_{\text{rad}}}{^{40}\text{K}} \left(\frac{\lambda}{\lambda \epsilon} \right) + 1 \right] \quad (1)$$

A more thorough discussion of the conventional K-Ar technique is given in Dalrymple and Lanphere (1969).

In the $^{40}\text{Ar}/^{39}\text{Ar}$ technique, the potassium and argon are measured on the same sample aliquant in a single experiment. First the sample is irradiated in a nuclear reactor, where fast neutrons convert some of the ^{39}K to ^{39}Ar by the reaction $^{39}\text{K}(n,p)^{39}\text{Ar}$, which has a threshold of 0.22 MeV. After irradiation, the sample is fused and the argon ratios are measured by mass spectrometry in the usual way. If the fraction of ^{39}K converted to ^{39}Ar were known exactly, then the age could be calculated directly from the ratio $^{40}\text{Ar}_{\text{rad}}/^{39}\text{Ar}_{\text{K}}$ by

$$t = \frac{1}{\lambda} \ln \left[\frac{^{40}\text{Ar}_{\text{rad}}}{C \ ^{39}\text{Ar}_{\text{K}}} \left(\frac{\lambda}{\lambda \epsilon} \right) + 1 \right] \quad (2)$$

where C is a constant that includes factors for both the fraction of ^{39}Ar produced from ^{39}K and the fraction of potassium that is ^{40}K . The conversion constant for the $^{39}\text{K}(n,p)^{39}\text{Ar}$ reaction, however, is not easy to measure accurately by direct methods, so a monitor mineral, whose age has been carefully determined by conventional techniques, is used. An aliquant of the monitor mineral is irradiated alongside the unknown mineral so that both receive the same neutron fluence. The age of the unknown is then calculated using

$$t_{\text{u}} = \frac{1}{\lambda} \ln \left[\frac{(^{40}\text{Ar}_{\text{rad}}/^{39}\text{Ar}_{\text{K}})_{\text{u}}}{(^{40}\text{Ar}_{\text{rad}}/^{39}\text{Ar}_{\text{K}})_{\text{m}}} (e^{\lambda t_{\text{m}}} - 1) + 1 \right] \quad (3)$$

where the subscripts u and m refer to the unknown and the monitor minerals, respectively. To simplify, it is conventional to define the quantity

$$J = \frac{(e^{\lambda t_{\text{m}}} - 1)}{(^{40}\text{Ar}_{\text{rad}}/^{39}\text{Ar}_{\text{K}})_{\text{m}}} \quad (4)$$

then rewrite equation (3)

$$t_{\text{u}} = \frac{1}{\lambda} \ln \left[J (^{40}\text{Ar}_{\text{rad}}/^{39}\text{Ar}_{\text{K}})_{\text{u}} + 1 \right] \quad (5)$$

which is the $^{40}\text{Ar}/^{39}\text{Ar}$ age equation. The derivation of this equation is given at the end of this report after the "References Cited."

If the only contaminant present were atmospheric argon, then $^{40}\text{Ar}_{\text{rad}}/^{39}\text{Ar}_{\text{K}}$ could be calculated from the measured $^{40}\text{Ar}/^{39}\text{Ar}$ and $^{36}\text{Ar}/^{39}\text{Ar}$ ratios using

$$\frac{^{40}\text{Ar}_{\text{rad}}}{^{39}\text{Ar}_{\text{K}}} = \frac{^{40}\text{Ar}}{^{39}\text{Ar}} - \left(\frac{^{40}\text{Ar}}{^{36}\text{Ar}} \right)_{\text{atm}} \left(\frac{^{36}\text{Ar}}{^{39}\text{Ar}} \right) \quad (6)$$

where $(^{40}\text{Ar}/^{36}\text{Ar})_{\text{atm}}$ is the composition of atmospheric argon. Several interfering argon isotopes, however, are produced by undesirable neutron reactions with other elements, principally ^{36}Ar and ^{39}Ar from calcium and ^{40}Ar from potassium. Fortunately, ^{37}Ar is also produced from calcium, and accurate corrections can be made for the interfering argon isotopes using

$$\frac{^{40}\text{Ar}_{\text{rad}}}{^{39}\text{Ar}_{\text{K}}} = \frac{(^{40}\text{Ar}/^{39}\text{Ar}) - 295.5 [(^{36}\text{Ar}/^{39}\text{Ar}) - (^{36}\text{Ar}/^{37}\text{Ar})_{\text{Ca}} (^{37}\text{Ar}/^{39}\text{Ar})] - (^{40}\text{Ar}/^{39}\text{Ar})_{\text{K}}}{1 - (^{39}\text{Ar}/^{37}\text{Ar})_{\text{Ca}} (^{37}\text{Ar}/^{39}\text{Ar})} \quad (7)$$

where $(^{36}\text{Ar}/^{37}\text{Ar})_{\text{Ca}}$, $(^{39}\text{Ar}/^{37}\text{Ar})_{\text{Ca}}$, and $(^{40}\text{Ar}/^{39}\text{Ar})_{\text{K}}$ are constants determined experimentally for a given reactor. (This equation is derived and the corrections discussed in detail in later sections.)

In spite of the necessity to correct for the interfering argon isotopes produced during irradiation, the $^{40}\text{Ar}/^{39}\text{Ar}$ technique has several important advantages over the conventional technique. First, both the potassium and the argon are measured on the same aliquant, eliminating problems of sample inhomogeneity and reducing significantly the required sample amount. Second, no elemental abundance measurements are required, so the technique is both easier and potentially more precise than the conventional technique. Finally, instead of releasing the argon all at once in a single fusion (the total fusion technique), it is possible to release the gas fractionally by incremental heating (the incremental heating, stepwise heating, or age spectrum technique). The result is a series of apparent ages at successively higher temperatures, known as an age spectrum or release curve, from which useful information about the geologic history, the condition of the sample, and the age of the sample can be inferred. The selected bibliography at the end of this report lists sources for the use of the incremental heating and the total fusion $^{40}\text{Ar}/^{39}\text{Ar}$ techniques.

THE GSTR FACILITY

The GSTR, located in the Nuclear Science Building (Building 15) of the Denver Federal Center, Denver Colo., is administered by the Geological Survey's Geologic Division. It first reached criticality in February 1969, and since then has been in operation 8 hours a day, 5 days a week. It has proved to be a very valuable tool for the Geological Survey's research programs in geology and hydrology. Among its many uses, in addition to $^{40}\text{Ar}/^{39}\text{Ar}$ experiments, are neutron activation analyses of a variety of geological materials, fission-track dating, uranium-thorium disequilibrium studies, delayed-neutron analyses for uranium and thorium concentrations, and hydrologic tracing with activatable materials. Since it first went into operation, the GSTR has generated over 8,000 MWH of thermal energy in the course of irradiating samples for scientific studies.

The GSTR (fig. 1) is a light-water-cooled and -reflected reactor that uses uranium-zirconium hydride (U-ZrH) fuel moderator elements (fig. 2). The reactor is capable of continuous steady-state operation at 1,000 kW (thermal) and may be pulsed repeatedly to yield a burst having a prompt energy release of about 15 MW-seconds, a peak power of about 1,600 MW, and a pulse width at half maximum of about 11 milliseconds.

For $^{40}\text{Ar}/^{39}\text{Ar}$ dating, samples are irradiated in the central thimble, located in the center of the core at the point of maximum fast neutron flux (figs. 1 and 2). The central thimble is an aluminum tube 3.81 cm (1.50 in.) in outside diameter, with a wall thickness of 0.211 cm (0.083 in.). It extends from the reactor support bridge straight down through the central hole in the top grid plate. The central thimble is supported at its lower end by a safety plate about 40 cm beneath the bottom grid plate. Use of the central thimble has the advantages of maximizing the fast neutron flux and minimizing horizontal flux gradients.

The bulk water in the reactor has an operational temperature limit of 60° C but is normally kept within the range of 42°-45° C. The water is circulated within the reactor by convection. Although the central thimble space is enclosed by an aluminum tube, the tube is open to the water supply through several holes at its lower end (fig. 1) and thus is also subjected to some convection cooling. In addition, the top of the central thimble tube is open to the atmosphere, and therefore the water in the central thimble can not exceed the boiling point. Because the water in the central thimble has never been observed to boil, the central thimble temperatures are probably actually less than about 95° C. Temperature-sensitive color tabs placed in the central thimble indicated an upper limit of 90° C, while direct thermocouple measurements indicated that the temperatures in the rabbit tube (fig. 2) are about 70° C. Thus, the data suggest that the temperature in the central thimble is probably between 70° C and 90° C.

Though the primary mission of the facility is the performance of experiments for the research groups within the Geological Survey, irradiations are done, as space is available, for other Government agencies, educational institutions, hospitals, and nonprofit research organizations. Persons interested in using the GSTR should contact the Reactor Supervisor, U. S. Department of the Interior, Geological Survey, Denver Federal Center, Denver, CO 80225.

SAMPLE ENCAPSULATION

Because the central thimble is water-filled, sample encapsulation must be leak tight. For adequate safety, two levels of containment are required. The rock or mineral samples are first encapsulated in heat-sealed quartz vials. These vials are then arranged in a multi-level aluminum sample holder (fig. 3) and placed in a cold-welded aluminum reactor tube that is lowered into the central thimble for irradiation.

The quartz sample vials are made from fused quartz tubing of various outside diameters (O.D.) and standard wall thicknesses. The most common are 6 and 8 mm O.D., but vials as small as 3mm O.D. and as large

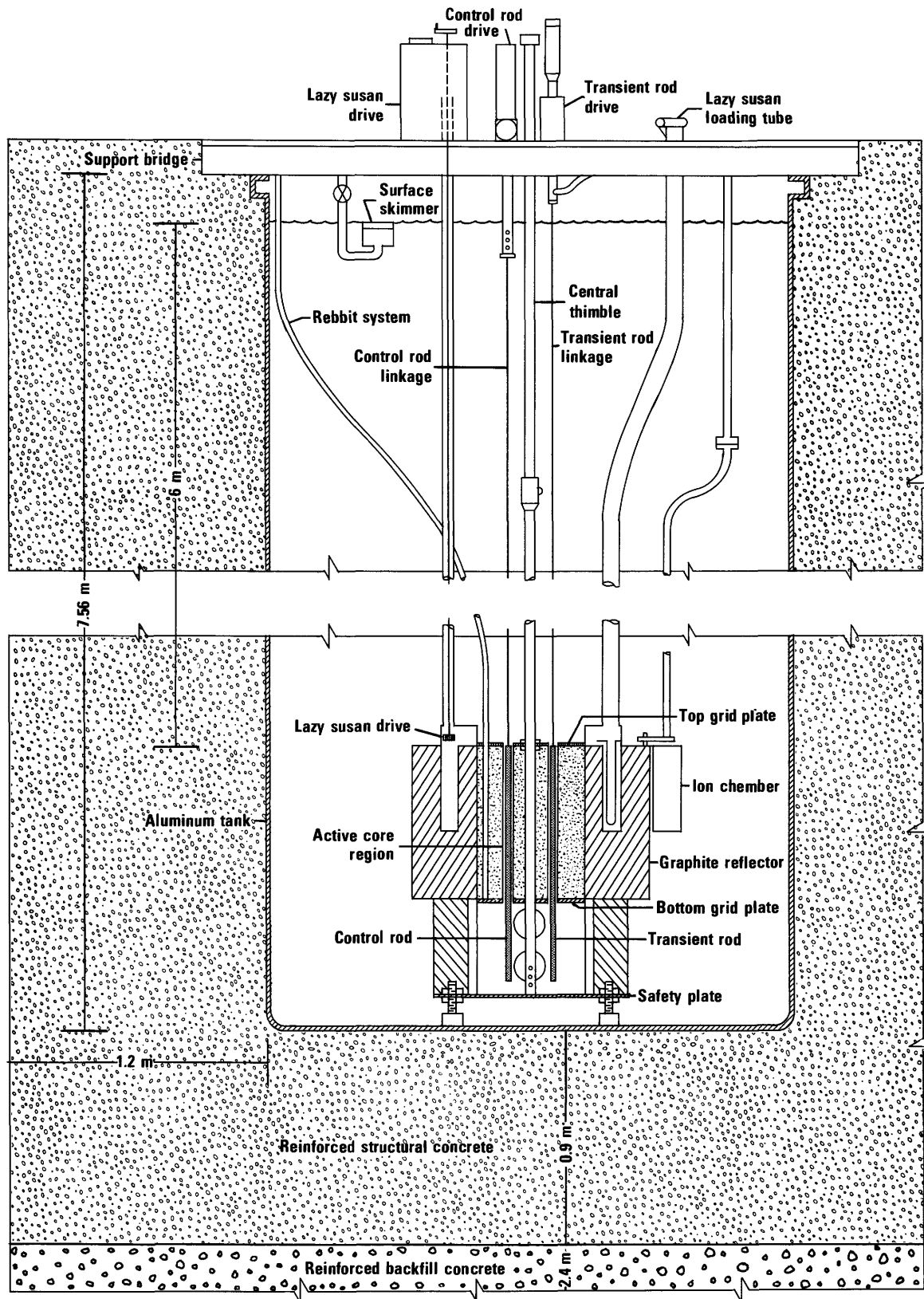


FIGURE 1.—Schematic cross section through U. S. Geological Survey TRIGA reactor.

as 12mm O.D. have been used. Other forms of glass, including vycor (96 percent silica), are not suitable either because of low strength or because other cations in the glass yield activation products of high activity and long half-life, making handling of the vials after irradiation a problem. Pure fused quartz (100 percent silica) yields only ^{28}Si and ^{30}Si , both of which decay rapidly, allowing safe handling of the vials within a few days of irradiation. Because of vertical fluence gradients in the reactor, the vials are made with flat bottoms (fig. 4), and the sample amounts are adjusted so

that all the samples on a level, including the monitors, are the same height and thus intercept the same fast neutron flux.

Each vial must be numbered for positive identification. Conventional inks and marking pens will not survive irradiation. A diamond marking scribe will leave a permanent mark, but the numbers lack contrast and are difficult to read. The two most satisfactory methods are to use either a ceramic ink or small glass-marking decals, both of which are available from most glass-blowing supply companies. After the vials have been

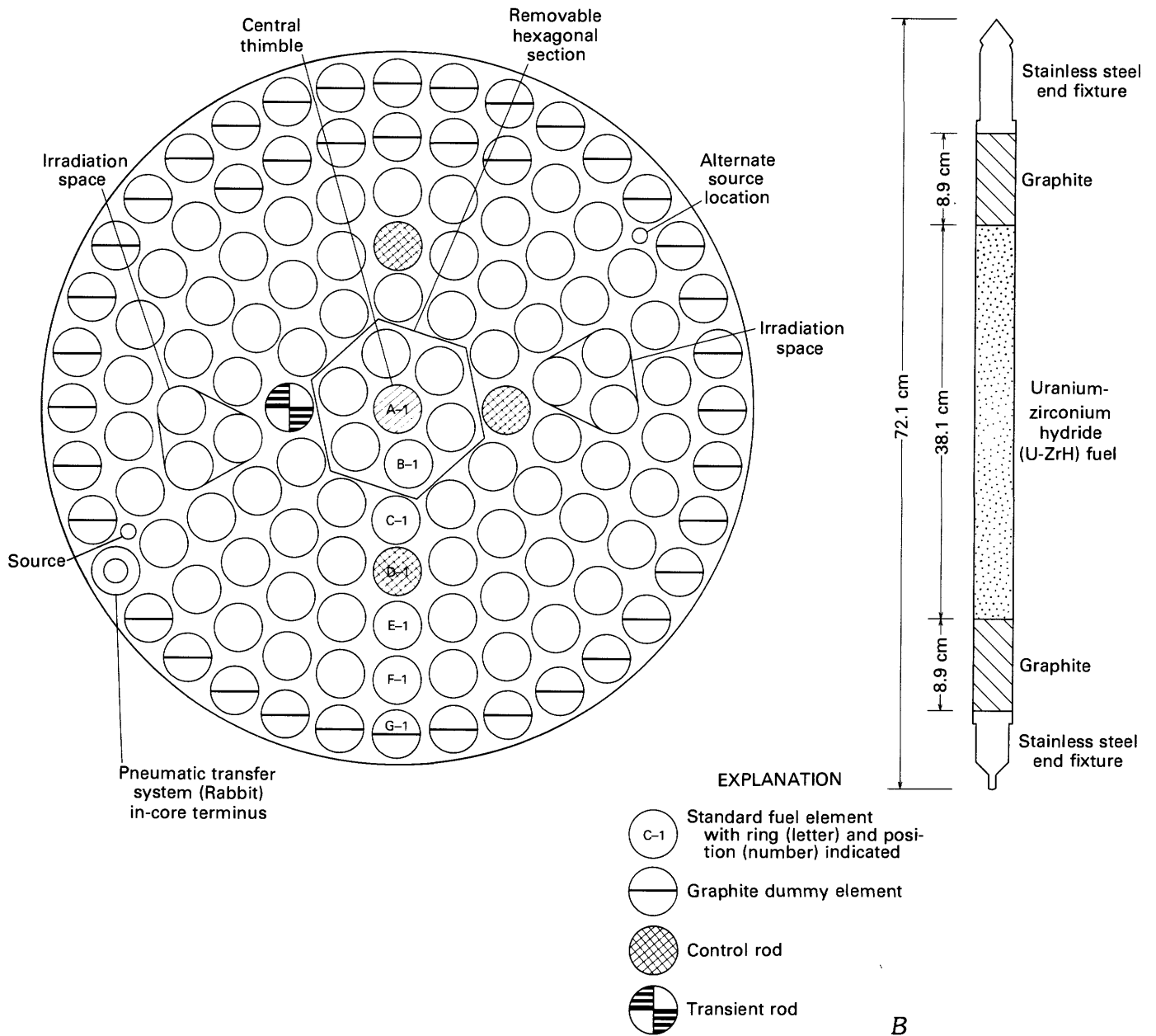


FIGURE 2.—Details of GSTR core. A. Plan view of core, showing location of central thimble facility. B. Configuration of typical fuel moderator element.

marked, the numbers are heated to red heat with a hand torch, whereupon they fuse onto the quartz and become permanent.

The samples may be fine powders, mineral grains, rock chips, or rock cores. Mineral grains, rock chips,

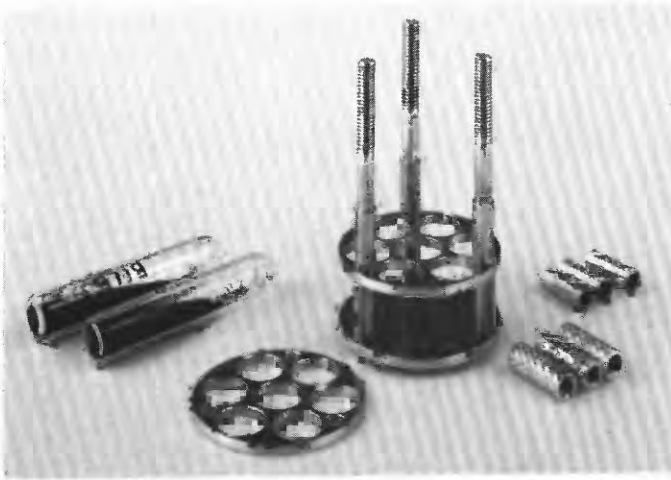


FIGURE 3.—Partly assembled aluminum sample holder and 8-mm-diameter flat-bottomed quartz sample vials. Vials fit into holes in sample holder. Shown at right are spacers and knurled top nuts.

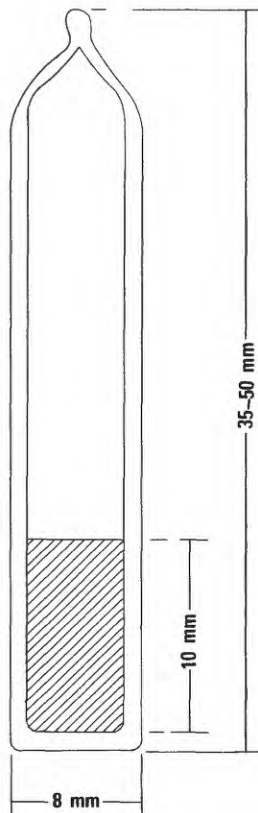


FIGURE 4.—Cross section of a sealed 8-mm quartz sample vial with 10-mm high sample (shaded). Tubing wall is 1 mm thick.

and cores are usually placed directly into the vials. Fine powders or fine mineral grains may be wrapped in household-type aluminum foil before insertion into the vial for ease of handling after irradiation. Cores of rocks are preferable to chips, because they maximize the mass of sample within a given vertical space. Cores cut with standard diamond core bits of 5/16-inch and 7/16-inch O.D. slip conveniently into 8-mm and 12-mm tubing, respectively. After the samples are placed in the vials, the tops of the vials are sealed with a hydrogen-oxygen torch and inspected for adequacy of seal. We have not found it necessary to evacuate the vials before sealing. During sealing, care should be taken to avoid overheating the sample. A method that we have found satisfactory is to hold the vial in a split aluminum cylinder, which is attached to a laboratory clamp (fig. 5). The lower part of the cylinder is immersed in a beaker of water. The heat from the vial is rapidly conducted by the aluminum to the water, preventing the sample from becoming hot.

The sample holder (fig. 6), made of 6061T6 aluminum, keeps one level of samples in the same vertical position within the central thimble. This ensures that all the samples on a given level receive the same integrated fast neutron flux. To prevent galling and freezing during irradiation, the knurled nuts that hold the assembly together are coated with a permanently bonded, monomolecular layer of graphite or with a graphite lubricant. Sample holders of from one to four

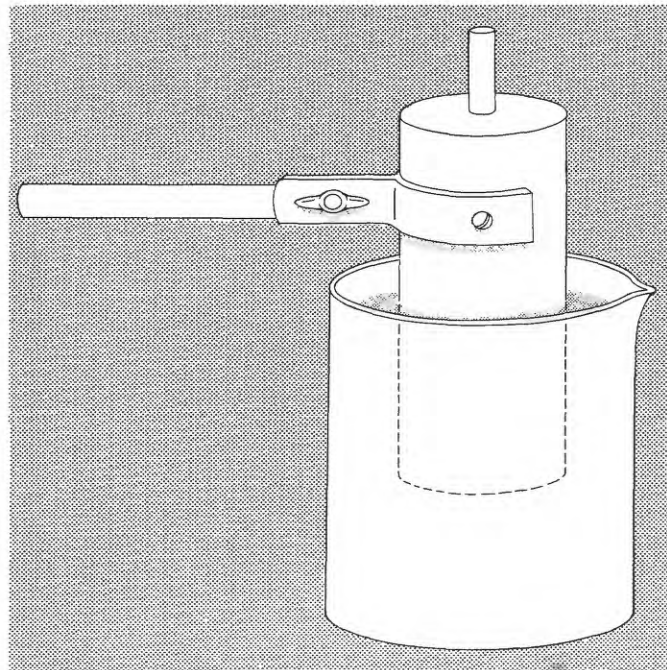
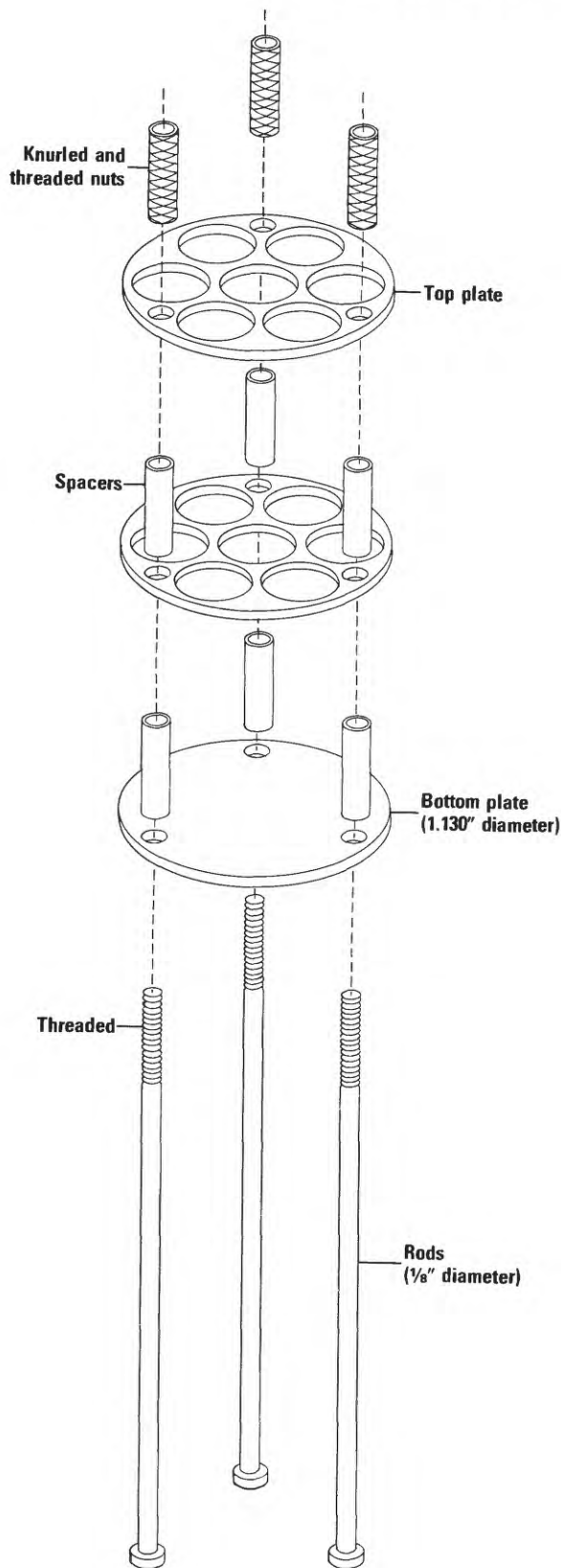


FIGURE 5.—Clamp for cooling quartz vials while they are being sealed. Vial (8 mm in diameter) is clamped in split aluminum cylinder, which is partly immersed in a beaker of water.



levels may be assembled quickly from the various pieces by using rods of appropriate length. In addition, we have used top plates machined to hold a wide variety of quartz vials (fig. 7). The 7-sample plates shown in figure 7C are the most frequently used for terrestrial samples and hold as many as 28 samples (four levels) for a single irradiation. Filled to a height of 1 cm, each of the 8-mm vials will hold about 0.3-0.8 g of material. For smaller amounts of material, such as lunar and meteorite samples, the plates shown in figure 7A, and B are used. The plate configuration shown in figure 7A permits up to 48 samples to be irradiated together. The plate configuration in figure 7D is used for young basalt samples, usually rock cores of up to 5 g each; the 3-mm holes in this plate hold the monitor minerals.

The sample holder (fig. 6) fits into the aluminum reactor tube, which has an outside diameter of 3.18 cm (1.25 in.), a maximum length of 30 cm (12 in.) (fig. 8), and is supplied by the researcher. The reactor tube is sealed by the reactor staff by cold-welding and then leak tested in a column of ethylene glycol evacuated to less than 0.8 atm. As the interior of the reactor tube is at atmospheric pressure, even a minute leak in the seals is clearly and quickly detected by a stream of small bubbles.

The sealed, leak-tested aluminum reactor tube is suspended in the central thimble between aluminum leaders with 60-lb test monofilament nylon line. Fishing weights are used to sink the tube, and they physically contact the bottom plug to ensure consistency in vertical positioning of the sample. After irradiation, the reactor tube is pulled out of the neutron flux and left suspended in the water column for several days to allow the radioactivity from products with short half-life to decrease. The tube is then removed from the reactor and opened. The aluminum tube is disposed of by the reactor staff, the sample holder is disassembled and saved at the reactor center for reuse, and the samples are shipped to the experimenter using packaging and shipping procedures specified by the Department of Transportation for radioactive materials.

MONITOR MINERALS

As explained above, the calculation of a K-Ar age using the $^{40}\text{Ar}/^{39}\text{Ar}$ technique depends on the use of a monitor mineral whose age is precisely known. The criteria for a suitable monitor mineral have been dis-

FIGURE 6.—Diagram of aluminum sample holder. Only one sample level is shown, but as many as four levels may be assembled on longer rods. Top plates shown hold seven 8-mm O. D. vials, but other configurations are also possible (see fig. 7).

cussed by Alexander and Davis (1974). Briefly, they are:

1. The mineral should have a uniform ratio of radiogenic ^{40}Ar to ^{40}K .
2. Both potassium and radiogenic ^{40}Ar should be homogeneously distributed.
3. The monitor should be similar in age and K/Ca ratio to the samples being dated.
4. The monitor should be fairly coarse grained.
5. The monitor should be available in reasonable quantity.

Because a $^{40}\text{Ar}/^{39}\text{Ar}$ age is calculated with reference to the $^{40}\text{Ar}_{\text{rad}}/^{39}\text{Ar}_{\text{K}}$ ratio of the monitor, criterion 1 is necessary to minimize errors due to monitor inhomogeneity. Criterion 2 is required because the monitor is calibrated by conventional K and Ar measurements, which are done on separate aliquants of the sample. Criterion 3 arises because the optimum parameters (primarily irradiation time and sample size) for an irradiation are a function of both age and K/Ca ratio. If the monitor and the samples are greatly different in either age or K/Ca, then the irradiation may be less than optimum for one or both and interfer-

ing neutron reactions may lead to unacceptable errors. The satisfaction of criterion 4 eliminates radiological safety difficulties involved in handling a radioactive powder, which may easily become airborne. Criterion 5 is desirable to provide continuity in measurements over a period of years.

We have used three different monitors (BS-1, SB-2, and St. Severin) in the GSTR, and a fourth (MMhb-1) (Alexander and others, 1978) has been recently prepared and calibrated (table 2). The first three are intralaboratory monitors and are not generally available. Hornblende MMhb-1 is available to other laboratories for use as a $^{40}\text{Ar}/^{39}\text{Ar}$ monitor mineral. Interested investigators should write to E. Calvin Alexander, Jr., Department of Geology and Geophysics, University of Minnesota, 310 Pillsbury Drive, S. E., Minneapolis, MN 55455.

BS-1, which is no longer in use, was biotite separated from 162-m.y.-old quartz diorite (sample 62A Lel) from the Aleutian Range, Alaska (Reed and Lanphere, 1969). The size range of BS-1 was nominally 420 to 177 micrometers, but the actual variation ranged from 420 to 88 micrometers. K_2O was measured by both flame photometry, using lithium metaborate fusion (Ingamells, 1970), and by isotope dilution. The argon measurements were by isotope-dilution mass spectrometry using two independently calibrated ^{38}Ar tracer systems. The separate was far from ideal for a standard because it contained about 4 percent impurities of hornblende, epidote, apatite, and chlorite. This inhomogeneity is reflected in the errors of the K_2O

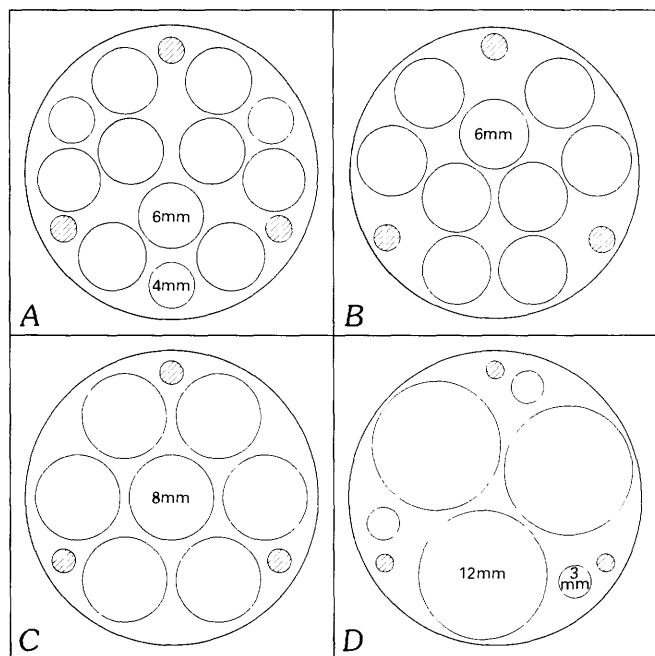


FIGURE 7.—Schematic diagram of aluminum sample holder plates, showing four useful arrangements of quartz vials of various sizes within an irradiation level. Outside diameter of vials accommodated to each size hole is indicated. Shaded holes accept 1/8- or 5/32-in. rods used to assemble plates into a complete sample holder. A, Smaller amounts of material, for lunar and meteorite samples. B, Smaller amounts of material, for lunar and meteorite samples. C, Most frequently used for terrestrial samples. D, For young basalt samples.

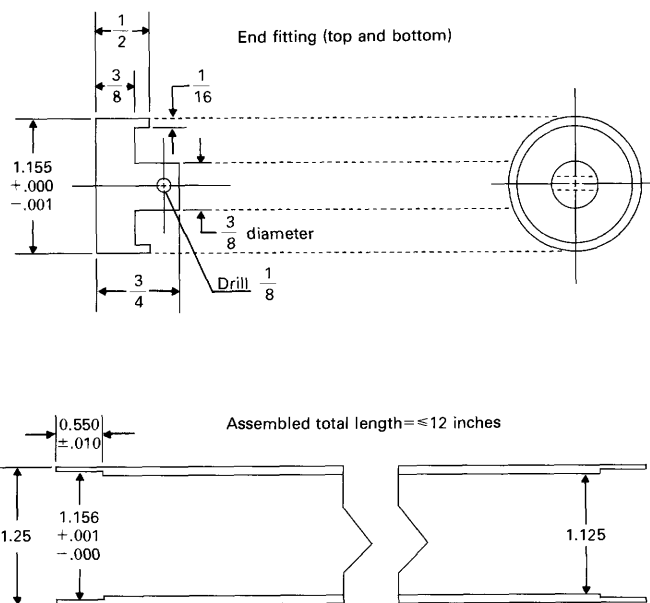


FIGURE 8.—Typical reactor tube for central thimble. Tube is constructed from 6061T6 aluminum. All dimensions are in inches.

measurements (table 2) and no doubt contributed some error to the age calibration of this monitor. However, as all the impurities are the same age as the biotite, BS-1 had a relatively uniform $^{40}\text{Ar}_{\text{rad}}/^{40}\text{K}$ ratio and proved to be a useful $^{40}\text{Ar}/^{39}\text{Ar}$ monitor.

SB-2 was prepared by resizing and recleaning BS-1. Grains smaller than 177 micrometers were removed by sieving, and the remaining impurities were removed with heavy liquid and magnetic separation techniques. SB-2 contains less than 0.3 percent impurities, and the improvement in the homogeneity of this monitor is apparent from the small dispersion of the K_2O measurements (table 2). The potassium measurements were done by both flame photometry and by isotope dilution, and the values obtained by both methods agree to within 0.004 percent K_2O . The isotope dilution value, however, was used in the monitor age calculations. The radiogenic ^{40}Ar value was measured using three independently calibrated ^{38}Ar tracer systems. SB-2 is currently in routine use in the Menlo Park laboratories.

The St. Severin monitor consisted of about 400 g of the 250- to 149-micrometer silicate fraction from the St. Severin chondrite from which Lewis (1975) separated 0.242 g of whitlockite. The material was not initially prepared as a monitor and was polyminerale. It eventually became evident that the K and therefore $^{40}\text{Ar}_{\text{rad}}$ were concentrated in a minor phase. Since the St. Severin monitor violated criterion 2 above, Alexander and Davis (1974) were forced to calibrate the monitor via an indirect comparison with other monitors. In stepwise heating analyses it was shown that the sites in the monitor that degassed below 800°C had lost $^{40}\text{Ar}_{\text{rad}}$ and so only those sites which degas at more than 800°C were calibrated. Finally, since the monitor was prepared from a meteorite that had been exposed to cosmic rays, a significant portion of the ^{36}Ar in the monitor is of nonatmospheric, cosmogenic origin. These problems notwithstanding, Alexander and Kahl (1974) demonstrated that the St. Severin monitor contains an extremely reproducible $^{40}\text{Ar}_{\text{rad}}/^{40}\text{K}$ ratio and its age and K/Ca ratio are appropriate for the dating of most meteoritic samples. Therefore, the monitor

meets criteria 1 and 3-5 listed above. Alexander and others (1981) recalculated the age of the St. Severin monitor to be $4.425 \pm 0.018 \times 10^9$ yr, using the new constants recommended in Steiger and Jäger (1977).

The hornblende monitor MMhb-1 was separated from syenite from the Cambrian McClure Mountain Complex in Fremont County, Colorado. Alexander and others (1978) described the preparation of this monitor. Analytical data for the K and $^{40}\text{Ar}_{\text{rad}}$ contents of MMhb-1 are listed in table 2, and the initial results of interlaboratory comparisons are given in Alexander and others (1978). The monitor is a 250- to 177-micrometer-sized hornblende separated with an age of about 520×10^6 yr.

Since 1970, several standards and monitors used by other laboratories have been run using our monitors and the GSTR. The results of 20 measurements on four of these standards are summarized in table 3. The pooled $^{40}\text{Ar}/^{39}\text{Ar}$ age of six measurements on SB-2 differ by only 0.1 percent from the reference age determined by conventional techniques.

The agreement on P-207 is not nearly as good. The pooled $^{40}\text{Ar}/^{39}\text{Ar}$ age of 80.8 ± 0.5 m.y. for eight measurements on P-207 is 2.2 percent younger than the mean age of 82.6 ± 1.0 m.y. based on 146 measurements made in 33 laboratories (Lanphere and Dalrymple, 1976). The $^{40}\text{Ar}/^{39}\text{Ar}$ age of P-207 is 2.8 percent younger than the mean of 15 conventional measurements made in the U.S.G.S. Menlo Park laboratory. The reason for this discrepancy is not known. However, SM-1, a finer size fraction of muscovite from the same rock as P-207, yielded $^{40}\text{Ar}/^{39}\text{Ar}$ ages in excellent agreement with the results from P-207.

FLUX CHARACTERISTICS OF THE GSTR

Although the TRIGA is not a large reactor, its flux characteristics are quite suitable for $^{40}\text{Ar}/^{39}\text{Ar}$ dating. The neutron energy distribution in the central thimble of the GSTR is given in table 4. The fast/thermal ratio on the centerline of the central thimble is 1.17 for fast

TABLE 2.—Analytical data for monitor minerals

[Values given are for mean and standard error of the mean. FP = flame photometry and ID = isotope dilution. The K_2O ID measurements were supplied by the National Bureau of Standards (E. L. Garner, L. A. Machlan, and W. P. Shields, written commun., 1973). The isotope dilution values and constants from table 1 were used in the age calculations.]

Monitor	K_2O (weight percent)	$^{40}\text{Ar}_{\text{rad}}$ (mol/g)	Calculated age (10^6 years)
BS-1Biotite	8.841 \pm 0.027 (FP, 13) 8.907 (ID, 2)	(2.183 \pm 0.006) $\times 10^{-9}$ (14)	162.7
SB-2Biotite	9.188 \pm 0.004 (FP, 14) 9.192 (ID, 2)	(2.245 \pm 0.008) $\times 10^{-9}$ (12)	162.1
MMhb-1Hornblende	1.874 \pm 0.001 (FP, 12)	(1.624 \pm 0.005) $\times 10^{-9}$ (4)	519.4

TABLE 3.—Results for mineral standards irradiated in GSTR

[Mineral standards analyzed are P-207 muscovite (interlaboratory standard), NL-25 hornblende (State University of New York at Stony Brook monitor), and SB-2 biotite and SM-1 muscovite (intralaboratory standards, U.S. Geological Survey, Menlo Park). The pooled ages were calculated by weighting each age according to the inverse of its estimated variance. The sources for reference ages were P-207 (Lanphere and Dalrymple, 1976); NL-25 (Ar data, Hanson and others, 1971; K₂O data, E. L. Garner, L. A. Machlan, and W. P. Shields, written commun., 1973); SB-2 and SM-1 (G. B. Dalrymple and M. A. Lanphere, unpub. data)]

Date of irradiation	Mineral standard	Monitor used	Irradiation time (MWH)	Calculated age (10 ⁶ yr)	Pooled age (10 ⁶ yr)	Reference age (10 ⁶ yr)
8-73	P-207	SB-2	10	81.6 ± 1.4		
11-73	P-207	SB-2	5	81.2 ± 1.9		
11-73	P-207	SB-2	5	80.6 ± 1.7		
11-73	P-207	SB-2	5	80.4 ± 1.5		
3-75	P-207	SB-2	40	79.4 ± 1.0		
4-75	P-207	SB-2	20	82.7 ± 1.1		
6-75	P-207	SB-2	10	80.1 ± 1.1		
6-75	P-207	SB-2	5	80.8 ± 1.0	80.8 ± 0.5	82.6 ± 1.0
6-72	NL-25	BS-1	40	2389. ± 26.		
6-72	NL-25	BS-1	40	2631. ± 21.		
11-72	NL-25	BS-1	40	2598. ± 21.		
11-72	NL-25	BS-1	40	2621. ± 21.	2576 ± 11	2674
3-73	SB-2	BS-1	80	163.0 ± 1.9		
3-73	SB-2	BS-1	80	161.9 ± 2.2		
3-73	SB-2	BS-1	80	163.1 ± 2.0		
5-73	SB-2	BS-1	30	161.8 ± 1.9		
5-73	SB-2	BS-1	30	162.0 ± 1.8		
5-73	SB-2	BS-1	30	161.9 ± 1.8	162.3 ± 0.8	162.1 ± 2.1
3-75	SM-1	SB-2	25	80.1 ± 1.0		
3-75	SM-1	SB-2	25	80.4 ± 1.0	80.2 ± 0.7	

neutron energies greater than 0.6 MeV, and the cadmium ratio is 9.24; the fluence over the entire energy spectrum is about 3.2×10^{13} n/cm²-s at 1 MW or 1.1×10^{17} n/cm²-MWH. Turner (1971a) used the relation between J and the integrated fast neutron flux (ϕ) as a basis for comparing various irradiation facilities for ⁴⁰Ar/³⁹Ar dating. For the GSTR, $J=0.4 \times 10^{-20} \phi$ where ϕ is for neutron energies greater than 0.6 MeV. The value given by Turner (1971a) for the core of the Herald reactor, Atomic Weapons Research Establishment, Aldermaston, U. K., is $J = 0.6 \times 10^{-20} \phi$ for neutron energies greater than 0.18 MeV; the comparable figure for the pool outside of the core of the GETR (General Electric Vallecitos Reactor), Pleasanton, Calif., is $J = 1 \times 10^{-20} \phi$.

For many reactors, the calculation of Turner's (1971a) relation using the available published data is ambiguous or impossible, because different authors de-

fine "fast" neutrons with different energy cutoffs or do not define them at all. We have therefore adopted another relation to compare the flux of neutrons capable of producing ³⁹Ar from ³⁹K in any given reactor. The relation is simply the irradiation parameter J (as defined in equation (4)) divided by the length of the irradiation in hours. The resulting quantity, J/hr, is a measure of the rate at which ³⁹K is converted into ³⁹Ar during any irradiation.

Table 5 lists J/hr and the thermal and "fast" fluxes of ten reactors that have been used for ⁴⁰Ar/³⁹Ar dating. The rate at which ³⁹K is converted to ³⁹Ar varies by two orders of magnitude between the reactors, with the GSTR in Denver being sixth on the list. The High Flux Beam Reactor at Brookhaven has the highest usable flux, and the HIFAR reactor in Australia has the lowest flux. All the fluxes are clearly adequate, and the only penalty for using a low flux reactor is the longer irradiation time required to reach any needed J value.

As the threshold for the ³⁹K(n,p)³⁹Ar reaction is 0.22 MeV (Everling and others, 1961), the exposure of the samples to energies of less than that value simply introduces unnecessary, unwanted, and potentially dangerous radioactivity into the samples and increases the probability that radiation damage will affect any results. The groups at Bern and Heidelberg routinely shield their samples from the thermal neutron fluence during the irradiation by wrapping the sample containers in cadmium foil (Stettler and others, 1974; Kirsten and others, 1972). We have not tried cadmium shielding because one of us (G.P.K.) thought it inadvisable to place a large neutron absorber into the core of the GSTR.

TABLE 4.—Neutron energy distribution on the centerline of the central thimble of the GSTR

[Data from W. M. Quam and T. M. Devore, U.S. Geological Survey TRIGA Mapping and Counter Calibration, unpublished report for the U.S. Geological Survey, May 19, 1969]

Energy (MeV)	Foil	Fluence (n/cm ² -s)
Thermal (< 0.4)	Au	1.46×10^{13}
> .6	Rh	1.54×10^{13}
> .6	Np	1.88×10^{13}
> 1.5	U	1.14×10^{13}
> 1.5	Th	1.12×10^{13}
> 3.0	S	2.98×10^{12}
> 3.0	Ni	2.98×10^{12}
> 7.5	Al	1.57×10^{11}
> 14.	Zr	5.15×10^8

The fast neutron flux in the GSTR is such that sufficient ^{39}Ar is produced in most samples in 10-40 hours of irradiation at 1 MW (fig. 9). Using data from 24 analyses of biotite monitor BS-1, the average ^{39}Ar production rate for 1 MWH on the centerline of the central thimble is

$$^{39}\text{Ar} = (7.1 \pm 0.4) \times 10^{-13} \text{ mole/gram-}\% \text{K}_2\text{O} \quad (8)$$

This is equivalent to a cross section for the reaction $^{39}\text{K}(n,p)^{39}\text{Ar}$ of about 34 ± 2 millibarns for all neutrons or 65 ± 4 millibarns for epithermal (>0.6 MeV) neutrons. For $^{40}\text{Ar}/^{39}\text{Ar}$ dating, it is desirable to choose the irradiation time so that the $^{40}\text{Ar}_{\text{rad}}/^{39}\text{Ar}_{\text{K}}$ ratio is between 300 and 1, and preferably less than 10 (Turner, 1971b). Figure 10 shows $^{40}\text{Ar}_{\text{rad}}/^{39}\text{Ar}_{\text{K}}$ as a function of age and irradiation time in the GSTR.

Users of the GSTR should be aware that values taken from figures 9 and 10 are approximate as the true power level in the reactor fluctuates as much as 20 percent (but usually only 5-10 percent) within the fueling cycle. Typically, the addition of new fuel rods, done annually near the first of the year, causes a depression in the true (versus indicated) power level. This is probably a result of both the increase in core size and the geometric relation between the new fuel and the linear ionization chamber that is used to monitor the power level. This ionization chamber sits outside of the graphite reflector surrounding the core (fig. 1) and thus does not measure the core power level directly. The power level is calibrated twice each year, after fueling in January and again in June. Between calibra-

tions, the true thermal power level gradually increases relative to the indicated power level, thus the typical power level fluctuation over the year probably looks like figure 11.

VERTICAL GRADIENTS

A significant problem in irradiations for $^{40}\text{Ar}/^{39}\text{Ar}$ dating is the inhomogeneity of the neutron flux. The primary concern is that vertical or horizontal flux gradients will result in significant differences in fluence between the monitor minerals and the unknown samples. In some reactors, the gradients are severe. For example, McDougall (1974) reported a change in the fast neutron flux in Facility X33 of the HIFAR reactor of more than 30 percent over a vertical distance of less than 3.5 cm (>8 percent/cm). In contrast, the vertical fast neutron flux gradient in the core of the Karlsruhe FR-2 reactor (Stettler and others, 1974) is less than 2 percent over 4.5 cm (<0.5 percent/cm).

The vertical flux gradients in the GSTR, while not extreme, are still large enough so that the resulting effects must be either corrected for or eliminated. There have been two experiments specifically designed to measure the vertical fluence gradient in the central thimble of the GSTR in detail. The first, using sulfur pills, was done by E. G. & G., Inc., shortly after the reactor achieved criticality. The results (fig. 12) indicated that the fast neutron flux was relatively symmetrical about the centerline. We did another experiment on November 16, 1976, using nickel washers placed at 2.5-cm intervals within the central thimble and irradiated for 1 hour at 1 MW. After irradiation, the

TABLE 5.—Comparison of nuclear reactors used for $^{40}\text{Ar}/^{39}\text{Ar}$ irradiations

[J is defined in equation 4; it is a measure of the fraction of ^{39}K converted to ^{39}Ar . The energy definition of "fast" neutrons varies from author to author if it is defined at all. Consult the original references for details]

Reactor and location (irradiation position)	J/hr	Thermal flux (n/cm ² -s)	Fast flux (n/cm ² -s)	References
GSTR-Denver, U.S. (Centerline, core position)	2.5×10^{-4}	1.5×10^{13}	1.7×10^{13}	This work.
Herald-Aldermaston, U.K. (Core)	7.2×10^{-4}	---	3.7×10^{13}	Turner (1970a, b; 1971a).
GEIR-Pleasanton, U.S. (Shuttle tube in pool)	4.1×10^{-4}	1.3×10^{14}	1.7×10^{13}	This work; Turner and others (1972); Podosek and others (1973); Huneke, Podosek, and Wasserburg (1972).
HIFAR-Lucas Heights, Australia (Core-X33, face 6, 4H-3)	3.3×10^{-5}	5×10^{13}	3.5×10^{12}	McDougall and Roksandic (1974); McDougall (1974).
HFBR-Brookhaven, U.S. (Core)	4.1×10^{-3}	1.3×10^{14}	2×10^{14}	Bogard, Husain, and Wright (1976).
FR-2 Karlsruhe, Germany (Core-Isotope Channel Facility)	6.1×10^{-5}	(1)	3.4×10^{12}	Stettler and others (1974); Kirsten and others (1972).
BR-2 - Mol, Belgium (Core)	7.5×10^{-4}	(1)	3.7×10^{13}	Kirsten and others (1972); Kirsten, Horn, and Heymann (1973); Kirsten and Horn (1977).
RRF-Columbia, Mo., U.S. (Flux trap)	2.9×10^{-3}	5.8×10^{14}	1×10^{13}	Bernatowicz and others (1978).
(Pool)	6.2×10^{-5}	4.0×10^{13}	3×10^{12}	Podosek (private communication, 1978).
JMTR-Oarai, Japan	1.3×10^{-4}	1×10^{13}	1×10^{12}	Ozima and others (1976).
McMaster University- Hamilton, Canada	1.1×10^{-4}	$\sim 1.5 \times 10^{13}$	$\sim 8 \times 10^{11}$	Berger and York (1970).

¹Samples were irradiated inside a cadmium-shielded container to eliminate the thermal fluence.

washers were counted in the NaI gamma-counting system at the GSTR in Denver, using the 0.8 MeV gamma from the decay of ^{58}Co . We placed each washer in the same position relative to the counting crystal; the more active washers near the centerline were counted for 4 minutes, and the less active washers were counted for up to 20 minutes. The results (fig. 12) show that the flux for fast neutrons is relatively symmetrical but that the point of maximum flux is displaced downward from the physical centerline about 4 cm. We are unsure why our results do not agree with the earlier results of E. G. & G., Inc., Both sulfur and nickel respond only to neutron energies above 3.0 MeV, and both experiments resulted in nearly identical flux curves. We suspect that the sulfur pills used in the earlier experiment may not have been as precisely located with respect to the physical centerline as the nickel washers.

The data in figure 12 show that the gradient over the central 20 cm, the part of the central thimble normally used in $^{40}\text{Ar}/^{39}\text{Ar}$ dating, ranges from a small fraction of a percent to as much as 3.5 percent per centimeter. We have used two methods to minimize the effects of this gradient.

The first method is to carefully control the vertical position of the unknown samples relative to the monitors. The use of flat-bottomed quartz vials (fig. 4) and an aluminum sample holder (fig. 6) ensures that the bottom of each sample on a level is coincident with its corresponding monitors to within a fraction of a millimeter. In addition, the amounts of the samples and the monitors on each level are carefully adjusted so that all are the same height in the quartz vials. This ensures that all the samples on a level intercept the same fast neutron flux as the monitors.

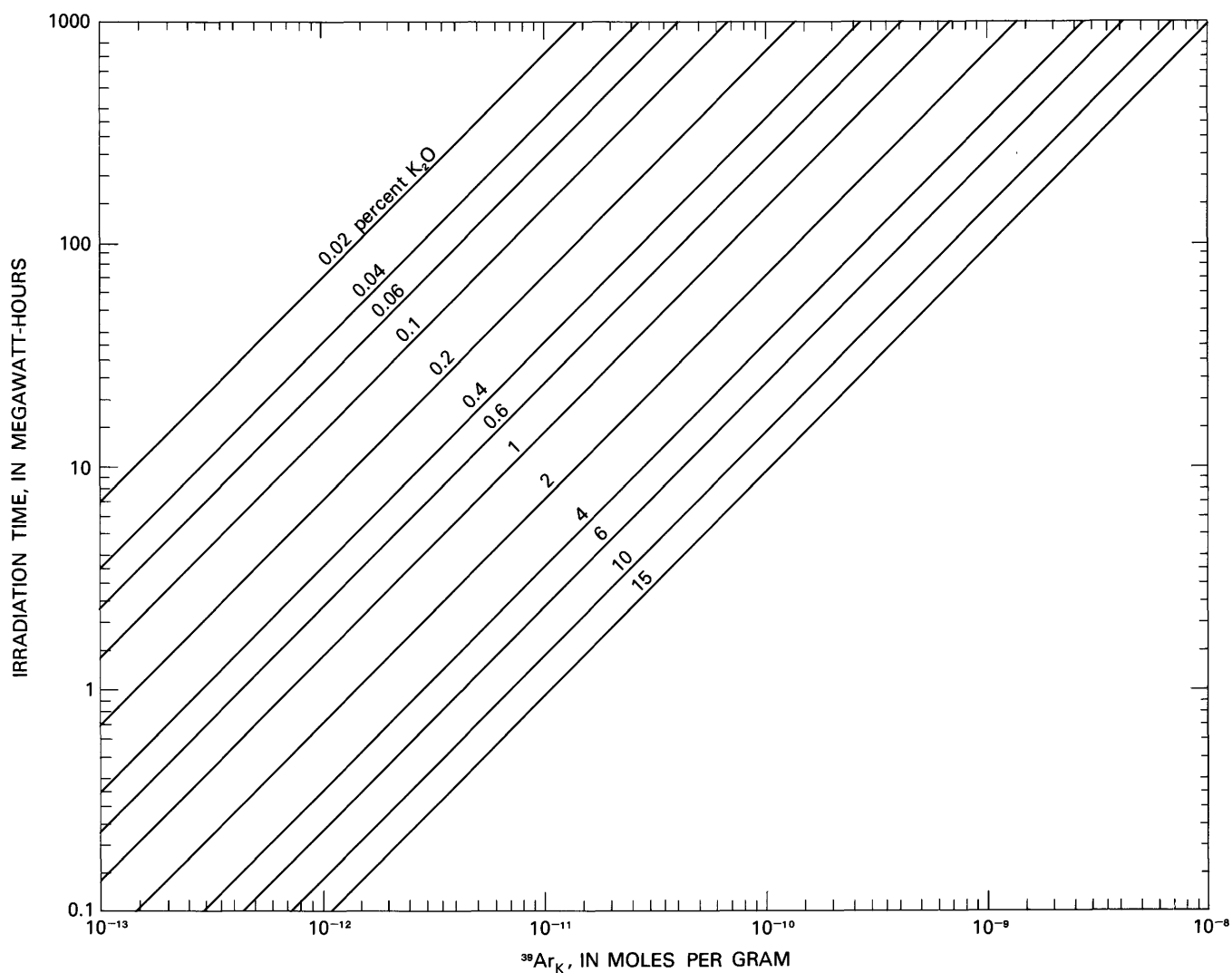


FIGURE 9.—Approximate $^{39}\text{Ar}_K$ productivity at centerline of central thimble as a function of K_2O content and irradiation time (in MWH). Curves are based on equation (8) and were calculated using data obtained on BS-1 biotite. Each curve shows weight percent K_2O .

The second method is to monitor the fluence received by each sample and each monitor with a nickel wire. The wire is cut to the same length as the sample

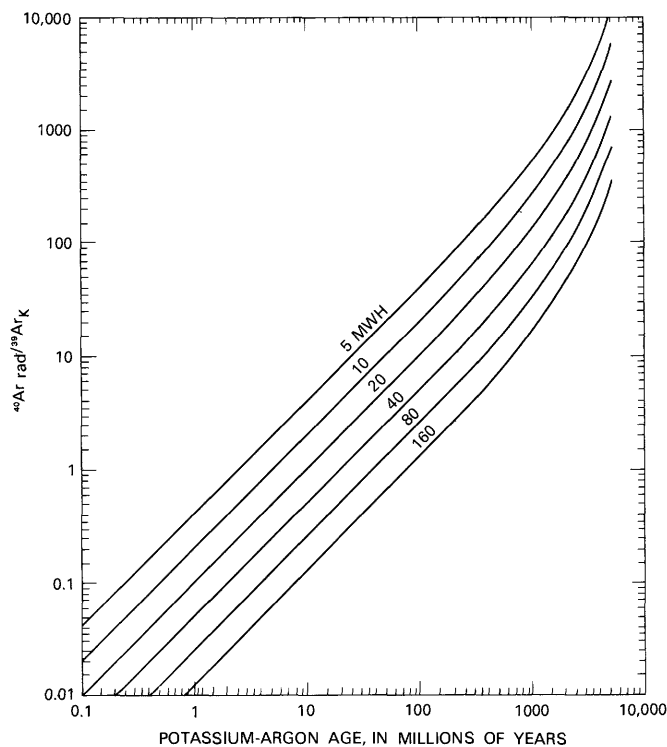


FIGURE 10.— $^{40}\text{Ar}_{\text{rad}}/^{39}\text{Ar}_K$ ratio as a function of K-Ar age and irradiation time (in MWh) in central thimble of GSTR. Ratio is independent of K_2O content of sample.

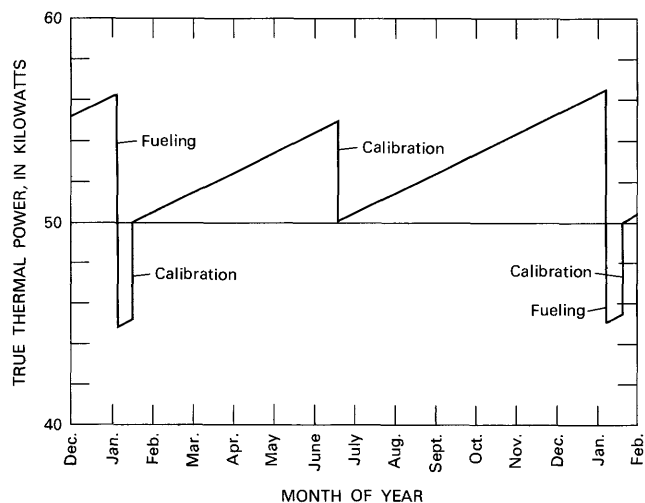


FIGURE 11.—Schematic diagram of change in true thermal-power level for 50 kW indicated power level as a function of fueling and calibration. Fueling causes an instantaneous depression in true power level, whereas fuel consumption causes a gradual power increase over time. True and indicated power levels are made equal at time of calibration.

height, and the two are wrapped together in aluminum foil and placed in the quartz vial. Subsequent counting of the wires provides data to correct the monitor constant, J , to a value appropriate for each sample. This technique is especially useful when it is not possible to keep the vertical heights of all samples on a level identical. Data obtained in a single irradiation from both nickel wires and the St. Severin monitor (fig. 13) show that the use of nickel wires provides an accurate and effective method of monitoring the relative fast neutron fluence in the GSTR.

HORIZONTAL GRADIENTS

Horizontal flux gradients in the central thimble of

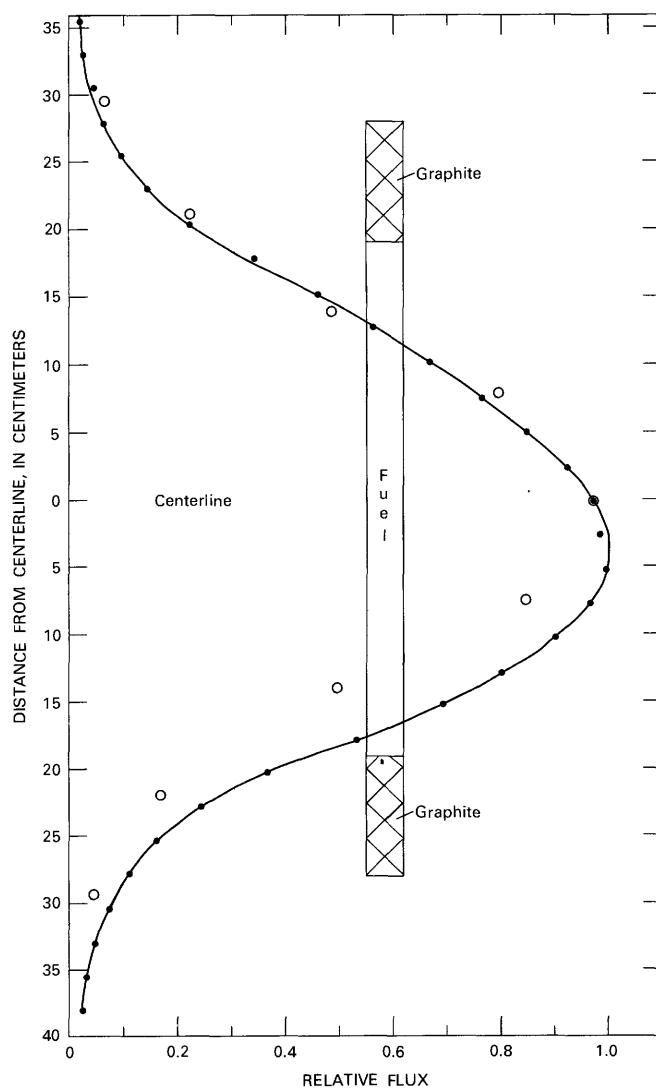


FIGURE 12.—Vertical flux gradient in central thimble of GSTR. Solid dots are data obtained using nickel washers, open circles with sulfur pills. Sulfur data are from W. M. Quam and T. M. Devore. (unpub. data, 1969). Point of maximum flux is approximately 4 cm below physical center of fuel rods.

the GSTR are, for most purposes, negligible. They are so small (<0.5 percent) that they are barely detectable statistically and are not measurable with the techniques available to us.

Five different experiments were designed to determine the extent and effect of these gradients. The first three experiments were designed to test for flux gradients between the outside and the center of the central thimble facility.

Experiment 1. — On 47 levels in 19 irradiations done between December 1971 and October 1976, either BS-1 (16 levels) or SB-2 (31 levels) biotite monitors were arranged in pairs so that one monitor was exactly in the center of the level and the other was in the outer ring. The arrangement of samples on each level was as in figure 7C, and the horizontal separation between the centers of the vials was 0.95 cm. The measured $^{40}\text{Ar}_{\text{rad}}/^{39}\text{Ar}_{\text{K}}$ ratios for each biotite pair was normalized to eliminate difference in the fluence between levels and between irradiations by dividing the value of the center monitor by that of the outside monitor. The 47 normalized values have a mean of 1.0042 and a standard error of the mean of 0.0016. A t-test indicates that the null hypothesis — this mean is equal to 1.0 — must be rejected at the 5 percent level of significance. This fact suggests that the fast neutron flux is slightly less in the center of the central thimble than on the outside.

Experiment 2. — One aliquant of BS-1 was placed in the center of a level and five in the outer ring (fig. 7C). These data were normalized in a similar way as the data

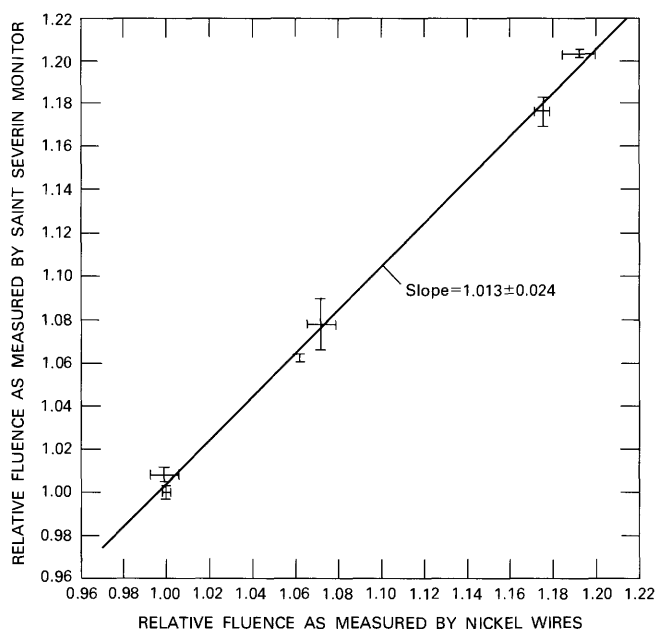


FIGURE 13.—Comparison of relative fluence in GSTR, as measured with nickel wires and with St. Severin monitor. Error bars are one standard deviation.

in experiment 1. The resulting mean is 1.0039 with a standard error of the mean of 0.0020. For these data, the null hypothesis that this mean is equal to 1.0 (two-tails test) cannot be rejected at the 5 percent level of significance, but the null hypothesis that the mean is equal to 1.0 against the alternative that it is greater than 1.0 (single-tails test) must be rejected. Though the results of this experiment are not so conclusive as those of experiment 1, they do suggest that there is a slight horizontal gradient in the central thimble with a lower flux in the center.

Experiment 3. — On six levels in two irradiations, nickel wires were so arranged that three were toward the center of the level and six to eight were in an outer ring (fig. 7A, B). The horizontal separation between the inner and outer wires on a given level ranged from 0.06-0.58 cm. The normalized data have a mean of 1.0006 and a standard error of the mean of 0.0011. In this experiment, no horizontal flux gradient was detected, but this may be because the horizontal separation was only about two-thirds or less of that in experiments 1 and 2.

Experiments 4 and 5 were designed to detect differences between dispersion within vials and within layers of vials. Such differences would be expected if horizontal fluence gradients were a significant factor in limiting the precision obtainable with the GSTR.

Experiment 4. — On nine levels in three irradiations, nickel wires were included with the samples in 85 quartz vials. Twenty-five of these sample vials contained two wires. After irradiation, the activity of each wire was measured. The pooled estimate of the standard deviation (Crow and others, 1960), s_p , of the 25 pairs of wires from the same vial is 0.619 percent. The statistic s_p for the groups of wires from the same layer was 0.672 percent. An F-test indicates that the null hypothesis—the dispersion of the two populations is equal—cannot be rejected at the 5 percent level of significance, that is, no difference was detected.

Experiment 5. — Thirteen samples of the St. Severin monitor were irradiated on seven levels in two irradiations. After irradiation, each sample was split into two aliquants, and each aliquant was analyzed separately. For the 13 pairs from the same vial, s_p is 0.527 percent; for the 5 levels that contained more than 1 vial of St. Severin, s_p is 0.598 percent. As in experiment 4, no significant difference in the dispersion of the two types of samples was detected.

Alexander and Kahl (1974), using the St. Severin monitor, performed an experiment similar to our experiment 4. Five pairs of the St. Severin monitor that were split after irradiation in the Vallecitos reactor have a pooled estimate of the standard deviation of precision of 0.077 percent; this reproducibility indi-

cates that the $^{40}\text{Ar}_{\text{rad}}/^{39}\text{Ar}_{\text{K}}$ ratio in St. Severin is very homogeneous. Because the reproducibility of the St. Severin analyses done in the GSTR does not approach that for the Vallecitos reactor, we suspect that the vertical fluence gradients in the GSTR are introducing inhomogeneities into the monitors and the nickel wires, and these effects are masking the effects of any horizontal gradients. It is quite likely that these inhomogeneities cannot be eliminated by mixing and splitting because the samples are small and are subject to significant sampling errors (Engels and Ingamells, 1970).

The results from experiments 1 and 2 indicate that there may be a small horizontal flux gradient in the GSTR, with the flux in the center of the central thimble slightly less (0.5 percent maximum) than toward the side. The results from experiment 5, however, suggest that the vertical gradient and not the horizontal gradient is the primary factor limiting the precision in the GSTR. The data indicate that the precision of $^{40}\text{Ar}/^{39}\text{Ar}$ dating using the GSTR may be limited to a standard deviation of about 0.5-0.6 percent.

SELF-SHIELDING

Mitchell (1968) was the first to raise the possibility that neutron absorption within a sample might result in a significant error. He looked for this effect in the Herald reactor by irradiating a sphere of muscovite, then analyzing several parts of the sphere. The analyses of mica from the inside and outside of the sphere agreed to within 2 percent, from which Mitchell concluded that the effect was negligible.

We have looked for self-shielding in the central thimble of the GSTR. A cylinder of Jurassic diabase (sample No. 8L691; L21 of Dalrymple and others, 1975) 2.40 cm in diameter and 2.54 cm high was irradiated for 5 MWH, receiving a neutron fluence of about 5×10^{17} n/cm². The axis of the cylinder was parallel to the axis of the central thimble. After irradiation, a 6-mm-diameter core was taken with a diamond core drill across the axis of the larger core (fig. 14). This smaller core was sliced with a diamond saw into six cylinders, each of which was analysed. The $^{40}\text{Ar}_{\text{rad}}/^{39}\text{Ar}_{\text{K}}$ ratios show a progressive increase of about 3 percent from the outside inward (fig. 15). The effect appears to be larger than can be accounted for by horizontal fluence gradients, and we conclude that self-shielding has been detected. For most purposes, however, the effect will be very small over the width of a typical sample, and negligible from sample to sample. The effect will be even less in samples that consist of mineral grains or powders.

ACTIVITY PREDICTIONS

Rocks and minerals used in $^{40}\text{Ar}/^{39}\text{Ar}$ dating contain a variety of elements that generate radioactive pro-

ducts when bombarded with fast neutrons. For reasons of radiological safety, it is necessary to predict what the activity of each sample will be after irradiation. These predictions are also required by the conditions of the U. S. Nuclear Regulatory Commission licenses that govern both reactor operation and the use of activated samples by the $^{40}\text{Ar}/^{39}\text{Ar}$ investigator.

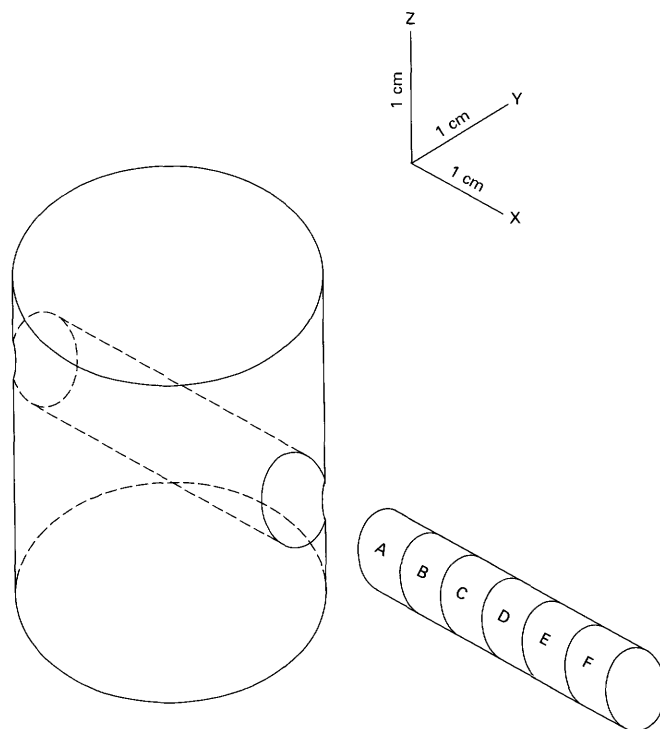


FIGURE 14.—Isometric drawing of sample locations in self-shielding experiment on diabase 8L691. Results for analyzed samples (A-F) are shown in figure 15.

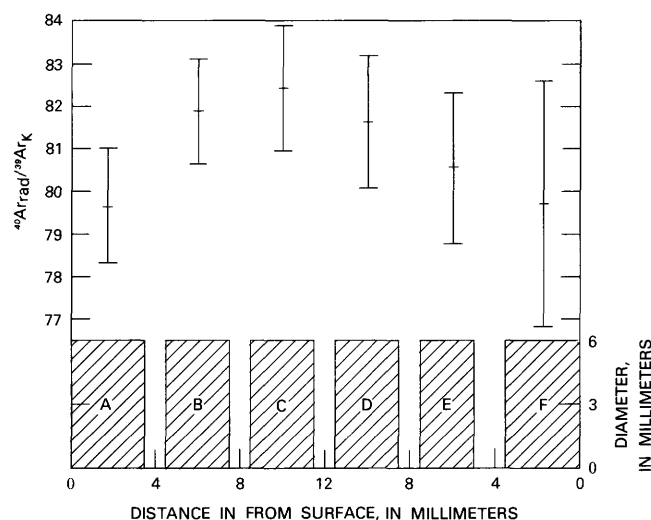


FIGURE 15.—Results of self-shielding experiment on diabase 8L691. Error bars are one standard deviation. Analyzed samples (A-F) (see fig. 14) are shown at bottom of diagram.

The basis for these activity predictions is as follows. The rate of formation R_f of an activation product when a quantity of a target element is bombarded by fast neutrons is

$$R_f = \frac{\phi m L f \sigma}{m_a} = \phi n \sigma \quad (9)$$

where ϕ is the neutron flux ($n/cm^2 \cdot s$), m is the mass of the element (grams), L is Avogadro's number (6.0225×10^{23} atoms/mole), f is the fractional abundance of the target isotope, σ is the nuclear reaction cross section ($cm^2/atom$), m_a is the atomic mass of the element (g/mole), and n is the number of target atoms. The disintegration rate of the radioactive product nuclide is

$$R_d = \lambda N \quad (10)$$

where λ is the decay constant (s^{-1}) and N is the number of radioactive parent atoms. The rate of change of a radioactive product nuclide is, therefore,

$$\frac{dN}{dt} = R_f - R_d = \phi n \sigma - \lambda N. \quad (11)$$

After an irradiation time t , the activity A of the product nuclide is

$$A_t = \phi n \sigma (1 - e^{-\lambda t}) \quad (12)$$

where A_t is in disintegrations per second. If the sample sits for a time t' after irradiation, then

$$A_{t'} = \phi n \sigma (1 - e^{-\lambda t}) e^{-\lambda t'}. \quad (13)$$

It is customary to express activity in curies, where 1 curie is 3.7×10^{10} disintegrations per second, so equation (13) becomes

$$A_{t'} = \frac{\phi n \sigma (1 - e^{-\lambda t}) e^{-\lambda t'}}{3.7 \times 10^{10}}. \quad (14)$$

In evaluating the radiological hazards from the irradiation of rock and mineral samples, we investigated more than 100 possible nuclear reactions involving 36 isotopes of 13 elements. Only 26 of these reactions result in products of significant activity (table 6). The reactions involving Cu and Cr were included primarily because these elements are found in the aluminum

TABLE 6.—Data for activity calculations, TRIGA reactor

[Half-life given in y=years, h=hours, and m=minutes. Atomic mass and percent abundance and half-life after Weast (1976). Product is stable except as noted. Q is based on data from Everling and others (1961). Fast-neutron cross sections based on data from activation analysis of Koch (1960)]

Target element	Atomic mass	Target isotope	Percent abundance	Reaction	Product	Q (MeV)	Cross section (barns)	Product half-life	Flux ($10^{13} n/cm^2 \cdot s$) at 1,000 kW
Na	22.99	²³ Na	100	n,γ	²⁴ Na	+6.96	0.53	15.0 h	1.7
Mg	24.31	²⁴ Mg	78.7	n,p	²⁴ Na	-4.73	.22	15.0 h	.1
Al	26.98	²⁷ Al	100	n,γ	²⁸ Al	+7.72	.21	2.31 m	1.7
				n,α	²⁴ Na	-3.14	.14	15.0 h	.3
Si	28.09	²⁸ Si	92.21	n,p	²⁸ Al	-3.86	.37	2.31 m	.2
		³⁰ Si	3.09	n,γ	³¹ Si	+6.59	.11	2.62 h	1.7
P	30.97	³¹ P	100	n,γ	³² P	+7.94	.19	14.3 d	1.7
				n,p	³¹ Si	-.69	.14	2.62 h	1.6
				n,α	²⁸ Al	-1.94	.15	2.31 m	.7
S	32.06	³² S	95.0	n,p	³² P	-.93	.30	14.3 d	1.4
		³³ S	.76	n,p	³³ P	+5.53	.015	25 d	1.7
		³⁴ S	4.22	n,γ	³⁵ S	+6.98	.26	88 d	1.7
				n,α	³¹ Si	-1.32	.14	2.62 h	1.0
K	39.10	⁴¹ K	6.88	n,γ	⁴² K	+7.53	1.1	12.4 h	1.7
Ca	40.08	⁴³ Ca	1.35	n,p	⁴³ K	-1.03	¹ 1.	22.4 h	1.3
		⁴⁴ Ca	2.08	n,γ	⁴⁵ Ca ¹	+7.42	.67	165 d	1.7
		⁴⁸ Ca	.18	n,γ	⁴⁹ Ca ²	+5.14	1.1	8.8 m	1.7
Cr	52.00	⁵⁰ Cr	4.31	n,γ	⁵¹ Cr	+9.25	13.5	27.8 d	1.7
Mn	54.94	⁵⁵ Mn	100	n,γ	⁵⁶ Mn	+7.27	13.3	2.58 h	1.7
Fe	55.85	⁵⁴ Fe	5.82	n,γ	⁵⁵ Fe	+9.30	2.5	2.6 y	1.7
				n,p	⁵⁴ Mn	+0.09	.023	303 d	1.7
				n,α	⁵¹ Cr	+8.4	.00037	27.8 d	1.7
		⁵⁶ Fe	91.66	n,p	⁵⁶ Mn	-2.93	.00044	2.58 h	.3
		⁵⁸ Fe	.33	n,γ	⁵⁹ Fe	+6.58	.98	45.1 d	1.7
Cu	63.54	⁶³ Cu	69.09	n,γ	⁶⁴ Cu	+7.92	4.3	12.9 h	1.7
Rb	85.47	⁸⁵ Rb	72.15	n,γ	⁸⁶ Rb	+8.58	.80	18.8 d	1.7
Ti	47.90	⁴⁶ Ti	7.93	n,p	⁴⁶ Sc	-1.58	.0041	83.8 d	.9
		⁴⁷ Ti	7.28	n,p	⁴⁷ Sc	+1.18	.00021	3.43 d	1.7
		⁴⁸ Ti	73.94	n,p	⁴⁸ Sc	-3.21	.000077	1.83 d	.3
Ni	58.71	⁵⁸ Ni	68.27	n,p	⁵⁸ Co	+4.0	.032	71.3 d	1.7
		⁶⁰ Ni	26.10	n,p	⁶⁰ Co	-2.04	.005	5.26 y	.7
		⁶² Ni	3.59	n,α	⁵⁹ Fe	-.43	.0057	45.1 d	1.7
		⁶⁴ Ni	.90	n,γ	⁶⁵ Ni	+6.13	1.6	2.52 h	1.7

¹Value is an estimate.

²Decays to ⁵⁸Sc, which decays by β⁻ to ⁵⁸Ti with a half-life of 57.5d.

alloy (6061T6) used for the sample holder and reactor tube. Sulfur was included because potassium sulfate is used in determining reactor correction factors. The remaining elements are commonly found in rocks and minerals.

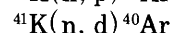
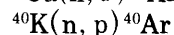
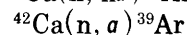
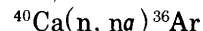
The reaction energies, Q , were used as an estimate of the threshold energy for reactions with negative Q . The appropriate neutron flux was then estimated from the data of table 4. For reactions with positive Q , the average epithermal flux (>0.6 MeV) was used. Fast-neutron cross sections based on data from activation analysis (Koch, 1960) were selected for the range of energies most appropriate for the particular reaction. Many of the cross sections are not well known or are known only for a range of energies different from those in the GSTR central thimble. Measurements of the activity of irradiated samples, however, have shown that the values in table 6 yield activity predictions that are accurate to within 20 percent.

The activity predictions are most conveniently done by computer. A BASIC computer program for predicting activities after irradiation in the GSTR is given in the section entitled "Computer Programs." If a computer is not available, activities may be estimated graphically using the curves in figure 16.

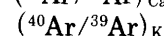
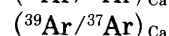
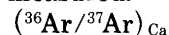
CORRECTIONS FOR INTERFERING ARGON ISOTOPES

Both Sigurgeirsson (1962) and Merrihue and Turner (1966) recognized that a principal difficulty with the

$^{40}\text{Ar}/^{39}\text{Ar}$ dating method was that the fast neutrons may react with nuclides in the sample other than ^{39}K to produce interfering isotopes of argon. These sources of interference were discussed in detail by Mitchell (1968), Brereton (1970), and Turner (1971b). Of the principal reactions (table 7), only four reactions occur with sufficient frequency to be of concern in most terrestrial samples (Turner, 1971b). These are:



Fortunately, ^{37}Ar is also produced by the (n, α) reaction with ^{40}Ca , which permits corrections to be made for both the undesirable Ca- and K-derived argon (equation 7). The corrections require that the following reactor constants be measured:



In the interval from November 1970 through June 1975, we irradiated 17 samples of optical grade CaF_2 crystals and 8 samples of reagent grade K_2SO_4 in 8 separate irradiations in the GSTR ranging from 5 to 80 MWH. After irradiation, the salts were fused in an extraction line, and the argon released was purified and analyzed by mass spectrometry. The results are given in table 8. Unirradiated samples of the CaF_2 and the K_2SO_4 have also been analyzed and, within experimental error, yielded argon of atmospheric composition. The values given in the table were calculated assuming

TABLE 7.—Principal neutron reactions leading to the production of argon isotopes
[After Brereton, (1970). The Q values, in MeV, are shown in brackets below each reaction (Everling and others, 1961)]

Target element	Argon isotopes produced				
	^{36}Ar	^{37}Ar	^{38}Ar	^{39}Ar	^{40}Ar
Calcium	$^{40}\text{Ca}(n, n\alpha)$ [−7.04]	$^{40}\text{Ca}(n, \alpha)$ [+1.75]	$^{42}\text{Ca}(n, n\alpha)$ [−6.24]	$^{42}\text{Ca}(n, \alpha)$ [+0.34] $^{43}\text{Ca}(n, n\alpha)$ [−7.59]	$^{43}\text{Ca}(n, \alpha)$ [+2.29] $^{44}\text{Ca}(n, n\alpha)$ [−8.85]
Potassium		$^{39}\text{K}(n, nd)$ [−9.73]	$^{40}\text{K}(n, d)$ [−4.14] $^{41}\text{K}(n, \alpha)^{38}\text{Cl} \beta$ [−0.10]	$^{39}\text{K}(n, p)$ [+0.22] $^{40}\text{K}(n, d)$ [−5.36]	$^{40}\text{K}(n, p)$ [+2.30] $^{41}\text{K}(n, d)$ [−5.58]
Argon		$^{36}\text{Ar}(n, \gamma)$ [+8.79]	$^{40}\text{Ar}(n, nd)^{38}\text{Cl} \beta$ [−12.11]	$^{38}\text{Ar}(n, \gamma)$ [+6.58] $^{40}\text{Ar}(n, d)^{39}\text{Cl} \beta$ [−10.30]	
Chlorine	$^{35}\text{Cl}(n, \alpha)^{36}\text{Cl} \beta$ [−8.57]		$^{37}\text{Cl}(n, \gamma)^{38}\text{Cl} \beta$ [+6.11]		

that all of the ^{40}Ar in the irradiated CaF_2 and all of the ^{36}Ar in the K_2SO_4 were atmospheric. These assumptions may not be correct, but their effects cancel out in equation (7) and do not introduce any error into a $^{40}\text{Ar}/^{39}\text{Ar}$ age.

Two of the three principal reactor constants ($(^{36}\text{Ar}/^{37}\text{Ar})_{\text{Ca}}$ and $(^{39}\text{Ar}/^{37}\text{Ar})_{\text{Ca}}$) are relatively reproducible and their values known for the GSTR to within less than 1 percent. We have been unable, however, to satisfactorily reproduce the value for $(^{40}\text{Ar}/^{39}\text{Ar})_{\text{K}}$ from one irradiation to the next (table 8). We are convinced that the variability is real and that it is not a property of the GSTR alone, for similar results have been reported for other reactors. For example, values of $(6.252 \pm 0.087) \times 10^{-2}$ and $(3.72 \pm 0.30) \times 10^{-2}$ have been found for the GETR at Vallecitos by Alexander and Davis (1974) and Davis (1977), respectively. Saito and Ozima (1977) have found that values for $(^{40}\text{Ar}/^{39}\text{Ar})_{\text{K}}$ vary by nearly a factor of ten within the JMTR. As noted by Alexander and Davis (1974), the variation in this correction factor between reactors also is much larger than the variation in the corrections for the Ca-derived isotopes. Saito and Ozima (1977) tabulated correction factors found for various reactors and noted that the values reported for $(^{40}\text{Ar}/^{39}\text{Ar})_{\text{K}}$ vary by nearly a factor of 50 whereas the values for $(^{36}\text{Ar}/^{37}\text{Ar})_{\text{Ca}}$ and $(^{39}\text{Ar}/^{37}\text{Ar})_{\text{Ca}}$ tend to be relatively uniform even from one reactor to another. Saito and Ozima (1977) and Davis (1977) suggested that $(^{40}\text{Ar}/^{39}\text{Ar})_{\text{K}}$ may be strongly dependent on the neutron energy distribution and can be expected to vary from reactor to reactor and even between locations within a single reactor. All of our measurements, however, were made in the same location in the GSTR and we cannot satisfactorily explain the wide variation in results in this way unless the neutron spectrum in the central thimble varies considerably over distances of only a few centimeters. One possibility that we have not explored is that $(^{40}\text{Ar}/^{39}\text{Ar})_{\text{K}}$ varies with the fueling cycle. What-

ever the cause, it is clear that where this correction is potentially an important source of error, it must be measured separately for each irradiation, preferably by placing the potassium salt as close as possible to the unknown sample.

The most serious interference is caused by the ^{36}Ar produced by the $(n, n\alpha)$ reaction with ^{40}Ca . This ^{36}Ar interferes with the atmospheric argon correction, which is made using ^{36}Ar as a reference isotope (equation 6). The extent of the interference is a function of integrated fast neutron flux, age, and the K/Ca ratio of the sample (figs. 17, 18). The effect becomes larger as the integrated fast neutron flux increases and as the age and K/Ca ratio of the sample decrease. Errors in this correction factor become increasingly important as the amount of $^{36}\text{Ar}_{\text{Ca}}$ increases. This interference has the same type of effect as the atmospheric argon correction, and in young, high-calcium samples these two corrections combine to seriously degrade the usefulness of the $^{40}\text{Ar}/^{39}\text{Ar}$ dating technique. Additional curves showing the effect of this correction as a function of age, irradiation time in the GSTR, and K/Ca, are given in the section entitled "Effect of $^{40}\text{Ca}(n, n\alpha)^{36}\text{Ar}$ Interference."

^{36}Ar and ^{38}Ar are produced by neutron capture followed by β^- decay from the two naturally occurring isotopes of chlorine, ^{35}Cl and ^{37}Cl . Since ^{35}Cl is three times as abundant as ^{37}Cl (table 1) and has much larger thermal and resonance integral capture cross sections, 45 and 15 barns, respectively versus 0.43 and 0.32 barns (Walker and others, 1977), neutron capture produces about 300 times more ^{36}Cl than ^{38}Cl . ^{36}Cl , however, has a half-life of 3×10^5 yr while ^{38}Cl has a half-life of 37.2 minutes (table 1). In most experimental situations, the ^{36}Cl does not decay appreciably to ^{36}Ar . Bernatowicz and others (1978) documented a case where the combination of a relatively high chlorine content of a monitor, a very high thermal fluence, and a long delay between irradiation and the analysis of the

TABLE 8.—Correction factors for Ca- and K-derived Ar isotopes for the U.S. Geological Survey TRIGA reactor

Irradiation date	MWH	Material	Number of measurements	$(^{36}\text{Ar}/^{37}\text{Ar})_{\text{Ca}}$ $\times 10^{-4}$	$(^{38}\text{Ar}/^{37}\text{Ar})_{\text{Ca}}$ $\times 10^{-5}$	$(^{39}\text{Ar}/^{37}\text{Ar})_{\text{Ca}}$ $\times 10^{-4}$	$(^{37}\text{Ar}/^{39}\text{Ar})_{\text{K}}$ $\times 10^{-3}$	$(^{36}\text{Ar}/^{39}\text{Ar})_{\text{K}}$ $\times 10^{-2}$	$(^{40}\text{Ar}/^{39}\text{Ar})_{\text{K}}$ $\times 10^{-2}$
Nov. 1970	80	CaF_2	4	2.72 ± 0.029		6.33 ± 0.043			
		K_2SO_4	3						0.594 ± 0.072
Mar. 1973	80	CaF_2	4	2.66 ± 0.054		6.57 ± 0.115			
Oct. 1973	80	K_2SO_4	3						1.01 ± 0.046
Mar. 1974	60	CaF_2	2	2.72 ± 0.018	3.174 ± 0.024	6.78 ± 0.026			
		K_2SO_4	2				2.20 ± 0.066	1.34 ± 0.024	0.1 ± 0.1
Apr. 1975	40	CaF_2	2	2.66 ± 0.014		6.76 ± 0.035			
Apr. 1975	20	CaF_2	2	2.68 ± 0.057		6.74 ± 0.007			
June 1975	10	CaF_2	2	2.54 ± 0.014		6.58 ± 0.106			
June 1975	5	CaF_2	1	2.63		6.70			
		Weighted means ¹		2.64 ± 0.017		6.73 ± 0.037			

¹Weighting is by the inverse of the variance. Errors are estimates of the standard error of the mean.

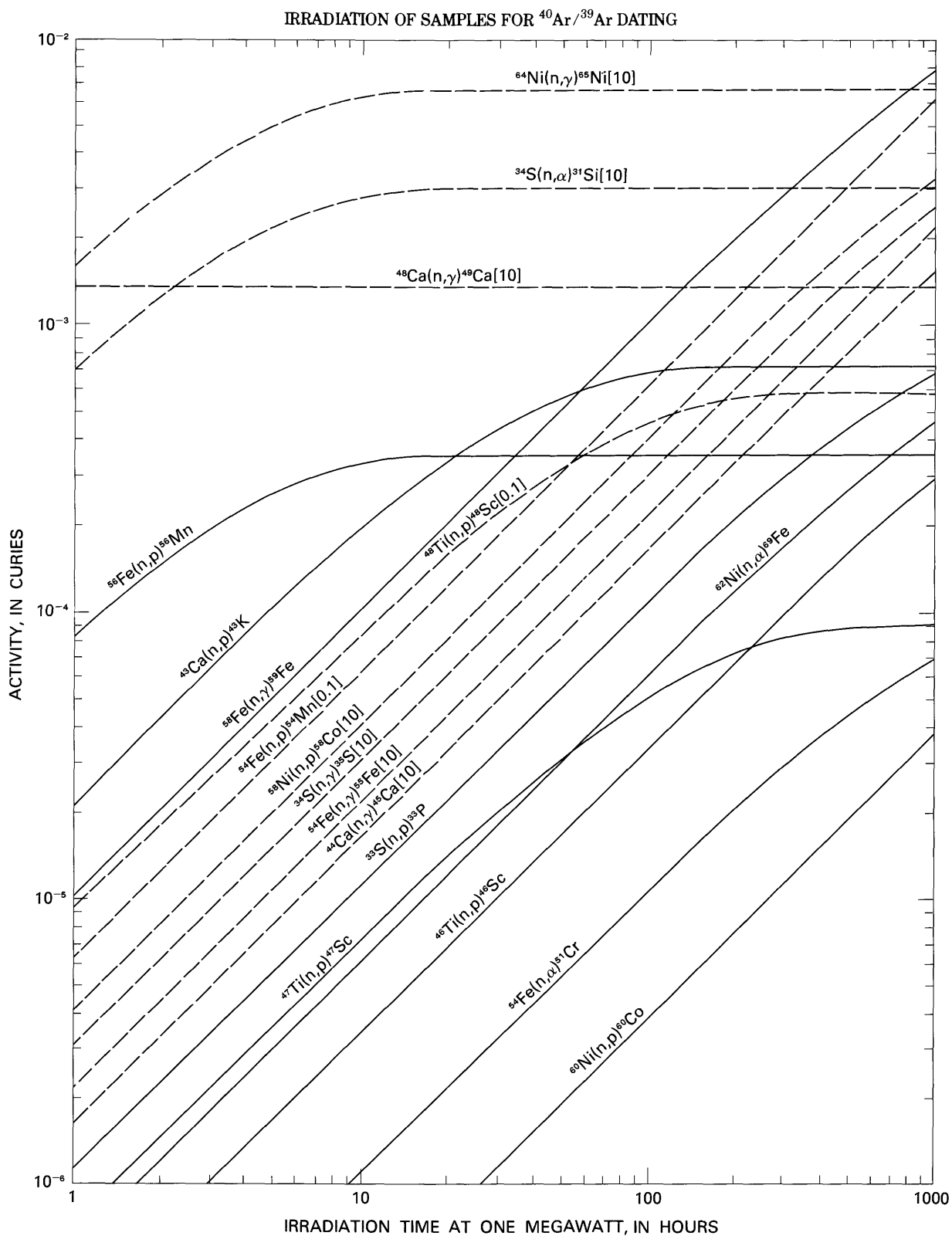
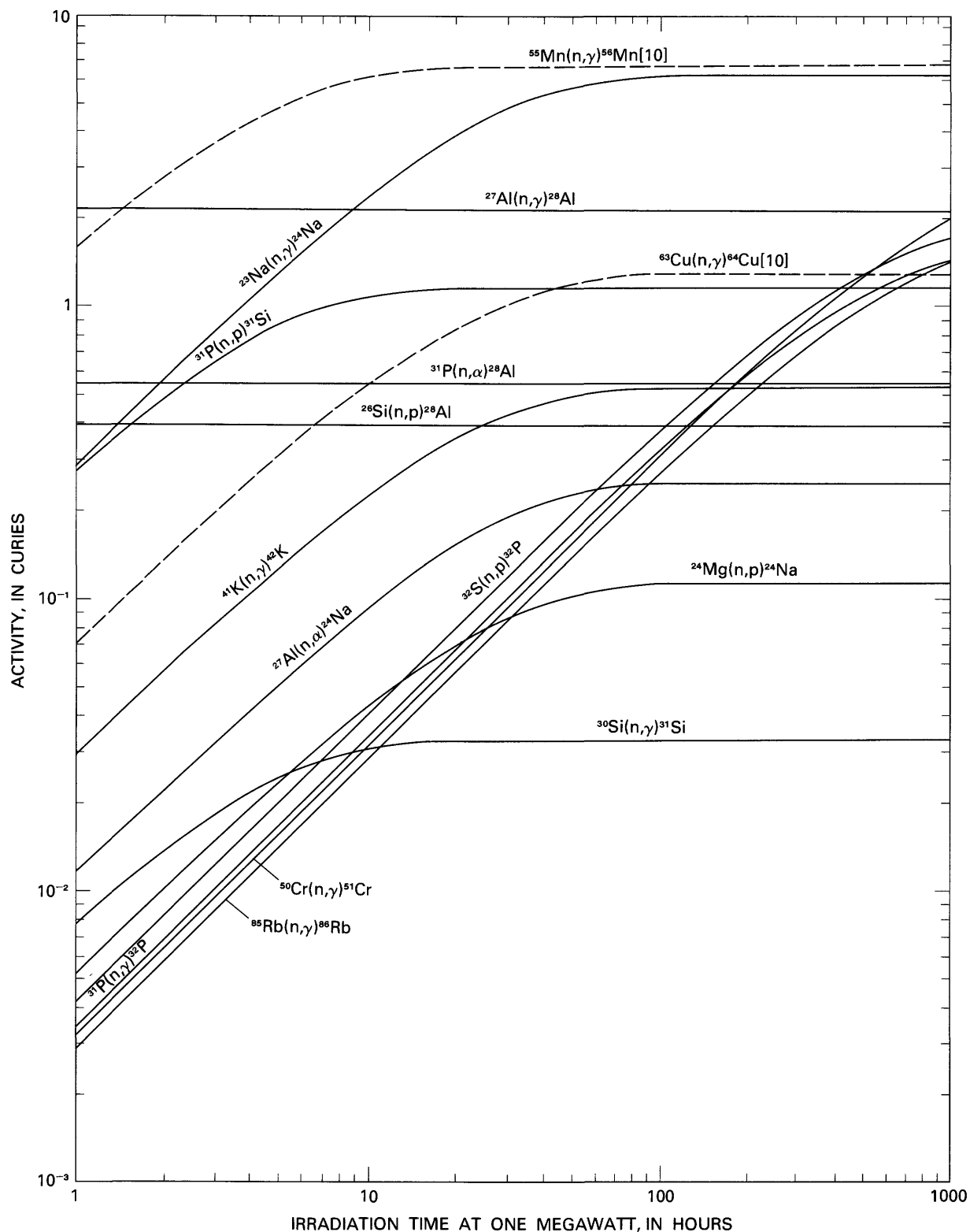


FIGURE 16.—Activity resulting from various neutron reactions in GSTR as a function of irradiation time at 1 MW. Curves are for 1 g of target from dashed curves must be



element; natural abundance of target nuclides has been taken into account. Solid curves yield activities directly, whereas activities read multiplied by factor in brackets.

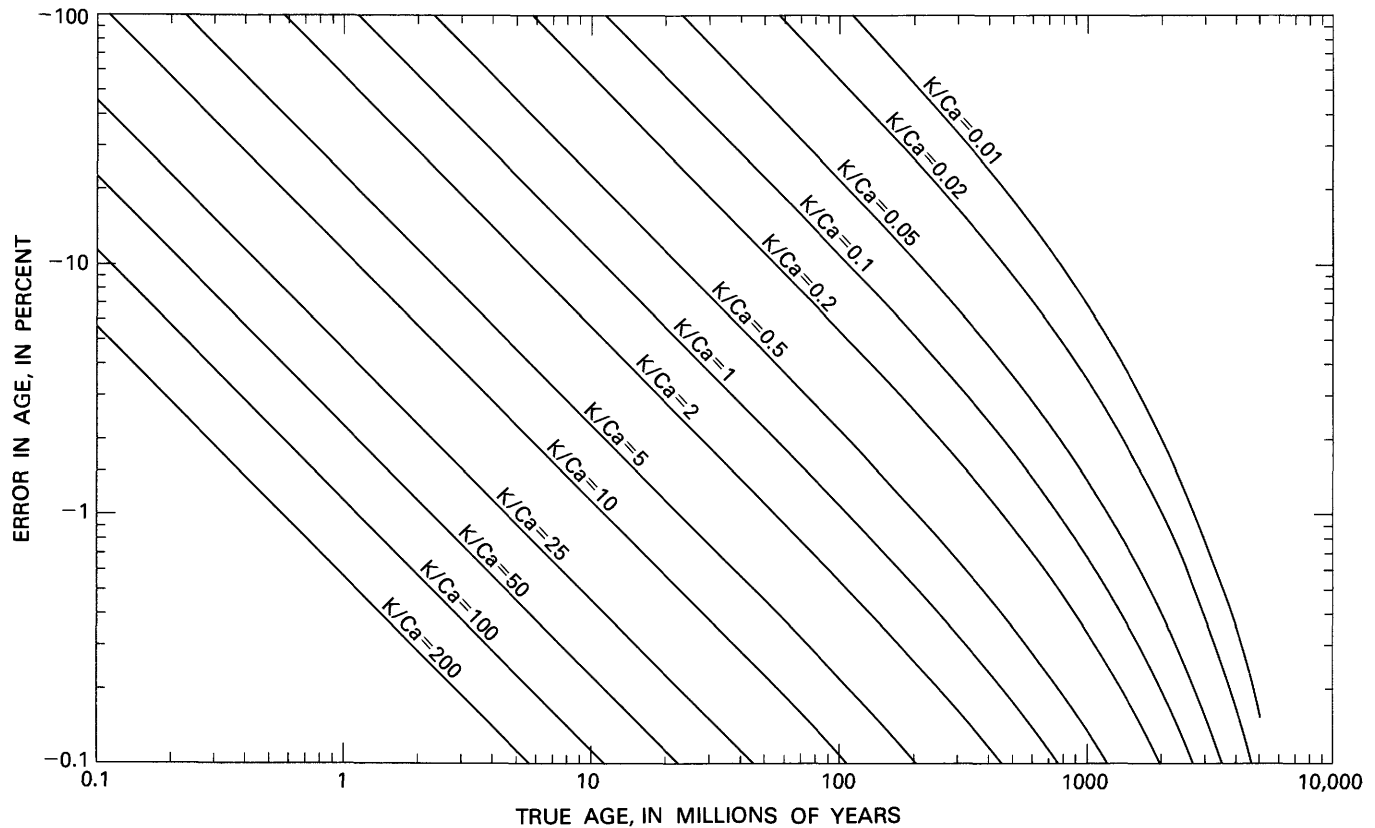


FIGURE 17.—Effect of reaction $^{40}\text{Ca}(n, na) ^{36}\text{Ar}$ on calculated $^{40}\text{Ar}/^{39}\text{Ar}$ age as a function of age and K/Ca ratio for irradiation time of 40 MWH. Graph gives approximate errors that would result if no corrections were made. Effect depends on age, K/Ca, and irradiation time. See also section entitled “Effect of $^{40}\text{Ca}(n, na) ^{36}\text{Ar}$ Interference” (figs. 24-36).

monitor resulted in a significant but indeterminable contribution to the measured ^{36}Ar in their monitor from neutron capture on ^{35}Cl . This indeterminable component introduced a major uncertainty into Bernatowicz and others' (1978) calibration of their irradiation.

^{38}Ar is produced by neutron-induced reactions on both K and Ca as well as the neutron capture reaction on ^{37}Cl via ^{38}Cl . In samples exposed to cosmic rays there is commonly a significant cosmogenic ^{38}Ar component, which can be used to calculate cosmic-ray exposure ages. The components of the measured ^{38}Ar due to reactor-induced reactions on K and Ca can be determined if the $(^{38}\text{Ar}/^{37}\text{Ar})_{\text{Ca}}$ and $(^{38}\text{Ar}/^{39}\text{Ar})_{\text{K}}$ values are measured on potassium and calcium salts. One measurement of each of these correction factors for the GSTR is listed in table 8.

In the analysis of terrestrial samples, the measured ^{36}Ar can usually be corrected to yield the atmospheric ^{36}Ar component. Any ^{38}Ar in excess of the atmospheric $^{38}\text{Ar}/^{36}\text{Ar}$ value, after the components from neutron-induced reactions on K and Ca are subtracted, can then be attributed to neutron capture on ^{37}Cl and can be used to measure the Cl contents of the samples (Stettler and Bochsler, 1979). In the analysis of extrater-

restrial samples, however, the subtraction of the reactor-produced ^{36}Ar and ^{38}Ar leaves a three-component mixture, cosmogenic ^{36}Ar and ^{38}Ar , atmospheric (or trapped) ^{36}Ar and ^{38}Ar , and Cl-derived ^{38}Ar . The measurement of ^{36}Ar and ^{38}Ar does not supply enough information to allow these components to be resolved.

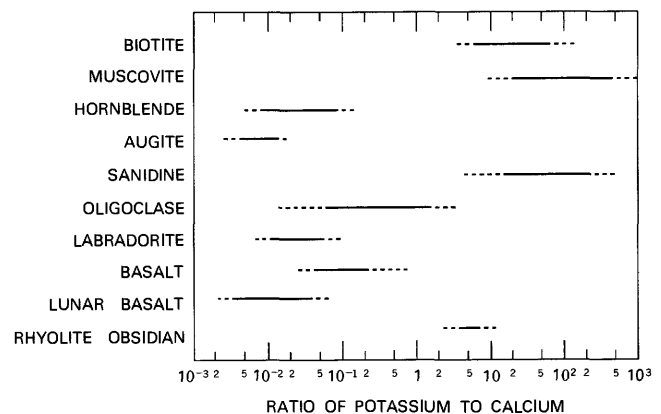


FIGURE 18.—Approximate ranges of K/Ca atomic ratios for some common minerals and rocks. K/Ca for an analyzed sample can be found by multiplying $\text{K}_2\text{O}/\text{CaO}$ (weight-percent ratio) by 1.190.

Only in those cases where one of the three components is negligible relative to the other two can the ^{36}Ar and ^{38}Ar data be resolved into individual components. Many lunar and meteoric samples are relatively depleted in Cl, and $^{38}\text{Ar}_{\text{Cl}}$ is negligible. In such cases, a cosmogenic component can be resolved and used to calculate cosmic-ray exposure ages. The same data set can therefore simultaneously yield $^{40}\text{Ar}/^{39}\text{Ar}$ formation ages and ^{38}Ar cosmic-ray exposure ages. The details of such calculations are given in several of the papers listed in the selected bibliography (table 10).

The effect of ^{39}Ar derived from neutron reactions with ^{42}Ca is an inverse function of the K/Ca ratio of the sample, is independent of the integrated fast neutron flux, and is essentially independent of age, except for old samples (fig. 19). For all but very low potassium samples, the effect of this interference is negligible and even large errors in the applicable correction factor would result in a negligible error in the age. In samples with very low K/Ca ratios such as lunar anorthosite, it is not uncommon for half of the measured ^{39}Ar to be $^{39}\text{Ar}_{\text{Ca}}$.

The magnitude of the K-derived ^{40}Ar correction is a direct function of the integrated fast neutron flux, an

inverse function of the age of the sample, and independent of the K/Ca ratio (fig. 20). For a 30-MWH irradiation in the GSTR, this interference produces an effect of about 0.1 m.y. for samples of any age. As noted above, however, this correction may vary from one irradiation to another for reasons that are as yet unknown. For most dating studies even a 100 percent error in the reactor constant ($^{40}\text{Ar}/^{39}\text{Ar}$)_K would produce a negligible error in the calculated age. For studies involving very young samples, however, the uncertainty and variability in this correction factor could be a serious source of error.

Occasionally, it is useful to know the relation between the atomic ratio K/Ca and the measured ratio $^{39}\text{Ar}_{\text{K}}/^{37}\text{Ar}_{\text{Ca}}$. For the GSTR the relation is

$$\text{K/Ca} = (0.49 \pm 0.09) ^{39}\text{Ar}_{\text{K}}/^{37}\text{Ar}_{\text{Ca}}. \quad (15)$$

The constant of proportionality was calculated using data from 19 samples for which K/Ca was measured independently (Dalrymple and Lanphere, 1971). Equation (15) is graphed in figure 21. Three of the samples give individually calculated constants that are unusu-

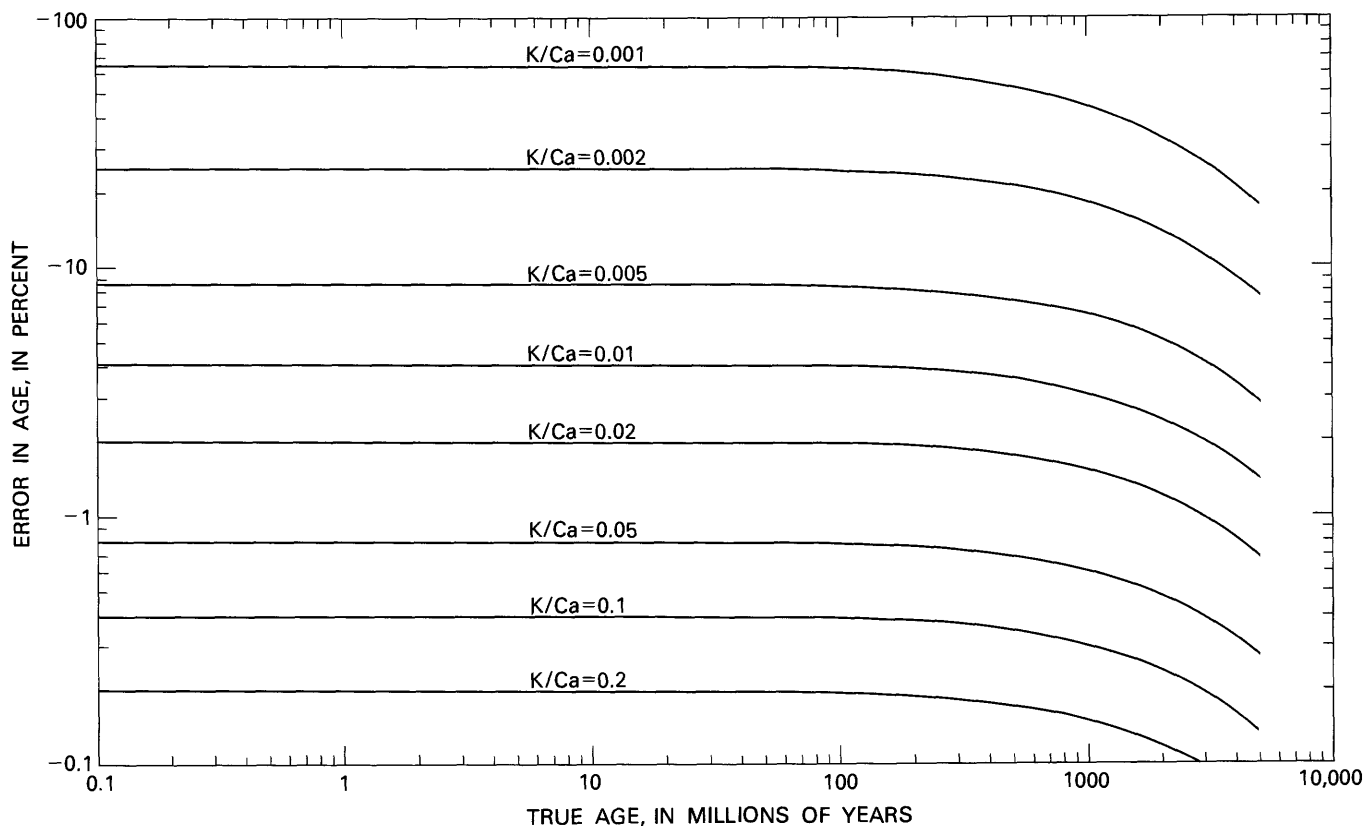


FIGURE 19.—Effect of $^{42}\text{Ca}(n, na) ^{39}\text{Ar}$ reaction on calculated $^{40}\text{Ar}/^{39}\text{Ar}$ age as a function of age and K/Ca ratio. Graph gives approximate errors that would result if no corrections were made. Effect is independent of irradiation time and is negligible for K/Ca greater than about 0.2.

ally high, but the remaining 16 values fall between 0.36 and 0.64 with mean and standard deviation as given in the equation above. Probably most of the variability, including the anomalous values, is due to inhomogeneities in the samples that makes it difficult to obtain representative splits for separate analyses. Another contributing factor is that either K or Ca is present in only trace amounts in nearly all these samples, and that fact adds to the difficulty in obtaining accurate analyses.

The ratios involving ^{37}Ar must be corrected for the decay (table 1) that occurs both during and after irradiation. For uninterrupted irradiation, this calculation can be done quickly with a desk calculator (equation 38, below). Because the GSTR is used for a variety of purposes, some of which require pulsing or very low power levels, samples for $^{40}\text{Ar}/^{39}\text{Ar}$ dating are frequently pulled up out of the core while other experiments are being accommodated. The aluminum capsule is not removed completely from the central thimble

tube; instead it is positioned out of the neutron flux but left deep enough for adequate radiological shielding by the column of water above. We are not sure that this procedure is necessary, but it seems worthwhile to try to ensure that the samples are irradiated at more or less constant power level. In addition, the reactor is normally operated 8 hours a day for 5 days a week. This means that samples for $^{40}\text{Ar}/^{39}\text{Ar}$ dating are irradiated in increments rather than continuously, a factor which complicates the ^{37}Ar correction procedure somewhat but does not degrade the accuracy of the calculations.

Formula 39 is used to calculate the ^{37}Ar decay correction for samples that have been irradiated in increments and at different power levels. This calculation can also be done with a desk calculator, but for more than a few increments the calculations become very cumbersome and a computer is much more convenient. A BASIC computer program for this calculation is given in the section entitled "Computer Programs."

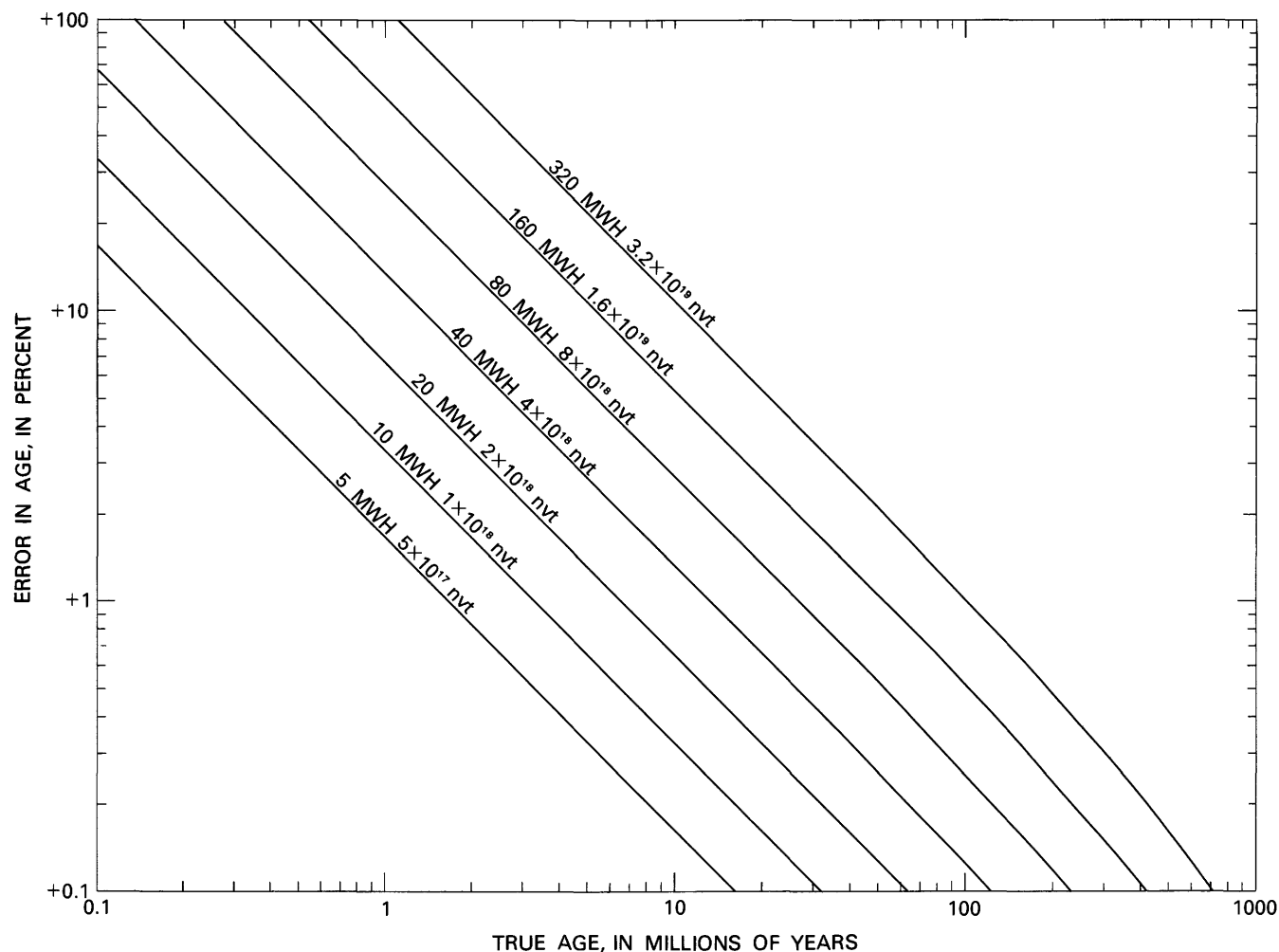


FIGURE 20.—Effect of $^{40}\text{K}(n, p) ^{40}\text{Ar}$ and $^{41}\text{K}(n, d) ^{40}\text{Ar}$ reactions on calculated $^{40}\text{Ar}/^{39}\text{Ar}$ age. Graph gives approximate errors that would result if no corrections were made. Effect is independent of K/Ca ratio.

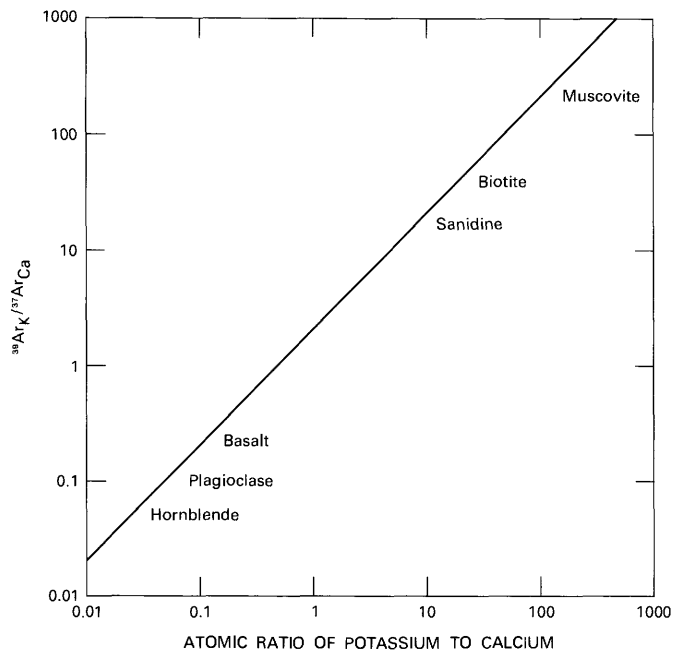


FIGURE 21.— $^{39}\text{Ar}_K/^{37}\text{Ar}_{Ca}$ as a function of K/Ca atomic ratio in GSTR (eq. 15).

OPTIMIZATION OF IRRADIATION PARAMETERS

Turner (1971b) showed that for any reactor the various interferences can be minimized by choosing an optimum irradiation time and an appropriate sample size. Following Turner (1971b) we analyzed our results from the GSTR, and we provide an irradiation optimization diagram as figure 22. The optimum irradiation is based on the satisfaction of three conditions: production of sufficient ^{39}Ar and minimization of interference from the reactions $^{40}\text{K}(n,p)^{40}\text{Ar}$ and $^{40}\text{Ca}(n,n\alpha)^{36}\text{Ar}$.

PRODUCTION OF SUFFICIENT ^{39}Ar

Theoretically, production of ^{39}Ar is controlled by sample size, K_2O content, and irradiation time. There are also several limiting practical considerations, including mass spectrometer sensitivity, the amount of reactor time available, and the maximum sample size that can be physically accommodated in the irradiation facility.

For the GSTR we have chosen 0.1 MWH as a lower practical limit for the irradiation time. The largest

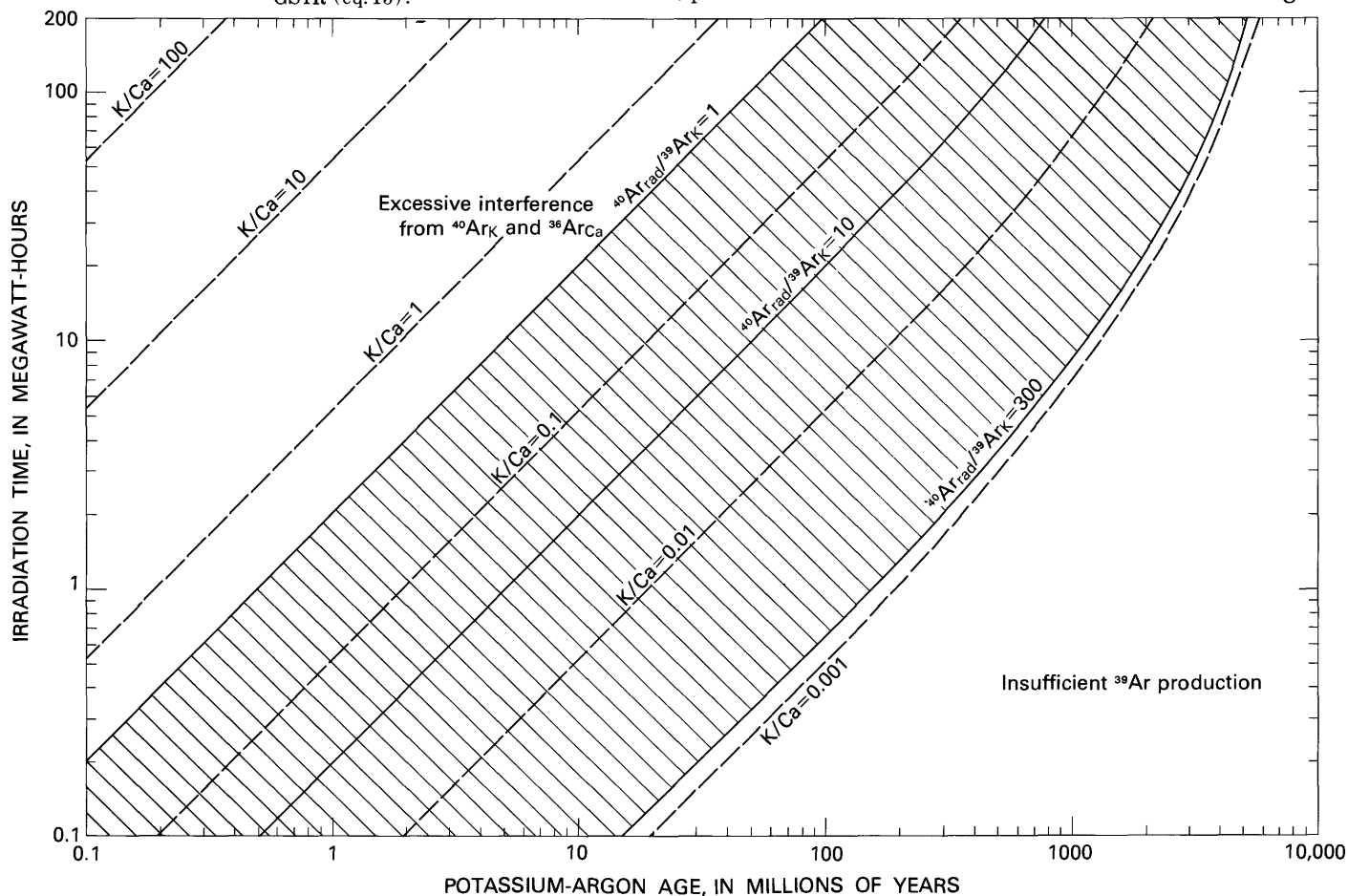


FIGURE 22.—Irradiation time in GSTR required to maximize ^{39}Ar produced from ^{39}K while minimizing interferences from $^{40}\text{Ar}_K$ and $^{36}\text{Ar}_{Ca}$. For irradiations in unshaded parts of graph, either ^{39}Ar production will be too low (lower right), or interference from $^{40}\text{Ar}_K$ will be too great (upper left). Dashed lines give maximum irradiation for minimization of $^{36}\text{Ar}_{Ca}$ interference.

sample that can fit easily in the larger quartz vials weighs about 5 grams. In 0.1 MWH, a 5-g sample that contained 10 percent K_2O would yield about 3.6×10^{-12} moles or $0.8 \times 10^{-8} \text{ cm}^3$ (STP) of ^{39}Ar (fig. 9), which is about as small a quantity as can be measured on most mass spectrometers and still maintain an accuracy of 1 percent or better. Two hundred hours is probably the upper limit, considering that the reactor is only available for a limited period of time (< 40 hours) each week, except under special circumstances.

The size of the sample should be chosen (fig. 9) to provide as much ^{39}Ar as can be conveniently measured, but the $^{40}\text{Ar}_{\text{rad}}/^{39}\text{Ar}_{\text{K}}$ ratio also must be limited to some reasonable value for accurate measurement. Turner (1971b) selected a ratio of 300 as probably the largest that could be measured without intolerable interference between the ^{40}Ar and ^{39}Ar mass beams. Thus, condition 1 requires that both the sample size and the irradiation time be adjusted to provide optimum amounts of both $^{40}\text{Ar}_{\text{rad}}$ and $^{39}\text{Ar}_{\text{K}}$, and to keep the $^{40}\text{Ar}_{\text{rad}}/^{39}\text{Ar}_{\text{K}}$ ratio less than 300.

MINIMIZATION OF $^{40}\text{K}(\text{n}, \text{p})^{40}\text{Ar}$ INTERFERENCE

As discussed above, the production ratio ($^{40}\text{Ar}/^{39}\text{Ar}$)_K varies considerably and may only be known for the GSTR to within a factor of two or so. If we select the maximum tolerable error from this interference as 0.5 percent, then the quantity of $^{40}\text{Ar}_{\text{K}}$ should be kept to less than 1 percent of the $^{40}\text{Ar}_{\text{rad}}$. In terms of ratios, this requires that

$$^{40}\text{Ar}_{\text{rad}}/^{39}\text{Ar}_{\text{K}} > 100(^{40}\text{Ar}/^{39}\text{Ar})_{\text{K}}$$

the largest value for ($^{40}\text{Ar}/^{39}\text{Ar}$)_K that we have measured for the GSTR is 1×10^{-2} (table 8), so conservatively, the desired ratio becomes

$$^{40}\text{Ar}_{\text{rad}}/^{39}\text{Ar}_{\text{K}} \geq 1.$$

All points that satisfy both the above conditions are included within the shaded area of figure 22. The line representing $^{40}\text{Ar}_{\text{rad}}/^{39}\text{Ar}_{\text{K}} = 10$ is also shown for reference. Generally, it is easier and more accurate to measure ratios if the two isotopes are within a factor of 10 or so in size, that is,

$$1 < ^{40}\text{Ar}_{\text{rad}}/^{39}\text{Ar}_{\text{K}} < 10,$$

but for very old samples this is not possible because impractically long irradiation times are required.

MINIMIZATION OF $^{40}\text{Ca}(\text{n}, \text{n}\alpha)^{36}\text{Ar}$ INTERFERENCE

The rate of production of $^{36}\text{Ar}_{\text{Ca}}$ relative to $^{37}\text{Ar}_{\text{Ca}}$ is known for the GSTR to within a few percent (table 8) so accurate corrections can be applied. It is desirable,

however, to limit the amount of $^{36}\text{Ar}_{\text{Ca}}$ produced to avoid magnifying the error. If we limit $^{36}\text{Ar}_{\text{Ca}}$ to 10 percent of the ^{36}Ar mass beam, then this condition becomes

$$^{36}\text{Ar}_{\text{Ca}} < 0.1 ^{36}\text{Ar}_{\text{atm}}$$

or

$$^{40}\text{Ar}_{\text{rad}}/^{36}\text{Ar}_{\text{Ca}} > 2955.$$

This condition depends not only on irradiation time and the age of the sample, but also on the K/Ca content. The dashed lines on figure 22 show the maximum irradiation times that will allow this condition to be met for various values of K/Ca.

As can be seen from figure 22, it is not difficult to satisfy all three of the conditions discussed above provided that K/Ca is greater than about 0.002. Theoretically, these conditions can always be satisfied for samples with K/Ca greater than 0.002, but there are also practical limitations imposed on the sample size and on the amount of gas that can be accurately measured by the mass spectrometer. All these factors need to be considered when choosing the irradiation parameters, and for many samples, it will be necessary to compromise.

REFERENCES CITED

- Alexander, E. C., Jr., 1975, $\text{Ar}^{39}/\text{Ar}^{40}$ studies of Precambrian cherts: An unsuccessful attempt to measure the time evolution of the atmospheric $\text{Ar}^{36}/\text{Ar}^{40}$ ratio: *Precambrian Research*, v. 2, no. 4, p. 329-344.
- Alexander, E. C., Jr., Coscio, M. R., Jr., Dragon, J. C., and Saito, Kazuo, 1981, K/Ar dating of lunar soils IV: Orange glass from 74220 and agglutinates from 14259 and 14163, *Proceedings of Eleventh Lunar and Planetary Science Conference, Geochimica et Cosmochimica Acta*, Supp. 12 (in press).
- Alexander, E. C., Jr., and Davis, P. K., 1974, ^{40}Ar - ^{39}Ar ages and trace element contents of Apollo 14 breccias; an interlaboratory cross-calibration of ^{40}Ar - ^{39}Ar standards: *Geochimica et Cosmochimica Acta*, v. 38, no. 6, p. 911-928.
- Alexander, E. C., Jr., and Kahl, S. B., 1974, ^{40}Ar - ^{39}Ar studies of lunar breccias: *Proceedings of Fifth Lunar Science Conference, Geochimica et Cosmochimica Acta*, Supplement 5, v. 2, p. 1353-1373.
- Alexander, E. C., Jr., Michelson, G. M., and Lanphere, M. A., 1978, MMhb-1: A new ^{40}Ar - ^{39}Ar dating standard, in Zartman, R. E., editor, *Short papers of the Fourth International Conference, Geochronology, Cosmochronology, Isotope Geology*: U. S. Geological Survey Open-File Report 78-701, p. 6-8.
- Beckinsale, R. D., and Gale, N. H., 1969, A reappraisal of the decay constants and branching ratio of ^{40}K : *Earth and Planetary Science Letters*, v. 6, no. 4, p. 289-294.
- Berger, G. W., 1975, $^{40}\text{Ar}/^{39}\text{Ar}$ step heating of thermally overprinted biotite, hornblende and potassium feldspar from Eldora, Colorado: *Earth and Planetary Science Letters*, v. 26, no. 3, p. 387-408.
- Berger, G. W., and York, Derek, 1970, Precision of the $^{40}\text{Ar}/^{39}\text{Ar}$ dating technique: *Earth and Planetary Science Letters*, v. 9, no. 1, p. 39-44.
- Bernatowicz, T. J., Hohenberg, C. M., Hudson, B., Kennedy, B. M.,

- and Podosek, F. A., 1978, Argon ages for lunar breccias 14064 and 15405: Proceedings of Ninth Lunar and Planetary Science Conference, *Geochimica et Cosmochimica Acta*, Supp. 10, v. 1, p. 905-919.
- Bogard, D. D., Husain, Liaquat, and Wright, R. J., 1976, $^{40}\text{Ar}/^{39}\text{Ar}$ dating of collisional events in chondrite parent bodies: *Journal of Geophysical Research*, v. 81, no. 32, p. 5664-5678.
- Brereton, N. R., 1970, Corrections for interfering isotopes in the $^{40}\text{Ar}/^{39}\text{Ar}$ dating method: *Earth and Planetary Science Letters*, v. 8, no. 6, p. 427-433.
- 1972, A reappraisal of the $^{40}\text{Ar}/^{39}\text{Ar}$ stepwise degassing technique: *Geophysical Journal of the Royal Astronomical Society*, v. 27, p. 449-478.
- Crow, E. L., Davis, F. A., and Maxfield, M. W., 1960, *Statistics manual*: New York, Dover Publishing, 288 p.
- Dallmeyer, R. D., 1975a, $^{40}\text{Ar}/^{39}\text{Ar}$ spectra of biotite and hornblende from the Cortlandt and Rosetown plutons, New York, and their regional implications: *Journal of Geology*, v. 83, no. 5, p. 629-643.
- 1975b, $^{40}\text{Ar}/^{39}\text{Ar}$ ages of biotite and hornblende from a progressively remetamorphosed basement terrane: Their bearing on interpretation of release spectra: *Geochimica et Cosmochimica Acta*, v. 39, no. 12, p. 1655-1669.
- 1975c, Incremental $^{40}\text{Ar}/^{39}\text{Ar}$ ages of biotite and hornblende from retrograded basement gneisses of the southern Blue Ridge: Their bearing on the age of Paleozoic metamorphism: *American Journal of Science*, v. 275, no. 4, p. 444-460.
- Dallmeyer, R. D., Maybin, A. H., and Durocher, M. E., 1975, Timing of Kenoran metamorphism in the eastern Abitibi greenstone belt, Quebec: Evidence from $^{40}\text{Ar}/^{39}\text{Ar}$ ages of hornblende and biotite from postkinematic plutons: *Canadian Journal of Earth Science*, v. 12, no. 11, p. 1864-1873.
- Dallmeyer, R. D., and Sutter, J. F., 1976, $^{40}\text{Ar}/^{39}\text{Ar}$ incremental-release ages of biotite and hornblende from variably retrograded basement gneisses of the northeasternmost Reading Prong, New York: Their bearing on early Paleozoic metamorphic history: *American Journal of Science*, v. 276, no. 6, p. 731-747.
- Dalrymple, G. B., 1979, Critical tables for conversion of K-Ar ages from old constants to new constants: *Geology*, v. 7, no. 11, p. 558-560.
- Dalrymple, G. B., and Clague, D. A., 1976, Age of the Hawaiian-Emperor bend: *Earth and Planetary Science Letters*, v. 31, no. 3, p. 313-329.
- Dalrymple, G. B., Grommé, C. S., and White, R. W., 1975, Potassium-argon age and paleomagnetism of diabase dikes in Liberia: Initiation of central Atlantic rifting: *Geological Society of America Bulletin*, v. 86, no. 3, p. 399-411.
- Dalrymple, G. B., and Lanphere, M. A., 1969, Potassium-argon dating: San Francisco, W. H. Freeman, 258 p.
- 1971, $^{40}\text{Ar}/^{39}\text{Ar}$ technique of K-Ar dating: A comparison with the conventional technique: *Earth and Planetary Science Letters*, v. 12, no. 3, p. 300-308.
- 1974, $^{40}\text{Ar}/^{39}\text{Ar}$ age spectra of some undisturbed terrestrial samples: *Geochimica et Cosmochimica Acta*, v. 38, no. 5, p. 715-738.
- Davis, P. K., 1977, Effects of shock pressure on $^{40}\text{Ar}/^{39}\text{Ar}$ radiometric age determinations: *Geochimica et Cosmochimica Acta*, v. 41, no. 2, p. 195-205.
- Deer, W. A., Howie, R. A., and Zussman, J., 1962, *Rock-forming minerals* (1st ed.): London, Longmans, v. 1-5.
- Dunham, K. C., Fitch, F. J., Ineson, P. R., Miller, J. A., and Mitchell, J. G., 1968, The geochronological significance of argon-40/argon-39 age determinations on White Whin from the northern Pennine orefield: *Proceedings of the Royal Society [London]*, A, v. 307, no. 1490, p. 251-266.
- Engels, J. C., and Ingamells, C. O., 1970, Effect of sample inhomogeneity in K-Ar dating: *Geochimica et Cosmochimica Acta*, v. 34, no. 9, p. 1007-1017.
- Everling, F., Koenig, L. A., Mattauch, J. H. E., and Wapstra, A. H., 1961, 1960 nuclear data tables, part 1, Consistent set of energies liberated in nuclear reactions I. Targets in the mass region $A < 66$: National Academy of Sciences — National Research Council, 214 p.
- Fitch, F. J., Hooker, P. J., and Miller, J. A., 1976, $^{40}\text{Ar}/^{39}\text{Ar}$ dating of the KBS Tuff in Koobi Fora Formation, East Rudolf, Kenya: *Nature*, v. 263, no. 5580, p. 740-744.
- Fitch, F. J., Miller, J. A., and Mitchell, J. G., 1969, A new approach to radio-isotopic dating in orogenic belts, in Kent, P. E., Satherthwaite, G. E., and Spencer, A. M., eds., *Time and place in orogeny*: Geological Society of London Special Publication 3, p. 157-195.
- Fleck, R. J., Sutter, J. F., and Elliot, D. H., 1977, Interpretation of discordant $^{40}\text{Ar}/^{39}\text{Ar}$ age spectra of Mesozoic tholeiites from Antarctica: *Geochimica et Cosmochimica Acta*, v. 41, no. 1, p. 15-32.
- Garner, E. L., Murphy, T. J., Gramlich, J. W., Paulsen, P. J., and Barnes, I. L., 1975, Absolute isotopic abundance ratios and the atomic weight of a reference sample of potassium: *Journal of Research of the National Bureau of Standards*, v. 79a, no. 6, p. 713-725.
- Hanson, G. N., Goldich, S. S., Arth, J. G., and Yardley, D. H., 1971, Age of the Early Precambrian rocks of the Saganaga Lake-Northern Light Lake area, Ontario-Minnesota: *Canadian Journal of Earth Sciences*, v. 8, no. 7/8, p. 1110-1124.
- Hanson, G. N., Simmons, K. R., and Bence, A. E., 1975, $^{40}\text{Ar}/^{39}\text{Ar}$ spectrum ages for biotite, hornblende, and muscovite in a contact metamorphic zone: *Geochimica et Cosmochimica Acta*, v. 39, no. 9, p. 1269-1277.
- Horn, Peter, Jessberger, E. K., Kirsten, T., and Richter, H., 1975, ^{39}Ar - ^{40}Ar dating of lunar rocks: Effects of grain and neutron irradiation: *Proceedings of Lunar Science Conference*, 6th, v. 2, p. 1563-1591.
- Huneke, J. C., 1976, Diffusion artifacts in dating by stepwise thermal release of rare gases: *Earth and Planetary Science Letters*, v. 28, no. 3, p. 407-417.
- Huneke, J. C., Jessberger, E. K., Podosek, F. A., and Wasserburg, G. J., 1973, $^{40}\text{Ar}/^{39}\text{Ar}$ measurements in Apollo 16 and 17 samples and the chronology of metamorphic and volcanic activity in the Taurus-Littrow region: *Proceedings of Lunar Science Conference*, 4th, v. 2, p. 1725-1756.
- Huneke, J. C., Podosek, F. A., and Wasserburg, G. J., 1972, Gas retention and cosmic-ray exposure ages of a basalt fragment from Mare Fecunditatis: *Earth and Planetary Science Letters*, v. 13, no. 2, p. 375-383.
- Huneke, J. C., and Smith, S. P., 1976, The realities of recoil: ^{39}Ar recoil out of small grains and anomalous age patterns in ^{39}Ar - ^{40}Ar dating: *Proceedings of Lunar Science Conference*, 7th, v. 2, p. 1987-2008.
- Ingamells, C. O., 1970, Lithium metaborate flux in silicate analysis: *Analytica Chimica Acta*, v. 52, no. 2, p. 323-334.
- Jackson, E. D., and Wright, T. L., 1970, Xenoliths in the Honolulu Volcanic Series, Hawaii: *Journal of Petrology*, v. 11, no. 2, p. 405-430.
- Jessberger, E. K., Huneke, J. C., Podosek, F. A., and Wasserburg, G. J., 1974, High resolution argon analysis of neutron-irradiated Apollo 16 rocks and separated minerals: *Proceedings of Lunar Science Conference*, 5th, v. 2, p. 1419-1449.
- Kaneoka, Ichiro, 1974, Investigation of excess argon in ultramafic rocks from the Kola Peninsula by the $^{40}\text{Ar}/^{39}\text{Ar}$ method: *Earth*

- and Planetary Science Letters, v. 22, no. 2, p. 145-156.
- Kirsten, T., Deubner, J., Horn, Peter, Kaneoka, Ichiro, Kiko, J., Schaeffer, O. A., and Thio, S. K., 1972, The rare gas record of Apollo 14 and 15 samples: Proceedings of Lunar Science Conference, 3rd, v. 2, p. 1865-1889.
- Kirsten, T., and Horn, P., 1977, ^{39}Ar - ^{40}Ar dating of basalts and rock breccias from Apollo 17 and Malvern Achondrite, in Pomeroy, J. H., and Hubbard, N. J., eds., The Soviet-American Conference on Cosmochemistry of the Moon and Planets: National aeronautics and Space Administration Special report 370, p. 525-540.
- Kirsten, T., Horn, P., and Heyman, Dieter, 1973, Chronology of the Taurus-Littrow region I: Ages of two major rock types from the Apollo 17 site: Earth and Planetary Science Letters, v. 20, no. 1, p. 125-130.
- Kirsten, T., Horn, P., and Kiko, J., 1973, $^{39}\text{Ar}/^{40}\text{Ar}$ dating and rare gas analysis of Apollo 16 rocks and soils: Proceedings of lunar Science Conference, 4th, v. 2, p. 1757-1784.
- Koch, R. C., 1960, Activation analysis handbook: New York, Academic Press, 219 p.
- Lanphere, M. A., and Albee, A. L., 1974, $^{40}\text{Ar}/^{39}\text{Ar}$ age measurements in the Worcester Mountains: Evidence of Ordovician and Devonian metamorphic events in northern Vermont: American Journal of Science, v. 274, no. 6, p. 545-555.
- Lanphere, M. A., and Dalrymple, G. B., 1965, P-207: An interlaboratory standard muscovite for argon and potassium analyses: Journal of Geophysical Research, v. 70, no. 14, p. 3497-3503.
- 1971, A test of the $^{40}\text{Ar}/^{39}\text{Ar}$ age spectrum technique on some terrestrial materials: Earth and Planetary Science Letters, v. 12, no. 4, p. 359-372.
- 1976, Identification of excess ^{40}Ar by the $^{40}\text{Ar}/^{39}\text{Ar}$ age spectrum technique: Earth and Planetary Science Letters, v. 32, no. 2, p. 141-148.
- 1976, Final compilation of K-Ar and Rb-Sr measurements on P-207, the USGS interlaboratory standard muscovite: U. S. Geological Survey Professional Paper 840, p. 127-130.
- Lewis, R. S., 1975, Rare gases in separated whitlockite from the St. Severin chondrite: Xenon and krypton from fission of extinct ^{244}Pu : Geochimica et Cosmochimica Acta, v. 39, no. 4, p. 417-432.
- McDougall, Ian, 1974, The $^{40}\text{Ar}/^{39}\text{Ar}$ method of K-Ar age determination of rocks using HIFAR reactor: Australian Atomic Energy Commission Journal, v. 17, no. 3, p. 3-12.
- McDougall, Ian, and Roksandic, Z., 1974, Total fusion $^{40}\text{Ar}/^{39}\text{Ar}$ ages using HIFAR reactor: Journal of the Australian Geological Society, v. 21, no. 1, p. 81-89.
- Mateen, Abdul, and Green, D. C., 1974, An assessment of irradiation parameters for $^{40}\text{Ar}/^{39}\text{Ar}$ age determinations in HIFAR reactor, Australia: Proceedings of the Royal Society of Queensland, v. 85, no. 8, p. 85-93.
- Merrihue, Craig, 1965, Trace element determinations and potassium-argon dating by mass spectroscopy of neutron-irradiated samples [abs.]: Transactions of the American Geophysical Union, v. 46, no. 1, p. 125.
- Merrihue, Craig, and Turner, Grenville, 1966, Potassium-argon dating by activation with fast neutrons: Journal of Geophysical Research, v. 71, no. 11, p. 2852-2857.
- Miller, J. A., Mitchell, J. G., and Evans, A. L., 1970, The argon-40/argon-39 dating method applied to basic rocks, in Runcorn, S. K., ed., Paleogeophysics: London and New York, Academic Press, p. 481-489.
- Mitchell, J. G., 1968, The argon-40/argon-39 method for potassium-argon age determinations: Geochimica et Cosmochimica Acta, v. 32, no. 7, p. 781-790.
- Nier, A. O., 1950, A redetermination of the relative abundances of the isotopes of carbon, nitrogen, oxygen, argon, and potassium: The Physical Review, v. 77, no. 6, p. 789-793.
- Ozima, Minoru, and Saito, Kazuo, 1973, $^{40}\text{Ar}/^{39}\text{Ar}$ stepwise degassing experiments on some submarine rocks: Earth and Planetary Science Letters, v. 20, no. 1, p. 77-87.
- Ozima, Minoru, Saito, Kazuo, Matsuda, Jun-ichi, Zashu, Sigeo, Aramaki, Shigeo, and Shido, Fumiko, 1976, Additional evidence of existence of ancient rocks in the mid-Atlantic ridge and the age of the opening of the Atlantic: Tectonophysics, v. 31, no. 1, p. 59-71.
- Pankhurst, R. J., Moorbath, Stephen, Rex, D. C., and Turner, Grenville, 1973, Mineral age patterns in ca. 3700 m.y. old rocks from West Greenland: Earth and Planetary Science Letters, v. 20, no. 2, p. 157-170.
- Podosek, F. A., 1971, Neutron-activation potassium-argon dating of meteorites: Geochimica et Cosmochimica Acta, v. 35, no. 2, p. 157-173.
- Podosek, F. A., and Huneke, J. C., 1973, Argon 40-argon 39 chronology of four calcium-rich achondrites: Geochimica et Cosmochimica Acta, v. 37, no. 3, p. 667-684.
- Podosek, F. A., Huneke, J. C., Gancarz, A. J., and Wasserburg, G. J., 1973, The age and petrography of two Luna 20 fragments and inferences for widespread lunar metamorphism: Geochimica et Cosmochimica Acta, v. 37, no. 4, p. 887-904.
- Reed, B. L., and Lanphere, M. A., 1969, Age and chemistry of Mesozoic and Tertiary plutonic rocks in south-central Alaska: Geological Society of America Bulletin, v. 80, no. 1, p. 23-44.
- Saito, Kazuo, and Ozima, Minoru, 1977, ^{40}Ar - ^{39}Ar geochronological studies on submarine rocks from the western Pacific area: Earth and Planetary Science Letters, v. 33, no. 3, p. 353-369.
- Schaeffer, O. A., and Husain, Liaquat, 1974, Chronology of lunar basin formation: Proceedings of Lunar Science Conference, 5th, v. 2, p. 1541-1555.
- Sigurgeirsson, Thorbjörn, 1962, Dating basalt by the potassium-argon method: Report of Physical Laboratory of the University of Iceland, 9 p. (in Icelandic).
- Steiger, R. H., and Jäger, Emilie, 1977, Subcommittee on geochronology: Convention on the use of decay constants in Geo- and Cosmochronology: Earth and Planetary Science Letters, v. 36, no. 3, p. 359-362.
- Stettler, A., and Bochsler, P., 1979, He, Ne, and Ar composition in a neutron irradiated activated sea-floor basalt glass: Geochimica et Cosmochimica Acta, v. 43, no. 1, p. 157-169.
- Stettler, A., Eberhardt, P., Geiss, J., Grögler, N., and Maurer, P., 1973, ^{39}Ar - ^{40}Ar ages and ^{37}Ar - ^{38}Ar exposure ages of lunar rocks: Proceedings of Lunar Science Conference, 4th, v. 2, p. 1865-1888.
- 1974, On the duration of lava flow activity in Mare Tranquillitatis: Proceedings of Lunar Science Conference, 5th, v. 2, p. 1557-1570.
- Stoerner, R. W., Schaeffer, O. A., and Katcoff, S., 1965, Half-lives of argon-37, argon-39, and argon-42: Science, v. 148, no. 3675, p. 1325-1328.
- Turner, F. J., and Verhoogen, John, 1960, Igneous and metamorphic petrology (2d ed.): New York, McGraw-Hill, 694 p.
- Turner, Grenville, 1969, Thermal histories of meteorites by the ^{39}Ar - ^{40}Ar method, in Millman, P. M., ed., Meteorite research: Dordrecht, Netherlands, D. Reidel, p. 407-417.
- 1970a, Argon-40/argon-39 dating of lunar rock samples: Proceedings of the Apollo 11 Lunar Science Conference, v. 2, p. 1665-1684.
- 1970b, ^{40}Ar - ^{39}Ar age determination of lunar rock 12013: Earth and Planetary Science Letters, v. 9, no. 2, p. 177-180.
- 1971a, ^{40}Ar - ^{39}Ar ages from the lunar maria: Earth and Planetary Science Letters, v. 11, no. 3, p. 169-191.

- 1971b, Argon 40-argon 39 dating: The optimization of irradiation parameters: *Earth and Planetary Science Letters*, v. 10, no. 2, p. 227-234.
- 1972, ^{40}Ar - ^{39}Ar age and cosmic ray irradiation history of the Apollo 15 anorthosite 15415: *Earth and Planetary Science Letters*, v. 14, no. 2, p. 169-175.
- Turner, Grenville, and Cadogan, P. H., 1974, Possible effects of ^{39}Ar recoil in ^{40}Ar - ^{39}Ar dating of lunar samples: *Proceedings of Lunar Science Conference*, 5th, v. 2, p. 1601-1615.
- 1975, The history of lunar bombardment inferred from ^{40}Ar - ^{39}Ar dating of highland rocks: *Proceedings of Lunar Science Conference*, 6th, v. 2, p. 1509-1538.
- Turner, Grenville, Huneke, J. C., Podosek, F. A., and Wasserburg, G. J., 1971, ^{40}Ar - ^{39}Ar ages and cosmic ray exposure ages of Apollo 14 samples: *Earth and Planetary Science Letters*, v. 12, no. 1, p. 19-35.
- 1972, $\text{Ar}^{40}/\text{Ar}^{39}$ systematics in rocks and separated minerals from Apollo 14: *Proceedings of Lunar Science Conference*, 3d, v. 2, p. 1589-1612.
- Turner, Grenville, Miller, J. A., and Grasty, R. L., 1966, The thermal history of the Bruderheim meteorite: *Earth and Planetary Science Letters*, v. 1, no. 4, p. 155-157.
- Walker, F. W., Kirouac, G. J., and Rourke, F. M., 1977, *Chart of the nuclides* (12th ed.): Schenectady, N.Y., Knowles Atomic Power Laboratory.
- Weast, R. C., ed., 1976, *Handbook of chemistry and physics* (57th ed.): Cleveland, The Chemical Rubber Company.
- York, Derek, and Berger, G. W., 1970, $^{40}\text{Ar}/^{39}\text{Ar}$ age determinations on nepheline and basic whole rocks: *Earth and Planetary Science Letters*, v. 7, no. 4, p. 333-336.

SUPPLEMENTAL DATA

DERIVATION OF EQUATIONS

 $^{30}\text{Ar}/^{39}\text{Ar}$ AGE EQUATION

Beginning with the basic equation for the production of radiogenic ^{40}Ar from the decay of ^{40}K ,

$$^{40}\text{Ar}_{\text{rad}} = ^{40}\text{K} \frac{\lambda_{\epsilon}}{\lambda_{\epsilon} + \lambda_{\beta}} (e^{\lambda t} - 1) \quad (1)$$

where λ_{ϵ} is the decay constant for electron capture, λ_{β} is the decay constant for β^{-} emission, $\lambda = \lambda_{\epsilon} + \lambda_{\beta}$, and t is time, and using the subscripts u and m for the unknown and monitor minerals, respectively, then

$$^{40}\text{Ar}_{\text{rad},u} = ^{40}\text{K}_u \frac{\lambda_{\epsilon}}{\lambda} (e^{\lambda t_u} - 1) \quad (2)$$

and

$$^{40}\text{Ar}_{\text{rad},m} = ^{40}\text{K}_m \frac{\lambda_{\epsilon}}{\lambda} (e^{\lambda t_m} - 1). \quad (3)$$

Dividing equation (2) by (3),

$$\frac{^{40}\text{Ar}_{\text{rad},u}}{^{40}\text{Ar}_{\text{rad},m}} = \frac{^{40}\text{K}_u}{^{40}\text{K}_m} \left(\frac{e^{\lambda t_u} - 1}{e^{\lambda t_m} - 1} \right). \quad (4)$$

If the unknown and the monitor minerals are irradiated together and receive the same neutron dose, and a fraction F of the ^{39}K in each is converted to $^{39}\text{Ar}_K$, then

$$^{39}\text{Ar}_{K,u} = F ^{39}\text{K}_u \quad (5)$$

and

$$^{39}\text{Ar}_{K,m} = F ^{39}\text{K}_m. \quad (6)$$

Dividing equation (5) by (6),

$$\frac{^{39}\text{Ar}_{K,u}}{^{39}\text{Ar}_{K,m}} = \frac{^{39}\text{K}_u}{^{39}\text{K}_m} = \frac{^{40}\text{K}_u}{^{40}\text{K}_m}. \quad (7)$$

Substituting equation (7) into (4),

$$\frac{^{40}\text{Ar}_{\text{rad},u}}{^{40}\text{Ar}_{\text{rad},m}} = \frac{^{39}\text{Ar}_{K,u}}{^{39}\text{Ar}_{K,m}} \left(\frac{e^{\lambda t_u} - 1}{e^{\lambda t_m} - 1} \right). \quad (8)$$

Solving for t_u ,

$$t_u = \frac{1}{\lambda} \ln \left[1 + \frac{(^{40}\text{Ar}_{\text{rad}}/^{39}\text{Ar}_K)_u}{(^{40}\text{Ar}_{\text{rad}}/^{39}\text{Ar}_K)_m} (e^{\lambda t_m} - 1) \right]. \quad (9)$$

To simplify, we define the quantity

$$J = \frac{(e^{\lambda t_m} - 1)}{(^{40}\text{Ar}_{\text{rad}}/^{39}\text{Ar}_K)_m} \quad (10)$$

and substitute equation (10) into (9), which becomes

$$t_u = \frac{1}{\lambda} \ln \left[1 + J(^{40}\text{Ar}_{\text{rad}}/^{39}\text{Ar}_K)_u \right]. \quad (11)$$

To determine the quantity $^{40}\text{Ar}_{\text{rad}}/^{39}\text{Ar}_K$ for use in equation (11), it is necessary to correct the isotope ratio $^{40}\text{Ar}/^{39}\text{Ar}$, measured in the mass spectrometer, for atmospheric Ar as well as for Ca- and K-derived Ar isotopes. If there were no Ca-derived ^{36}Ar , then the atmospheric component would be $(^{40}\text{Ar}/^{36}\text{Ar})_{\text{atm}}(^{36}\text{Ar}/^{39}\text{Ar})$ or 295.5 ($^{36}\text{Ar}/^{39}\text{Ar}$), which would be subtracted from the measured $^{40}\text{Ar}/^{39}\text{Ar}$ ratio. However, part of the ^{36}Ar is derived from neutron reactions with ^{40}Ca , and the appropriate atmospheric correction is

$$295.5 [(^{36}\text{Ar}/^{39}\text{Ar}) - (^{36}\text{Ar}/^{37}\text{Ar})_{\text{Ca}} (^{37}\text{Ar}/^{39}\text{Ar})] \quad (12)$$

where $(^{36}\text{Ar}/^{37}\text{Ar})_{\text{Ca}}$ is a constant for a particular reactor. In addition, there is ^{40}Ar generated by neutron reactions with potassium, and this component, $(^{40}\text{Ar}/^{39}\text{Ar})_K$ also a reactor constant, must be subtracted from the measured $^{40}\text{Ar}/^{39}\text{Ar}$ ratio. Finally, the measured $^{40}\text{Ar}/^{39}\text{Ar}$ ratio must be corrected for the ^{39}Ar generated by neutron reactions with Ca, which is $(^{39}\text{Ar}/^{37}\text{Ar})_{\text{Ca}} (^{37}\text{Ar}/^{39}\text{Ar})$, where $(^{39}\text{Ar}/^{37}\text{Ar})_{\text{Ca}}$ is a constant.

After incorporating these corrections, the complete expression becomes

$$\frac{^{40}\text{Ar}_{\text{rad}}}{^{39}\text{Ar}_K} = \frac{(^{40}\text{Ar}/^{39}\text{Ar}) - 295.5 [(^{36}\text{Ar}/^{39}\text{Ar}) - (^{36}\text{Ar}/^{37}\text{Ar})_{\text{Ca}} (^{37}\text{Ar}/^{39}\text{Ar})] - (^{40}\text{Ar}/^{39}\text{Ar})_K}{1 - (^{39}\text{Ar}/^{37}\text{Ar})_{\text{Ca}} (^{37}\text{Ar}/^{39}\text{Ar})} \quad (13)$$

ERROR FORMULAE

The basis for the derivation of the error formulae is as follows:

$$\text{If } y = F(x_1, x_2, \dots, x_k) \quad (14)$$

and the changes Δx_i are small, then

$$\Delta y \sim dy = \frac{\partial F}{\partial x_1} \Delta x_1 + \frac{\partial F}{\partial x_2} \Delta x_2 + \dots + \frac{\partial F}{\partial x_k} \Delta x_k. \quad (15)$$

Further, if the quantities Δx_i are independent, then the variance in Δy is approximately

$$\sigma_y^2 \sim \left(\frac{\partial F}{\partial x_1} \right)^2 \sigma_{x_1}^2 + \left(\frac{\partial F}{\partial x_2} \right)^2 \sigma_{x_2}^2 + \dots + \left(\frac{\partial F}{\partial x_k} \right)^2 \sigma_{x_k}^2. \quad (16)$$

To simplify notation, let

$$\begin{aligned} F &= {}^{40}\text{Ar}_{\text{rad}}/{}^{39}\text{Ar}_k \\ A &= {}^{40}\text{Ar}/{}^{39}\text{Ar} \\ B &= {}^{36}\text{Ar}/{}^{39}\text{Ar} \\ D &= {}^{37}\text{Ar}/{}^{39}\text{Ar} \text{ (corrected for } {}^{37}\text{Ar decay)} \\ C_1 &= ({}^{40}\text{Ar}/{}^{36}\text{Ar})_{\text{atm}} = 295.5 \\ C_2 &= ({}^{36}\text{Ar}/{}^{37}\text{Ar})_{\text{ca}} = \text{reactor constant} \\ C_3 &= ({}^{40}\text{Ar}/{}^{39}\text{Ar})_{\text{k}} = \text{reactor constant} \\ C_4 &= ({}^{39}\text{Ar}/{}^{37}\text{Ar})_{\text{ca}} = \text{reactor constant} \end{aligned}$$

Then equation (13) becomes

$$F = \frac{A - C_1 B + C_1 C_2 D - C_3}{1 - C_4 D}. \quad (17)$$

From equation (15),

$$\Delta F \cong dF = \frac{\partial F}{\partial A} \Delta A + \frac{\partial F}{\partial B} \Delta B + \frac{\partial F}{\partial D} \Delta D. \quad (18)$$

Differentiating equation (17) and rearranging it,

$$dF = \frac{(1 - C_4 D) \Delta A - C_1 (1 - C_4 D) \Delta B + [C_4 (A - C_1 B - C_3) + C_1 C_2] \Delta D}{(1 - C_4 D)^2} \quad (19)$$

Equation (19) can be simplified because for the GSTR (and probably for all reactors),

$$1 - C_4 D \cong 1$$

and

$$C_4 C_3 \cong 4 \times 10^{-6},$$

and is negligible.

Equation (19) then becomes

$$\Delta F \sim \Delta A - C_1 \Delta B + [C_4 A - C_1 C_4 B + C_1 C_2] \Delta D \quad (20)$$

and

$$\sigma_F^2 \sim \sigma_A^2 + C_1^2 \sigma_B^2 + [C_4 A - C_1 C_4 B + C_1 C_2]^2 \sigma_D^2 \quad (21)$$

where the errors σ are absolute errors.

It is usually more convenient to use percentage or fractional errors, σ' , whereupon equation (21) becomes

$$\sigma'^2_F \cong \frac{A^2 \sigma'^2_A + C_1^2 B^2 \sigma'^2_B + [C_4 A - C_1 C_4 B + C_1 C_2]^2 D^2 \sigma'^2_D}{F^2} \quad (22)$$

which can be used to estimate the error in ${}^{40}\text{Ar}_{\text{rad}}/{}^{39}\text{Ar}$.

Using the same approach and terminology, an expression for estimating the error in a ${}^{40}\text{Ar}/{}^{39}\text{Ar}$ age can be derived.

Starting with equation (11),

$$t = \frac{1}{\lambda} \ln [1 + FJ], \quad (23)$$

then

$$\Delta t \cong dt = \frac{\partial t}{\partial F} \Delta F + \frac{\partial t}{\partial J} \Delta J. \quad (24)$$

Differentiating (23) and rearranging,

$$\Delta t \cong \frac{1}{\lambda (1 + FJ)} (J \Delta F + F \Delta J) \quad (25)$$

and

$$\sigma_t^2 \cong \frac{1}{\lambda^2 (1 + FJ)^2} (J^2 \sigma_F^2 + F^2 \sigma_J^2). \quad (26)$$

Expressed in percentage or fractional errors, (26) becomes

$$\sigma'^2_t \sim \frac{J^2 F^2}{t^2 \lambda^2 (1 + FJ)^2} (\sigma'^2_F + \sigma'^2_J). \quad (27)$$

 ${}^{37}\text{Ar}$ DECAY CORRECTION

Let

- n = neutron density,
- v = neutron velocity,
- nv = flux,
- σ = nuclear cross section,
- t = irradiation time,
- T = number of ${}^{40}\text{Ca}$ target atoms,
- N = number of ${}^{37}\text{Ar}$ atoms at time t, and
- λ = decay constant of ${}^{37}\text{Ar}$.

The rate of change of ^{37}Ar is

$$\frac{dN}{dt} = nv\sigma T - \lambda N. \quad (28)$$

Equation (28) can be rewritten

$$e^{\lambda t} \frac{dN}{dt} + \lambda N e^{\lambda t} = nv\sigma T e^{\lambda t} \quad (29)$$

or

$$\frac{d}{dt} (N e^{\lambda t}) = nv\sigma T e^{\lambda t}. \quad (30)$$

Integrating (30) and rearranging,

$$N = \frac{nv\sigma T}{\lambda} + C e^{-\lambda t}. \quad (31)$$

Now $N = 0$ at $t = 0$, so

$$C + \frac{nv\sigma T}{\lambda} = 0 \quad (32)$$

or

$$C = \frac{-nv\sigma T}{\lambda}. \quad (33)$$

Substituting (33) into (31),

$$N = \frac{nv\sigma T}{\lambda} (1 - e^{-\lambda t}). \quad (34)$$

If a finite time t' elapses between irradiation and measurement, then at time $t + t'$,

$$N = \frac{nv\sigma T}{\lambda} (1 - e^{-\lambda t}) e^{-\lambda t'}. \quad (35)$$

Now the total number of ^{37}Ar atoms produced, including those that have decayed, is

$$N_0 = nv\sigma T t,$$

so

$$nv\sigma T = \frac{N_0}{t}. \quad (36)$$

Substituting (36) into (35) and rearranging,

$$N_0 = \frac{N \lambda t e^{\lambda t}}{(1 - e^{-\lambda t})}. \quad (37)$$

Expressing (37) in terms of Ar isotope ratios,

$$\frac{^{37}\text{Ar}_0}{^{39}\text{Ar}} = \frac{^{37}\text{Ar}}{^{39}\text{Ar}} \cdot \frac{\lambda t e^{\lambda t}}{(1 - e^{-\lambda t})}. \quad (38)$$

The above presumes that the irradiation is continuous for a time t and at the same reactor power level. If the irradiation I is done in n increments at various power levels, then equation (38) becomes

$$\frac{^{37}\text{Ar}_0}{^{39}\text{Ar}} = \frac{^{37}\text{Ar}}{^{39}\text{Ar}} \sum_{i=0}^n \left[\frac{P_i t_i}{I} \cdot \frac{t_i \lambda e^{\lambda t_i}}{1 - e^{-\lambda t_i}} \right] \quad (39)$$

where P_i = reactor power level, in megawatts, for the increment,

t_i = increment length,

t' = corresponding decay time for the increment (that is, the time from increment end to analysis), and

$$I = \sum_{i=0}^n P_i t_i \text{ in MWH.}$$

EFFECT OF $^{40}\text{Ca}(n, n\alpha)^{36}\text{Ar}$ INTERFERENCE

The following 13 graphs (figs. 23-35) supplement figure 17 and show the effect of the $^{40}\text{Ca}(n, n\alpha)^{36}\text{Ar}$ reaction on the calculated $^{40}\text{Ar}/^{39}\text{Ar}$ age as a function

of age and irradiation time in (MWH) for various K/Ca atomic ratios. The graphs give the approximate errors that would result if no corrections were made. On the centerline of the central thimble, 1 MWH results in a fluence of approximately $1 \times 10^{17} \text{ n/cm}^2$.

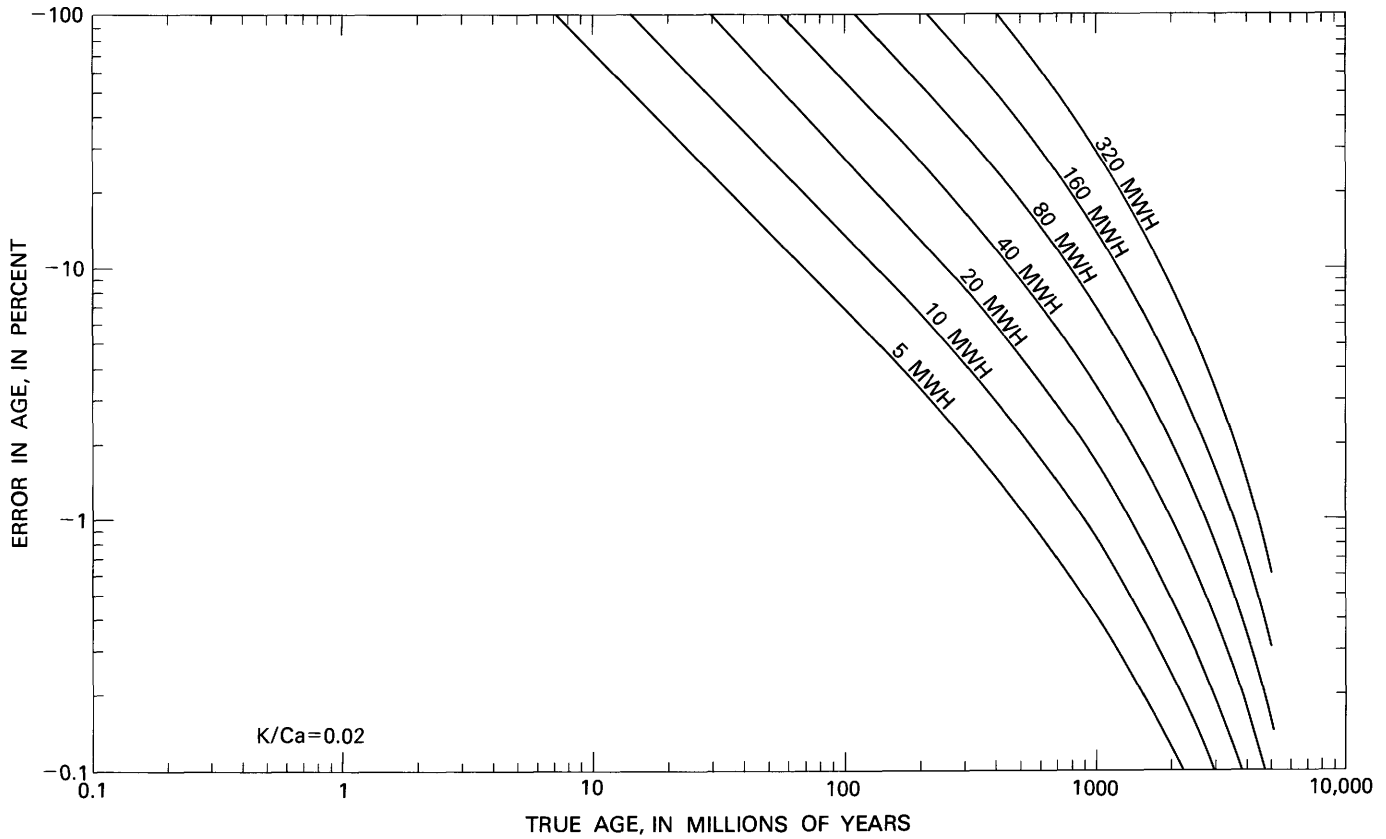
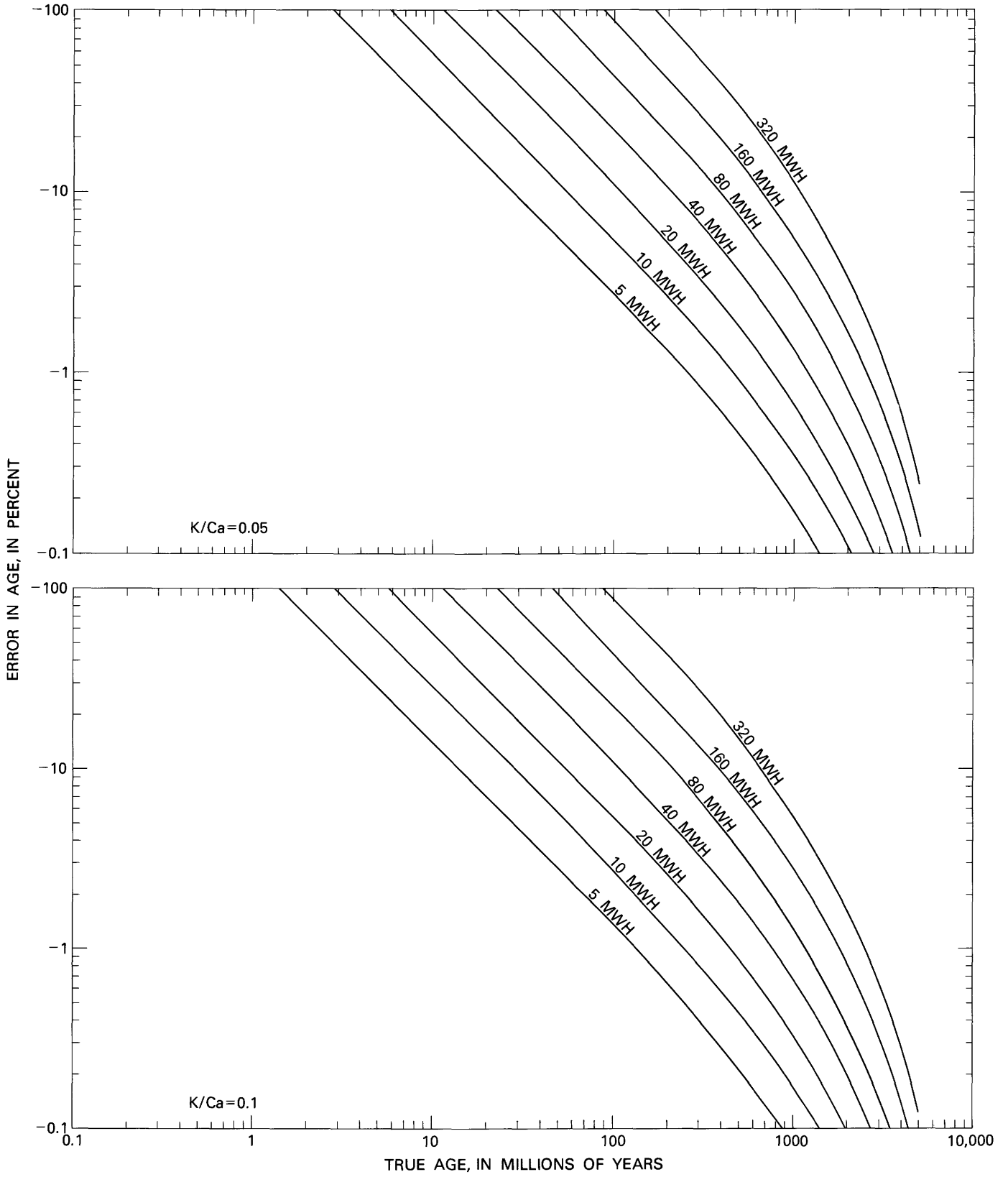
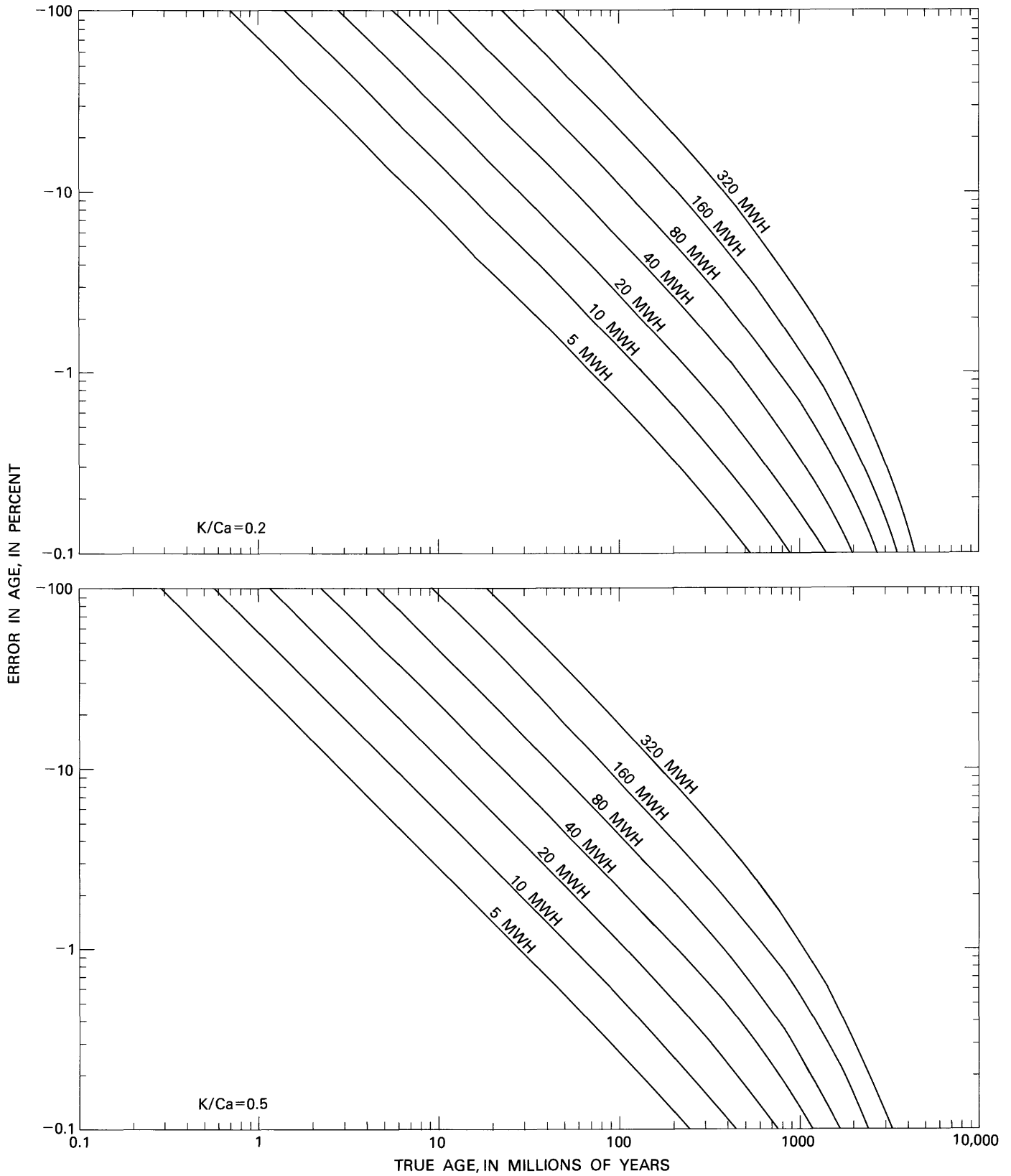


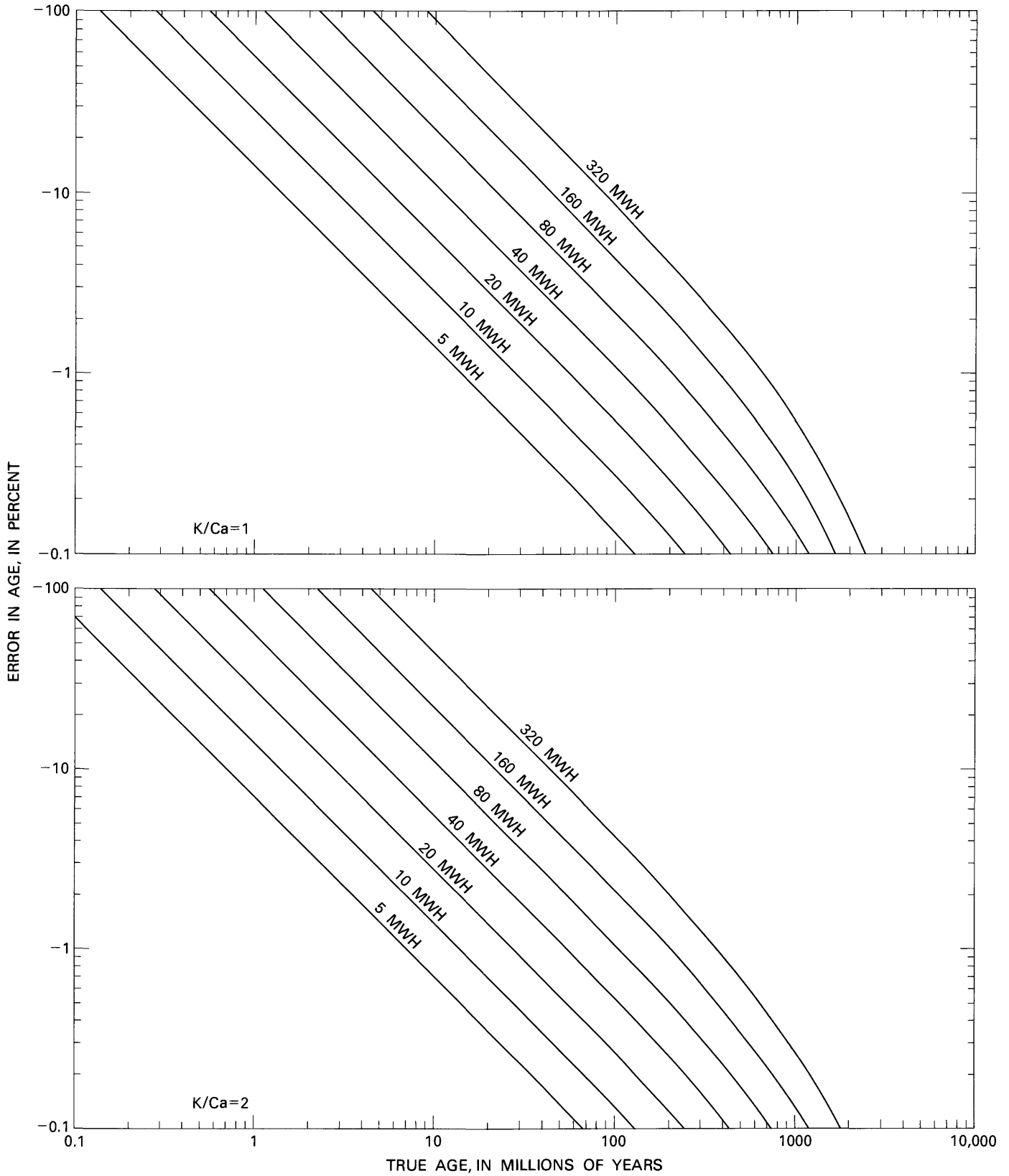
FIGURE 23.—Effects of reaction $^{40}\text{Ca}(n, n\alpha)^{36}\text{Ar}$ on calculated $^{40}\text{Ar}/^{39}\text{Ar}$ ages.



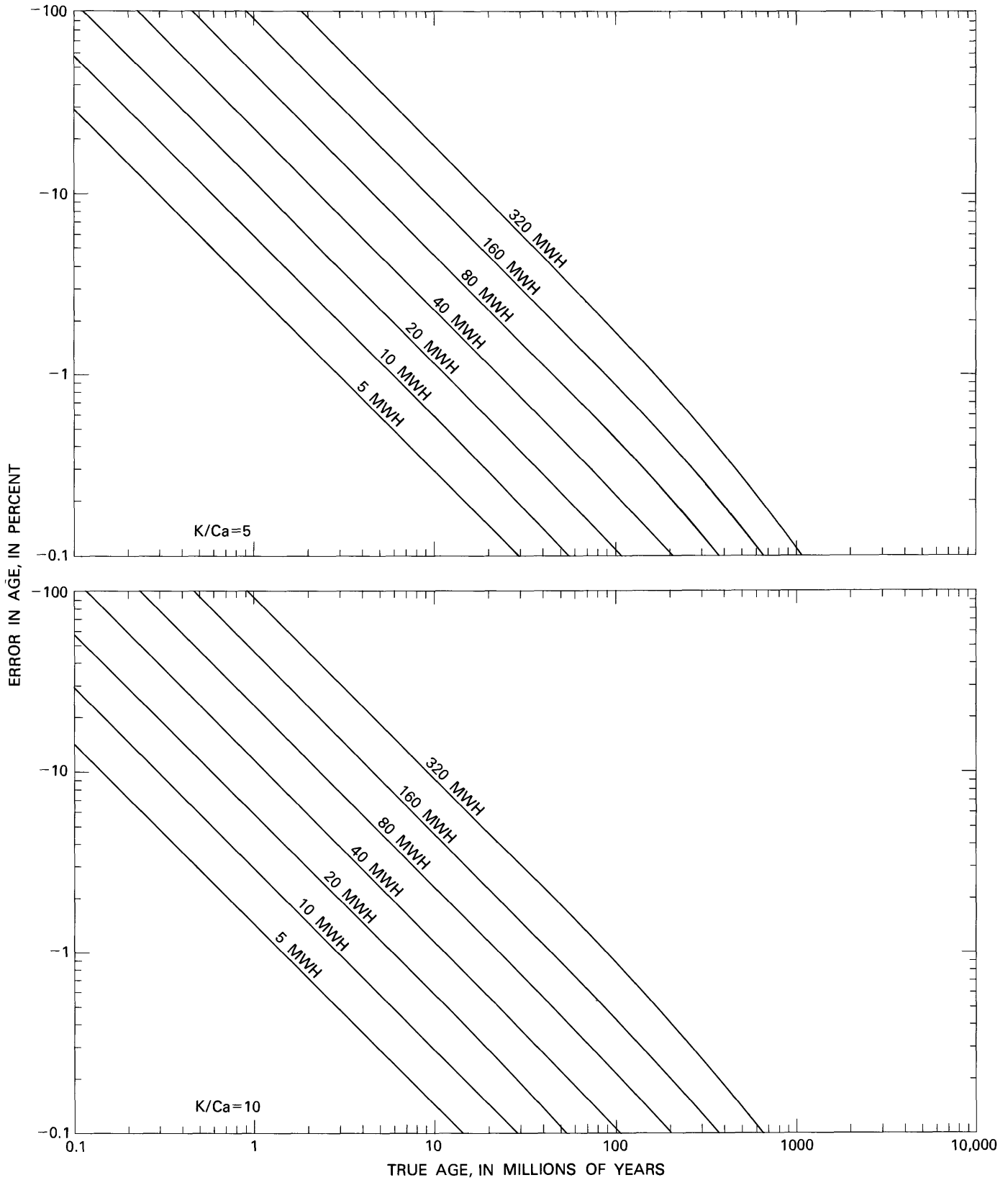
FIGURES 24 (top) and 25 (bottom).— Effects of the reaction $^{40}\text{Ca}(n, \alpha)^{36}\text{Ar}$ on calculated $^{40}\text{Ar}/^{39}\text{Ar}$ ages.

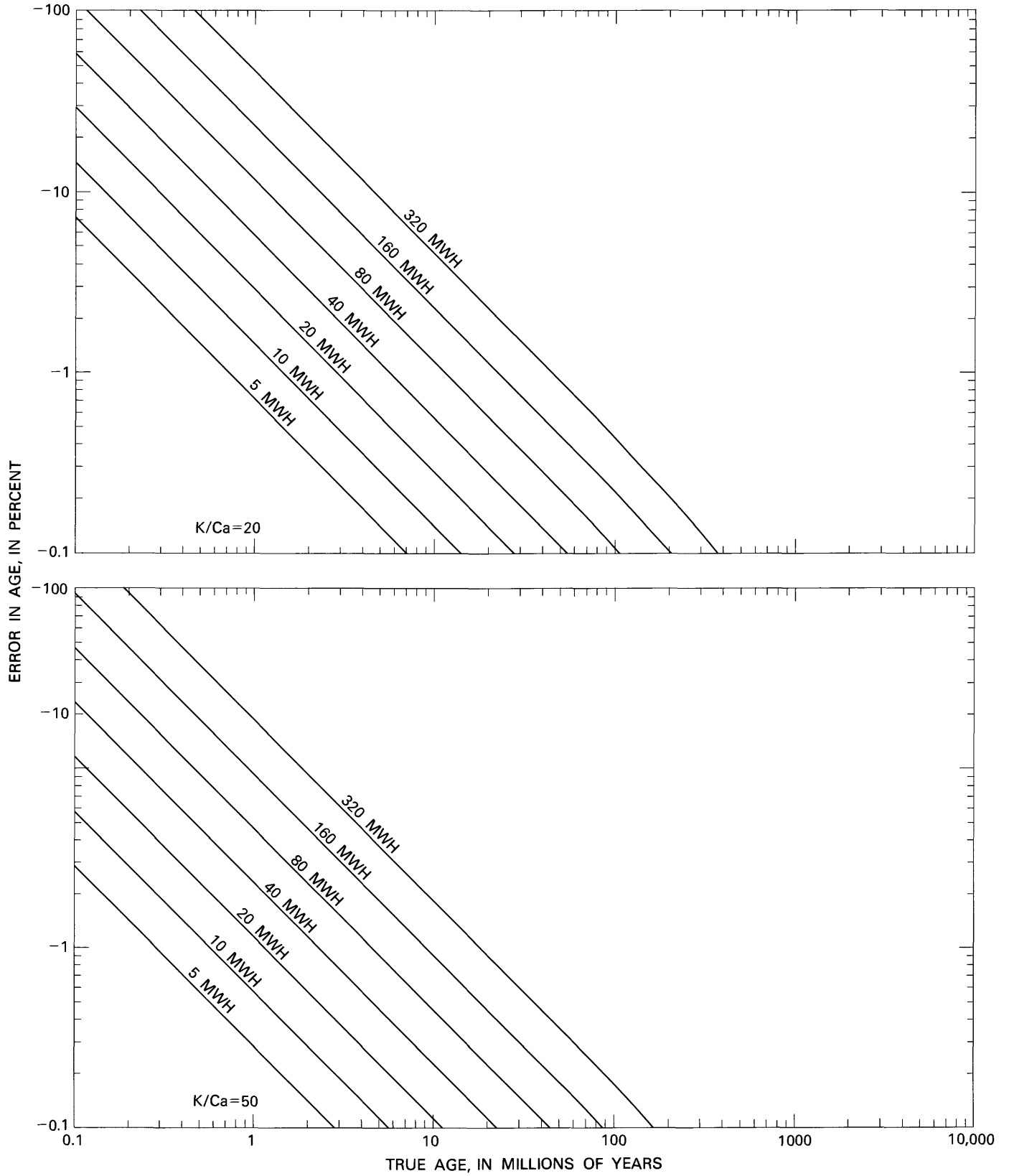


FIGURES 26 (top) and 27 (bottom).— Effects of reaction $^{40}\text{Ca}(n, n\alpha)^{36}\text{Ar}$ on calculated $^{40}\text{Ar}/^{39}\text{Ar}$ ages.

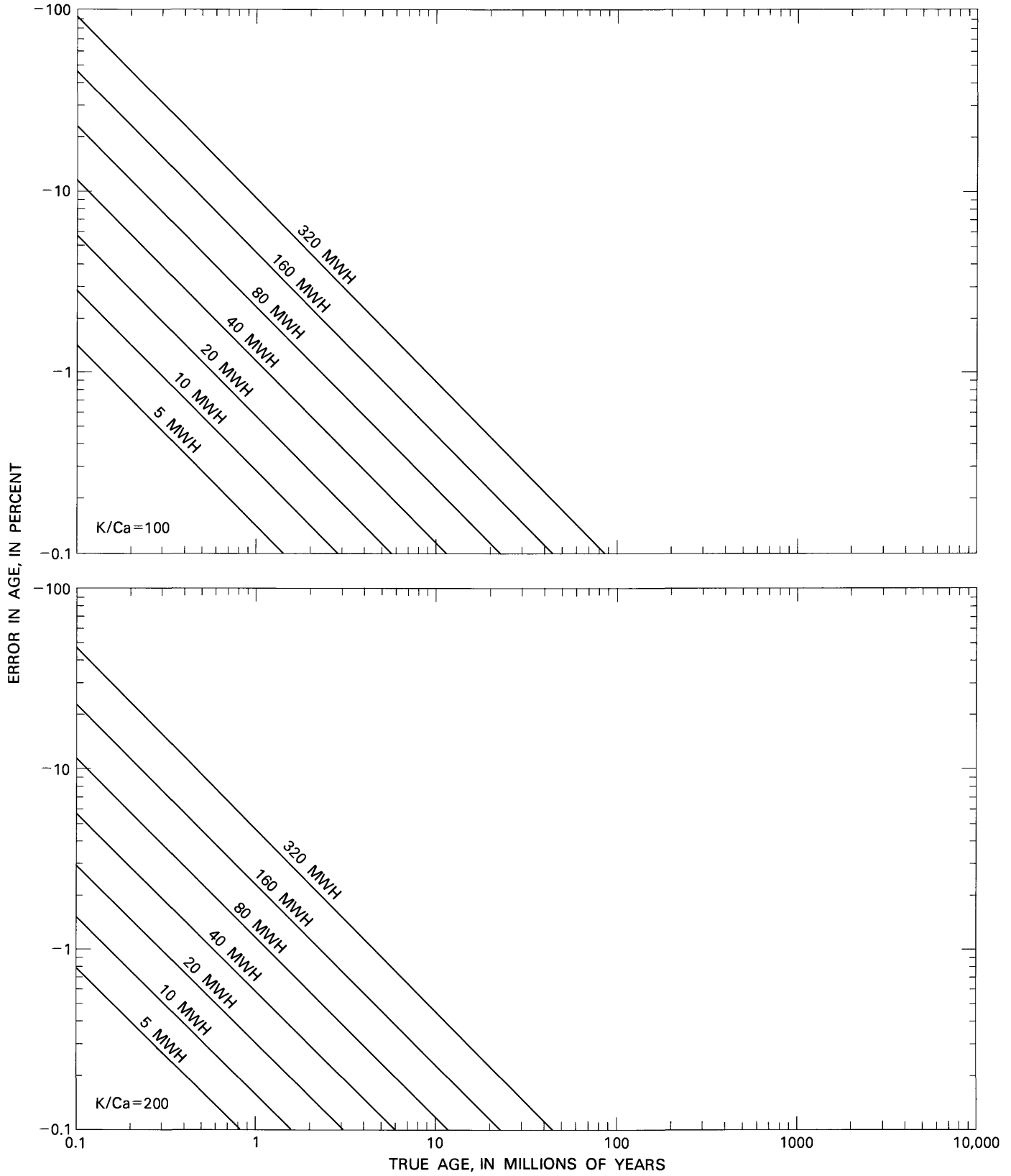


FIGURES 28 (top) and 29 (bottom).— Effects of reaction $^{40}\text{Ca}(n, n\alpha)^{36}\text{Ar}$ calculated $^{40}\text{Ar}/^{39}\text{Ar}$ ages.

FIGURES 30 (top) and 31 (bottom).— Effects of reaction $^{40}\text{Ca}(n,n\alpha)^{36}\text{Ar}$ on calculated $^{40}\text{Ar}/^{39}\text{Ar}$ ages.



FIGURES 32 (top) and 33 (bottom).— Effects of reaction $^{40}\text{Ca}(n, n\alpha)^{36}\text{Ar}$ on calculated $^{40}\text{Ar}/^{39}\text{Ar}$ ages.

FIGURES 34 (top) and 35 (bottom).— Effects of reaction $^{40}\text{Ca}(n, \alpha)^{36}\text{Ar}$ on calculated $^{40}\text{Ar}/^{39}\text{Ar}$ ages.

COMPUTER PROGRAMS

The following two computer programs are written in DEC (Digital Equipment Corporation) OS/8 Basic (version 5A) for a PDP8/e or PDP8/a computer. This version of BASIC runs as a true compiler under the DEC OS/8 operating system and contains certain file and string handling capabilities that may not be available in some versions of BASIC. Each program is sufficiently documented, however, so that the programs can be converted easily to other versions of BASIC or to other computer languages.

NEUT2 - ACTIVITY PREDICTION PROGRAM FOR THE GSTR

INTRODUCTION

This BASIC program predicts the activity of 18 radioisotopes upon irradiation of rock and mineral samples in the central thimble (core) of the U. S.

```
READY
RUN
```

```
NEUT2D BA 5A 30-JUL-80
```

```
NEUTRON 2 (VER. 1/6/78)
ACTIVITY PREDICTION FOR U.S.G.S. TRIGA REACTOR
07/30/80
```

MATERIAL CHOICES:

1-BIOTITE	5-ACTINOLITE	9-AUGITE	13-RHYOLITE
2-MUSCOVITE	6-HORNBLLENDE	10-CAF2	14-AL TUBE
3-BASALT	7-PLAGIOCLASE	11-K2SO4	15-QTZ VIALS
4-MGRAYWACKE	8-K-FELDSPAR	12-ANDESITE	99-YOUR CHOICE

Typical compositions for these 15 materials are contained in the DATA statements 9000-9300. There is also an option (99—your choice) to allow entry of any composition desired.

After the material list, the program requests an irradiation number and a sample number. Any combination of alphanumeric characters (up to 20) may be used as the information is for identification only. The weight is entered in grams. The irradiation time should be in hours at a 1 MW power level. The material is chosen by entering the appropriate material number, after which the program will print the material selected and the activity table.

Geological Survey TRIGA reactor (GSTR) at a 1 MW power level. Predictions are made for 0 day, 2 days, 7 days, and 20 days after irradiation so that an appropriate cooling time can be estimated. The program also sums the activity of the 18 isotopes at $t = 0$ for all the samples in an irradiation. Activity is in millicuries and is accurate to no more than two significant digits because the neutron cross sections of most of the nuclear reactions are poorly known. Data used by the program for the activity predictions are given in table 6 and discussed in the section entitled "Activity Predictions".

DESCRIPTION

Paging is done by the program, so it is advisable to begin at the top of a page if fanfold paper is used. The program begins by printing a heading, the current date, and a list of material choices as shown below:

IRRADIATION NO.?XXXVIII-C-7
 SAMPLE NO.?P-207
 WGT (GMS)?0.0706
 IRRAD. TIME (HRS)?25
 MATERIAL NO?2
 MUSCOVITE

PRODUCT	ACTIVITY (MCI) AFTER COOLING			
	0 DAYS	2 DAYS	7 DAYS	20 DAYS
AL-28	31.7284	0	0	0
SI-31	.505674	0	0	0
NA-24	3.34828	.364327	.00140912	0
FE-55	.00136735	.00136535	.00136037	.00134752
MN-54	0	0	0	0
CR-51	0	0	0	0
MN-56	4.26675	0	0	0
FE-59	.000588632	.000570828	.000528639	.000432972
K-43	0	0	0	0
CA-45	0	0	0	0
CA-49+SC-49	.000481701	0	0	0
K-42	2.3535	.160454	.000194736	0
P-32	.0011733	.00106527	.000836719	.000446576
P-33	0	0	0	0
S-35	0	0	0	0
S-31	0	0	0	0
RB-86	.00401179	.00372586	.00309706	.00191526
CU-64	0	0	0	0
TOTALS	42.2102	.531509	.00742665	.00414233

DATA OK?YES
 MORE SAMPLES?YES

If the optional material is chosen (99), the program will request a material name, then the *elemental* composition (weight percent) of the material.

IRRADIATION NO.?XXIV-B-4
 SAMPLE NO.?T-S235Z
 WGT (GMS)?0.3042
 IRRAD. TIME (HRS)?25
 MATERIAL NO?99
 MATERIAL?SERICITE

SI	?22.1
AL	?16.5
FE	?3.40
MG	?0.57
CA	?0.06
NA	?0.42
K	?8.66
MN	?0.09
CR	?0
P	?0.017
RB	?0.078
CU	?0
S	?0

After the activity table is printed, the program will ask DATA OK? A "YES" will accumulate the nuclide activities at 0 days for the summary table. A "NO" will exclude that sample from the irradiation totals. The next question MORE SAMPLES? tells the program whether to request data for another sample (YES) or to print the summary table (NO).

ACTIVITY SUMMARY AT T=0
GEOCHRONOLOGY PROJECT, MENLO PARK
ACCOMPANIES RADIOISOTOPE REQUEST FORM NO.
07/30/80
IRRADIATION NO. XLIV
3 SAMPLES

PRODUCT	MCI
AL-28	227.33
SI-31	4.07664
NA-24	25.9914
FE-55	.0336044
MN-54	.0009272
CR-51	.000131501
MN-56	34.4166
FE-59	.0144665
K-43	.000572499
CA-45	.000610968
CA-49+SC-49	.0207518
K-42	19.1344
P-32	.00547047
P-33	0
S-35	0
S-31	0
RB-86	.0208656
CU-64	0
TOTAL	311.046

For options 1-9 and 12-13, standard mineral and rock compositions have been used. Because of the poorly known neutron cross sections of most of the reactions involved, the use of an exact composition for any given sample generally would result in insignificant differences in the predicted activities. If an exact composition is required, option 99 can be used. The standard compositions and their sources are given in table 9.

VARIABLE LIST

W	Sample weight, grams.
I	Irradiation time, hours.
X	Irradiation time, seconds.
E(1)	Si, weight percent.
E(2)	Al
E(3)	Fe
E(4)	Mg
E(5)	Ca
E(6)	Na
E(7)	K
E(8)	Mn
E(9)	Cr
E(10)	P
E(11)	Rb
E(12)	Cu
E(13)	S
T	Amount of target isotope.
H	Product isotope half-life, seconds.
B	Neutron cross section, barns.
D	Neutron flux, n/cm^2-s .
N	Number of atoms in 1 gram of target isotope.
I\$	Irradiation number.
R\$	Sample number.
M	Material (option) number.
M\$	Material name.
AO	Activity in millicuries at 0 days for a particular reaction
A2	Activity in millicuries at 2 days for a particular reaction
A3	Activity in millicuries at 7 days for a particular reaction
A4	Activity in millicuries at 20 days for a particular reaction
S0, S2, S3, S4,	Sums of AO, A2, A3, A4 when several reactions have the same product nuclide.
Z0, Z2, Z3, Z4,	Sums of activities at 0, 2, 7, and 20 days.
L(J)	Sums of product activities for summary total.

TABLE 9.—Standard mineral and rock compositions (weight percent) used in BASIC program NEUT 2

[Numbers are material choices in computer program]

Elements and oxides	1 Biotite	2 Muscovite	3 Basalt	4 Metagraywacke	5 Actinolite	6 Hornblende	7 Plagioclase	8 K-feldspar	9 Augite	10 CaF ₂	11 K ₂ SO ₄	12 Andesite	13 Rhyolite	14 6061T6 A1	15 Qtz vials
Si	17.9	22.1	23.6	34.8	26.3	23.8	25.3	30.1	23.6	0	0	28.1	34.4	0.6	46.8
Al	7.4	16.5	7.65	6.0	1.13	5.0	15.5	10.3	1.3	0	0	9.4	7.4	97.2	0
Fe	18.5	3.4	7.65	3.0	8.52	8.7	.1	.3	11.5	0	0	4.2	1.4	.7	0
Mg	4.8	.57	5.46	1.5	9.71	8.7	.01	.04	7.9	0	0	2.1	.2	1.0	0
Ca	.64	.06	6.25	.9	7.36	8.5	7.9	.8	12.4	51.3	0	4.5	1.0	0	0
Na	.37	.42	1.94	1.6	1.01	.86	3.5	3.1	.2	0	0	3.1	3.0	0	0
K	6.9	8.66	.12	.6	.25	.1	.35	7.8	.02	0	44.9	1.1	3.6	0	0
Mn	.07	.09	.12	.05	.05	.2	0	0	.3	0	0	0	.2	0	0
Cr	0	0	.06	0	0	0	0	0	0	0	0	0	0	.2	0
P	0	.02	.09	.05	0	0	0	0	0	0	0	.1	.04	0	0
Rb	0	.08	0	0	0	0	0	.06	0	0	0	0	0	0	0
Cu	0	0	0	0	0	0	0	0	0	0	0	0	0	.27	0
S	0	0	0	0	0	0	0	0	0	0	18.4	0	0	0	0
SiO ₂	38.30	47.14	50.50	74.3	56.06	48.71	54.01	64.40	50.53	60.09	73.59	60.09	73.59	100	100
Al ₂ O ₃	13.99	31.28	14.47	11.4	2.14	9.48	29.28	19.50	2.49	17.85	14.03	17.85	14.03	0	0
Fe ₂ O ₃	3.98	3.98	3.43	0	2.22	2.33	.05	.35	.59	2.03	.42	2.03	.42	0	0
FeO	20.24	.79	6.76	3.8	8.97	9.12	.10	.05	14.25	3.45	1.43	3.45	1.43	0	0
MgO	7.96	.94	9.06	2.5	16.11	14.43	.02	.07	13.08	3.5	.36	3.5	.36	0	0
CaO	.90	.09	8.74	1.3	10.28	11.93	11.09	1.19	17.38	6.28	1.38	6.28	1.38	0	0
Na ₂ O	.50	.57	2.62	2.1	1.36	1.16	4.77	4.19	.23	4.17	4.04	4.17	4.04	0	0
K ₂ O	8.31	10.43	.14	.72	0	.15	.42	9.40	.03	1.31	4.34	1.31	4.34	0	0
P ₂ O ₅	..	.04	.21	.1223	.09	0	0
MnO	.09	.11	.15	.06	.23	.23	Trace	.2	0	0
Cr ₂ O ₃09	0	0
Rb ₂ O	0	0

NOTES. Source of data

1. Biotite: from southern California batholith. Deer, Howie, and Zussman (1962, v. 3, p. 59).
2. Muscovite: P-207 standard. Lanphere and Darymple (1965).
3. Basalt: tholeiite from Koolau Volcanic Series, Oahu, Hawaii. Jackson and Wright (1970).
4. Metagraywacke: 64YB-13. Unpublished data. M. C. Blake, Jr., U. S. Geological Survey.
5. Actinolite: Kanto Mountain, Japan. Deer, Howie, and Zussman (1962, v. 2, p. 252).
6. Hornblende: from gabbro, Pennsylvania. Deer, Howie, and Zussman (1962, v. 2, p. 276).
7. Plagioclase: labradorite from anorthosite, Wisconsin. Deer, Howie and Zussman (1962, v. 4, p. 116).
8. K-feldspar: sanidine from trachybasalt, Black Point, California. Deer, Howie, and Zussman (1962, v. 4, p. 40).
9. Augite: from diabase pegmatite, Virginia. Deer, Howie, and Zussman (1962, v. 2, p. 117).
12. Andesite: hypersilene andesite from Crater Lake, Oregon. Turner and Verhoogen (1960, p. 285).
13. Rhyolite: obsidian from Medicine Lake highland, California. Turner and Verhoogen (1960, p. 285).

```

10 PRINT "NEUTRON 2 (VER. 1/6/78)"
20 PRINT "ACTIVITY PREDICTION FOR U.S.G.S. TRIGA REACTOR"
30 REM - BY G. BRENT DALRYMPLE, U.S.G.S., MENLO PARK, CA
40 PRINT DAT$(X)
50 PRINT\PRINT
60 PRINT "MATERIAL CHOICES:\PRINT
65 PRINT "1-BIOTITE", "5-ACTINOLITE", "9-AUGITE", "13-RHYOLITE"
70 PRINT "2-MUSCOVITE", "6-HORNBLLENDE", "10-CAF2", "14-AL TUBE"
75 PRINT "3-BASALT", "7-PLAGIOCLASE", "11-K2SO4", "15-QTZ VIALS"
80 PRINT "4-MGRAYWACKE", "8-K-FELDSPAR", "12-ANDESITE", "99-YOUR CHOICE"
85 PRINT\PRINT\PRINT
90 GOSUB 7600\GOSUB 7600
100 DIM E(13),M$(16,20),K(19),L(19),R$(20)
105 DIM I$(20)
120 FOR J=1 TO 19
130 L(J)=0
140 NEXT J
150 F=1
160 PRINT "IRRADIATION NO. ";
170 INPUT I$
200 PRINT "SAMPLE NO. ";
210 INPUT R$
220 PRINT "WGT (GMS) ";
230 INPUT W
240 PRINT "IRRAD. TIME (HRS) ";
250 INPUT I
255 X=I*3600
260 PRINT "MATERIAL NO ";
270 INPUT M
280 IF M<0 THEN 350
290 IF M>15 THEN 310
300 GOTO 400
310 IF M><99 THEN 350
320 GOTO 400
350 PRINT "INVALID MATERIAL"
360 GOTO 260
400 IF M=99 THEN 500
410 FOR J=1 TO M
420 FOR K=1 TO 13
430 READ E(K)
440 NEXT K
450 NEXT J
460 GOTO 700
500 PRINT "MATERIAL ";
510 INPUT M$(1)
520 PRINT
530 PRINT "SI",\INPUT E(1)
540 PRINT "AL",\INPUT E(2)
550 PRINT "FE",\INPUT E(3)
560 PRINT "MG",\INPUT E(4)
570 PRINT "CA",\INPUT E(5)
580 PRINT "NA",\INPUT E(6)
590 PRINT "K",\INPUT E(7)
600 PRINT "MN",\INPUT E(8)
610 PRINT "CR",\INPUT E(9)
620 PRINT "P",\INPUT E(10)
630 PRINT "RB",\INPUT E(11)
640 PRINT "CU",\INPUT E(12)
650 PRINT "S",\INPUT E(13)
660 GOTO 1000
700 M$(1)="BIOTITE"\M$(2)="MUSCOVITE"\M$(3)="BASALT"
710 M$(4)="METAGRAYWACKE"\M$(5)="ACTINOLITE"\M$(6)="HORNBLLENDE"
720 M$(7)="PLAGIOCLASE"\M$(8)="K-FELDSPAR"\M$(9)="AUGITE"
730 M$(10)="CAF2"\M$(11)="K2SO4"\M$(12)="ANDESITE"\M$(13)="RHYOLITE"
740 M$(14)="AL TUBE"\M$(15)="QTZ VIALS"

```

```

750 PRINT M$(M)
1000 Z0=0\Z2=0\Z3=0\Z4=0
1010 PRINT\PRINT\PRINT
1020 PRINT "PRODUCT";TAB(28);"ACTIVITY (MCI) AFTER COOLING"
1030 PRINT , " 0 DAYS", " 2 DAYS", " 7 DAYS", " 20 DAYS"
1040 PRINT
1100 REM - SI-28(N,P)AL-28
1110 T=W*(1)*.9921E-2
1120 H=1.38E2\B=.37\D=2E12\N=2.15E22
1130 GOSUB 7070
1200 REM - AL-27(N,G)AL-28
1210 T=W*(2)*1E-2
1220 B=.21\N=1.7E13\N=2.23E22
1230 GOSUB 7100
1240 GOSUB 7400
1300 REM - P-31(N,A)AL-28
1310 T=W*(10)*1E-2
1320 B=.15\N=7E12\N=1.94E22
1330 GOSUB 7100
1340 GOSUB 7400
1400 GOSUB 7500
1410 PRINT "AL-28",S0,S2,S3,S4
1420 K(1)=S0
1500 REM - SI-30(N,G)SI-31
1510 T=W*(1)*.0309E-2
1520 H=9.43E3\B=.11\N=1.7E13\N=2.01E22
1530 GOSUB 7070
1600 REM - P-31(N,P)SI-31
1610 T=W*(10)*1E-2
1620 B=.14\N=1.94E22\N=1.6E13
1630 GOSUB 7100
1640 GOSUB 7400
1700 GOSUB 7500
1710 PRINT "SI-31",S0,S2,S3,S4
1720 K(2)=S0
1800 REM - AL-27(N,G)NA-24
1810 T=W*(2)*1E-2
1820 H=5.4E4\B=.14\N=3E12\N=2.23E22
1830 GOSUB 7070
1900 REM - MG-24(N,P)NA-24
1910 T=W*(4)*.787E-2
1920 B=.22\N=1E12\N=2.51E22
1930 GOSUB 7100
1940 GOSUB 7400
2000 REM - NA-23(N,G)NA-24
2010 T=W*(6)*1E-2
2020 B=.53\N=1.7E13\N=2.62E22
2030 GOSUB 7100
2040 GOSUB 7400
2100 GOSUB 7500
2110 PRINT "NA-24",S0,S2,S3,S4
2120 K(3)=S0
2200 REM - FE-54(N,G)FE-55
2210 T=W*(3)*.0582E-2
2220 H=8.2E7\B=2.5\N=1.12E22
2230 GOSUB 7010
2240 PRINT "FE-55",A0,A2,A3,A4
2250 K(4)=A0
2300 REM - FE-54(N,P)MN-54
2310 H=2.62E7\B=0.023
2320 GOSUB 7010
2330 PRINT "MN-54",A0,A2,A3,A4
2340 K(5)=A0
2400 REM - FE-54(N,A)CR-51

```

```

2410 H=2.4E6\B=.00037
2420 GOSUB 7070
2500 REM - CR-50(N,G)CR-51
2510 T=W*(9)*.0431E-2
2520 B=13.5\N=1.2E22
2530 GOSUB 7100
2540 GOSUB 7400
2600 GOSUB 7500
2610 PRINT "CR-51",S0,S2,S3,S4
2620 K(6)=S0
2700 REM - FE-56(N,P)MN-56
2710 T=W*(3)*.9166E-2
2720 H=9.29E3\B=.00044\D=3E12\N=1.08E22
2730 GOSUB 7070
2800 REM - MN-55(N,G)MN-56
2810 T=W*(8)*1E-2
2820 B=13.3\D=1.7E13\N=1.1E22
2830 GOSUB 7100
2840 GOSUB 7400
2900 GOSUB 7500
2910 PRINT "MN-56",S0,S2,S3,S4
2920 K(7)=S0
3000 REM - FE-58(N,G)FE-59
3010 T=W*(3)*33E-6
3020 H=3.9E6\B=.98\N=1.04E22
3030 GOSUB 7010
3040 PRINT "FE-59",A0,A2,A3,A4
3050 K(8)=A0
3100 REM - CA-43(N,P)K-43
3110 T=W*(5)*135E-7
3120 H=8.06E4\B=.1\N=1.4E22\D=1.3E13
3130 GOSUB 7010
3140 PRINT "K-43",A0,A2,A3,A4
3150 K(9)=A0
3200 REM - CA-44(N,G)CA-45
3210 T=W*(5)*208E-6
3220 H=1.43E7\B=.67\N=1.37E22\D=1.7E13
3230 GOSUB 7010
3240 PRINT "CA-45",A0,A2,A3,A4
3250 K(10)=A0
3300 REM - CA-48(N,G)CA-49+SC-49
3310 T=W*(5)*18E-6
3320 H=3.6E3\B=1.1\N=1.25E22
3330 GOSUB 7010
3340 PRINT "CA-49+SC-49",A0,A2,A3,A4
3350 K(11)=A0
3400 REM - K-41(N,G)K-42
3410 T=W*(7)*688E-6
3420 H=4.46E4\B=1.1\N=1.47E22
3430 GOSUB 7010
3440 PRINT "K-42",A0,A2,A3,A4
3450 K(12)=A0
3500 REM - P-31(N,G)P-32
3510 T=W*(10)*1E-2
3520 H=1.24E6\B=.19\N=1.94E22
3530 GOSUB 7070
3600 REM - S-32(N,P)P-32
3610 T=W*(13)*.95E-2
3620 B=.3\D=1.4E13\N=1.88E22
3630 GOSUB 7100
3700 GOSUB 7500
3710 PRINT "P-32",S0,S2,S3,S4
3720 K(13)=S0
3800 REM - S-33(N,P)P-33
3810 T=W*(13)*76E-6

```

```
3820 H=2.16E6\B=.015\D=1.7E13\N=1.82E22
3830 GOSUB 7010
3840 PRINT "P-33",A0,A2,A3,A4
3850 K(14)=A0
3900 REM - S-34(N,G)S-35
3910 T=W*(13)*422E-6
3920 H=7.6E6\B=.26\N=1.77E22
3930 GOSUB 7010
3940 PRINT "S-35",A0,A2,A3,A4
3950 K(15)=A0
4000 REM - S-34(N,A)S-31
4010 H=9.4E3\B=.14\D=1E13
4020 GOSUB 7010
4030 PRINT "S-31",A0,A2,A3,A4
4040 K(16)=A0
4100 REM - RB-85(N,G)RB-86
4110 T=W*(11)*.7215E-2
4120 H=1.62E6\B=.8\N=.709E22\D=1.7E13
4130 GOSUB 7010
4140 PRINT "RB-86",A0,A2,A3,A4
4150 K(17)=A0
4200 REM - CU-63(N,G)CU-64
4210 T=W*(12)*.691E-2
4220 H=4.64E4\B=4.3\N=.96E22
4230 GOSUB 7010
4240 PRINT "CU-64",A0,A2,A3,A4
4250 K(18)=A0
5000 PRINT
5010 PRINT "TOTALS",Z0,Z2,Z3,Z4
5020 K(19)=Z0
5030 PRINT\PRINT
5035 RESTORE
5040 PRINT "DATA OK";
5050 INPUT E$
5060 IF E$="YES" THEN 5080
5065 GOSUB 7600\PRINT
5070 GOTO 160
5080 FOR J=1 TO 19
5090 L(J)=L(J)+K(J)
5100 NEXT J
5200 PRINT "MORE SAMPLES";
5210 INPUT E$
5220 IF E$="NO" THEN 5300
5230 GOSUB 7600
5240 F=F+1
5250 GOTO 160
5300 REM - PRINT SUMMARY TABLE
5305 GOSUB 7600
5310 PRINT "ACTIVITY SUMMARY AT T=0"
5320 PRINT "GEOCHRONOLOGY PROJECT, MENLO PARK"
5330 PRINT "ACCOMPANIES RADIOISOTOPE REQUEST FORM NO."
5340 PRINT DAT$(X)
5350 PRINT "IRRADIATION NO. ";I$
5360 PRINT F;" SAMPLES"
5370 PRINT\PRINT\PRINT
5380 PRINT "PRODUCT";TAB(19);"MCI"
5390 PRINT "AL-28",L(1)
5400 PRINT "SI-31",L(2)
5410 PRINT "NA-24",L(3)
5420 PRINT "FE-55",L(4)
5430 PRINT "MN-54",L(5)
5440 PRINT "CR-51",L(6)
5450 PRINT "MN-56",L(7)
5460 PRINT "FE-59",L(8)
5470 PRINT "K-43",L(9)
```

```

5480 PRINT "CA-45",L(10)
5490 PRINT "CA-49+SC-49",L(11)
5500 PRINT "K-42",L(12)
5510 PRINT "P-32",L(13)
5520 PRINT "P-33",L(14)
5530 PRINT "S-35",L(15)
5540 PRINT "S-31",L(16)
5550 PRINT "RB-86",L(17)
5560 PRINT "CU-64",L(18)
5570 PRINT
5580 PRINT "TOTAL",L(19)
6000 PRINT\PRINT\PRINT\PRINT\PRINT
6010 STOP
7000 REM - SUBROUTINES
7010 REM - SUBR CALL 1
7020 GOSUB 7100
7030 GOSUB 7300
7040 GOSUB 7400
7050 GOSUB 7500
7060 RETURN
7070 REM - SUBR CALL 2
7075 GOSUB 7100
7080 GOSUB 7300
7085 GOSUB 7400
7090 RETURN
7100 REM - CALCULATE ACTIVITY
7110 A0=T*D*N*B*1E-21*(1-EXP(-.69315*X/H))/3.7E10
7120 G=-5.989E4/H
7130 IF A0>1E-4 THEN 7160
7140 A0=0\A2=0\A3=0\A4=0
7150 GOTO 7190
7160 A2=A0*EXP(2*G)
7162 IF A2>1E-4 THEN 7170
7164 A2=0\A3=0\A4=0
7166 GOTO 7190
7170 A3=A0*EXP(7*G)
7172 IF A3>1E-4 THEN 7180
7174 A3=0\A4=0
7176 GOTO 7190
7180 A4=A0*EXP(20*G)
7182 IF A4>1E-4 THEN 7190
7184 A4=0
7190 RETURN
7300 REM - INITIALIZE SUM VARIABLES
7310 S0=0\S2=0\S3=0\S4=0
7320 RETURN
7400 REM - SUM INDIVIDUAL PRODUCT ACTIVITIES
7410 S0=S0+A0
7420 S2=S2+A2
7430 S3=S3+A3
7440 S4=S4+A4
7450 RETURN
7500 REM - SUM SAMPLE TOTAL ACTIVITIES
7510 Z0=Z0+S0
7520 Z2=Z2+S2
7530 Z3=Z3+S3
7540 Z4=Z4+S4
7550 RETURN
7600 PRINT\PRINT\PRINT\PRINT\PRINT\PRINT\PRINT\PRINT\PRINT\PRINT
7610 PRINT\PRINT\PRINT\PRINT\PRINT\PRINT\PRINT\PRINT\PRINT\PRINT
7620 PRINT\PRINT\PRINT\PRINT\PRINT\PRINT\PRINT\PRINT\PRINT\PRINT
7630 RETURN
9000 REM - COMPOSITION DATA
9010 REM - BIOTITE (1)
9020 DATA 17.9,7.4,18.5,4.8,.64,.37,6.9,.07,0,0,0,0,0

```

```

9030 REM - MUSCOVITE (2)
9040 DATA 22.1,16.5,3.4,.57,.06,.42,8.66,.09,0,.02,.08,0,0
9050 REM - THOLEIITIC BASALT (3)
9060 DATA 23.6,7.65,7.65,5.46,6.25,1.94,.12,.12,.06,.09,0,0,0
9070 REM - METAGRAYWACKE (4)
9080 DATA 34.8,6.0,3.0,1.5,.9,1.6,.6,.05,0,.05,0,0,0
9090 REM - ACTINOLITE (5)
9100 DATA 26.3,1.13,8.52,9.71,7.36,1.01,.25,.05,0,0,0,0,0
9110 REM - HORNBLENDE (6)
9120 DATA 22.8,5.8,7.8,7.8,5.86,.1,.2,0,0,0,0,0
9130 REM - PLAGIOCLASE (7)
9140 DATA 25.3,15.5,.1,.01,7.9,3.5,.35,0,0,0,0,0,0
9150 REM - K-FELDSPAR (8)
9160 DATA 30.1,10.3,.3,.04,.8,3.1,7.8,0,0,0,.06,0,0
9170 REM - AUGITE (9)
9180 DATA 23.6,1.3,11.5,7.9,12.4,.2,.02,.3,0,0,0,0,0
9190 REM - CAF2 (10)
9200 DATA 0,0,0,0,51.3,0,0,0,0,0,0,0,0
9210 REM - K2SO4 (11)
9220 DATA 0,0,0,0,0,0,44.9,0,0,0,0,0,18.4
9230 REM - ANDESITE (12)
9240 DATA 28.1,9.4,4.2,2.1,4.5,3.1,1.1,0,0,.1,0,0,0
9250 REM - RHYDLITE (13)
9260 DATA 34.4,7.4,1.4,.2,1,3,3.6,.2,0,.04,0,0,0
9270 REM - AL TUBE (14)
9280 DATA .6,97.2,.7,1,0,0,0,0,.2,0,0,.27,0
9290 REM - QTZ VIALS (15)
9300 DATA 46.8,0,0,0,0,0,0,0,0,0,0,0,0
9999 END

```

AR 37-³⁷Ar DECAY CORRECTION PROGRAM INTRODUCTION

This program calculates the ³⁷Ar decay correction factor used in ⁴⁰Ar/³⁹Ar dating. The calculation allows for episodic irradiation at various reactor power levels and is equal to

$$\sum_{i=0}^n \left[\frac{P_i t_i}{I} \cdot \frac{t_i \lambda e^{\lambda t_i}}{1 - e^{-\lambda t_i}} \right]$$

where P_i = power (megawatts) for the increment,
 t_i = length (hours) of increment,
 t'_i = time (hours) between irradiation
 increment and ³⁷Ar measurement,
 λ = decay constant of ³⁷Ar = $8.25 \times 10^{-4} \text{hr}^{-1}$
 (half-life = 35.1 days),

$$I = \sum_{i=0}^n P_i t_i, \text{ and}$$

n = number of increments in the irradiation.
 The derivation of the formula is given above.

DESCRIPTION

The irradiation history of each irradiation is stored in a file (IRHIST.DA) called by the program upon entry of

the irradiation number. This file is maintained using a symbolic editor, available on most computer systems. If the data for that irradiation are not in the file, an error message results.

Upon execution, a limited amount of information about the irradiation (number of increments, date and time the last increment ended, and total MWH) is printed so the operator can verify that the irradiation history is correct. The operator also has the option of printing the entire irradiation history.

Data for each sample are entered (sample number, day, and time measured) and the program prints the ³⁷Ar correction factor, which is applied as a multiplier directly to the measured ³⁷Ar/³⁹Ar ratio. The day measured should be the Julian day, that is, Jan. 1 = 1, Dec. 31 = 365. As the day numbers are subtracted to determine the decay times, it may be necessary to add 365 to the day number if the measurement was made in the year following the irradiation. (If a sample was irradiated in December and measured on the mass spectrometer the following January 15, for instance, then the day number would be entered as 380.) The hour is entered as a decimal in 24-hour notation, so 3:12 in the afternoon is entered as 15.2.

The program continues to request sample data and calculates correction factors until execution is halted by the operator.

A sample program execution is given below.

IRRADIATION OF SAMPLES FOR $^{40}\text{Ar}/^{39}\text{Ar}$ DATING

VARIABLE LIST

E\$	Sample No. [DIM (20)]	M1	Day measured
E1\$	Irradiation number	M2	Hour
E2\$	Date last increment ended	X	Number of sets in data file
E3\$	Last person to modify file	Z	Set counter
E4\$	Date modified	Q(J)	$=W(J) * T(J) = P_i * t_i$
N	Number of increments in the irradiation	D(J)	$=t_i$
Y	Total MWH $= \sum W(J) = \sum P_i * t_i$	P(J)	$= P_i * t_i / I = Q(J) / Y$
T(J)	Length of increment (hrs)	A(J)	$= \lambda t_i / (1 - e^{-\lambda t_i})$
E(J)	Day increment ended	C(J)	$= A(J) * P(J) * e^{-\lambda t_i}$
H(J)	Hour	C	$= \sum C(J) = \text{correction factor}$
W(J)	Power level of increment		

READY
RUN

AR37 BA 5A 30-JUL-80

AR37.BA (VER.12/30/77)
AR-37 DECAY CORRECTIONS
ISOTOPE GEOLOGY BRANCH, U.S.G.S., MENLO PARK
07/30/80

IRRADIATION NO. 750
6 INCREMENTS
LAST INCREMENT ENDED AT 16.4 ON 15APR1980
TOTAL MWH= 25

PRINT IRRADIATION HISTORY?YES

TIME	DAY	HOUR	PWR
8	100	16.1	1
8	101	16	1
1.633	102	12.5	1
.6	102	15.5	1
4.583	106	13.5	1
2.184	106	16.4	1

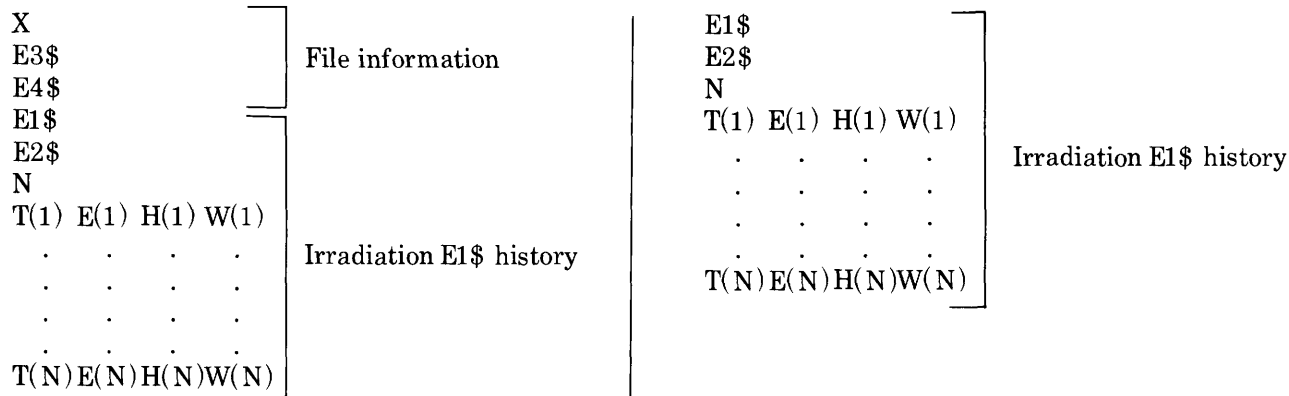
SAMPLE NO. ?L-C-4
MEASURED ON DAY NO. ?164
TIME ?10.4
AR-37 CORRECTION FACTOR= 3.39324

SAMPLE NO. ?L-B-5
MEASURED ON DAY NO. ?156
TIME ?11.0
AR-37 CORRECTION FACTOR= 2.8987

SAMPLE NO. ?L-C-5
MEASURED ON DAY NO. ?164
TIME ?13.1
AR-37 CORRECTION FACTOR= 3.40078

FILE FORMAT

Data used by the program are stored in an ASCII file called IRHIST.DA. These data consist of irradiation histories, which occur in the file in the format shown below. The file can be maintained or updated using any symbolic editor. Variables are explained in the variable list.



```

10 PRINT "AR37.BA (VER.12/30/77)"
20 PRINT "AR-37 DECAY CORRECTIONS"
30 PRINT "ISOTOPE GEOLOGY BRANCH, U.S.G.S., MENLO PARK"
40 PRINT DAT$(X)
50 PRINT\PRINT\PRINT
100 DIM E$(20),E3$(20),E4$(12),E2$(12)
110 DIM T(50),E(50),H(50),W(50),Q(50),D(50),P(50),A(50),C(50)
200 PRINT "IRRADIATION NO.":#
210 INPUT E$
220 Z=0
300 FILE#1:"IRHIST.DA"
310 INPUT#1:X,C
320 INPUT#1:E3$,E4$
400 INPUT#1:E1$,E2$
410 INPUT#1:N,C
420 FOR J=1 TO N
430 INPUT#1:T(J),E(J),H(J),W(J),C
440 NEXT J
500 IF E1$=E$ THEN 600
510 Z=Z+1
520 IF Z=X+1 THEN 535
530 GOTO 400
535 CLOSE#1
540 PRINT "INPUT ERROR"
550 GOTO 200
600 CLOSE#1
610 Y=0
700 FOR J=1 TO N
710 Q(J)=W(J)*T(J)
720 Y=Y+Q(J)
730 NEXT J
800 PRINT N;" INCREMENTS"
810 PRINT "LAST INCREMENT ENDED AT"#H(N)#" ON "#E2$

```

IRRADIATION OF SAMPLES FOR $^{40}\text{Ar}/^{39}\text{Ar}$ DATING

```

820 PRINT "TOTAL MWH=";Y
830 PRINT\PRINT\PRINT
840 PRINT "PRINT IRRADIATION HISTORY";
845 INPUT E$
850 IF E$="YES" THEN 860
855 GOTO 900
860 PRINT "TIME";TAB(16);"DAY";TAB(29);"HOUR";TAB(44);"PWR"
865 PRINT
870 FOR J=1 TO N
880 PRINT T(J),E(J),H(J),W(J)
885 NEXT J
890 PRINT\PRINT\PRINT\PRINT
900 PRINT "SAMPLE NO. ";
910 INPUT E$
920 PRINT "MEASURED ON DAY NO. ";
930 INPUT M1
940 PRINT TAB(16);"TIME";
950 INPUT M2
960 PRINT
1000 G=0
1010 FOR J=1 TO N
1020 D(J)=24*(M1-E(J))-H(J)+M2
1030 P(J)=R(J)/Y
1040 A(J)=(8.23E-4)*T(J)/(1-EXP((-8.23E-4)*T(J)))
1050 C(J)=A(J)*P(J)*EXP((8.23E-4)*D(J))
1060 G=G+C(J)
1070 NEXT J
1100 PRINT "AR-37 CORRECTION FACTOR=";G
1110 PRINT
1120 PRINT "-----"
1130 PRINT\PRINT\PRINT
1140 GOTO 900
9999 END

```

SELECTED
BIBLIOGRAPHY

The following bibliography (table 10) was selected to illustrate the use of $^{40}\text{Ar}/^{39}\text{Ar}$ data in terrestrial, lunar, and cosmological studies. Ten subject categories have

been set up in the table. An "x" indicates that a particular subject category is covered in varying degree in the reference. The bibliography is not a complete list of $^{40}\text{Ar}/^{39}\text{Ar}$ dating references, but it should give the interested reader an introduction to the $^{40}\text{Ar}/^{39}\text{Ar}$ literature.

TABLE 10.—Selected bibliography of use of $^{40}\text{Ar}/^{39}\text{Ar}$ data in terrestrial, lunar, and cosmological studies

References	Theory	Technique development	Irradiation parameters/ reactors	Lunar samples	Meteorites	Terrestrial samples	Age spectra	Excess ^{40}Ar	Argon loss	Isochrons/ correlation diagrams
Alexander (1975)	--	--	--	--	--	X	X	X	--	X
Alexander and Davis (1974)	--	X	--	X	--	--	X	--	--	--
Alexander and Kahl (1974)	--	--	--	X	--	--	X	--	--	X
Berger (1975)	--	X	--	--	--	X	X	--	X	--
Berger and York (1970)	--	X	X	--	--	X	--	--	--	X
Bogard, Husain, and Wright (1976)	--	--	--	--	X	--	X	--	--	--
Brereton (1970)	X	--	X	--	--	--	--	--	--	--
Brereton (1972)	X	--	--	--	--	X	X	--	--	X
Dallmeyer (1975a)	--	--	--	--	--	X	X	X	X	--
Dallmeyer (1975b)	--	--	--	--	--	X	X	--	X	--
Dallmeyer (1975c)	--	--	--	--	--	X	X	--	--	--
Dallmeyer, Maybin, and Durocher (1975)	--	--	--	--	--	X	X	--	--	--
Dallmeyer and Sutter (1976)	--	--	--	--	--	X	X	--	--	--
Dalrymple and Clague (1976)	--	X	--	--	--	X	X	--	X	X
Dalrymple and Lanphere (1971)	--	X	X	--	--	X	--	--	--	--
Dalrymple and Lanphere (1974)	--	X	--	--	--	X	X	--	--	X
Davis (1977)	--	X	X	--	--	X	X	--	--	--
Dunham and others (1968)	--	X	--	--	--	X	--	--	--	--
Fitch, Miller, and Mitchell (1969)	X	--	--	--	--	X	X	--	--	--
Fitch, Hooker, and Miller (1976)	--	--	--	--	--	X	X	--	--	X
Fleck, Sutter, and Elliot (1977)	--	--	--	--	--	X	X	--	X	X
Hanson, Simmons, and Bence (1975)	--	--	--	--	--	X	X	--	X	--
Horn and others (1975)	--	X	--	X	--	--	X	--	--	--

TABLE 10.—Selected bibliography of use of $^{40}\text{Ar}/^{39}\text{Ar}$ data in terrestrial, lunar, and cosmological studies — Continued

References	Theory	Technique development	Irradiation parameters/ reactors	Lunar samples	Meteorites	Terrestrial samples	Age spectra	Excess ^{40}Ar	Argon loss	Isochrons/ correlation diagrams
Huneke (1976)	X	--	--	--	--	--	X	--	X	X
Huneke and others (1973)	--	--	--	X	--	--	X	--	--	X
Huneke and Smith (1976)	X	X	--	--	--	--	X	--	X	--
Jessberger and others (1974)	--	--	--	X	--	--	X	--	--	X
Kaneoka (1974)	--	--	--	--	--	X	X	X	--	--
Kirsten, Horn, and Kiko (1973)	--	--	--	X	--	--	--	--	--	--
Kirsten, Horn, and Heymann (1973)	--	--	--	X	--	--	--	--	--	--
Lanphere and Albee (1974)	--	--	--	--	--	X	X	--	--	X
Lanphere and Dalrymple (1971)	--	X	--	--	--	X	X	X	X	--
Lanphere and Dalrymple (1976)	--	X	--	--	--	X	X	X	--	X
McDougall (1974)	--	--	X	--	--	--	--	--	--	--
McDougall and Roksandic (1974)	--	--	X	--	--	X	--	--	--	--
Mateen and Green (1974)	--	--	X	--	--	X	--	--	--	--
Merrihue and Turner (1966)	X	X	--	--	X	--	--	--	--	X
Miller, Mitchell, and Evans (1970)	--	--	X	--	--	X	--	--	--	--
Mitchell (1968)	X	X	X	--	--	X	--	--	--	--
Ozima and Saito (1973)	--	--	--	--	--	X	X	X	--	X
Pankhurst and others (1973)	--	--	--	--	--	X	X	X	--	--
Podosek (1971)	--	--	--	--	X	--	X	--	--	X
Podosek and Huneke (1973)	--	--	--	--	X	--	X	--	--	--
Schaeffer and Husain (1974)	--	--	--	X	--	--	X	--	--	--
Sigurgeirsson (1962)	X	--	X	--	--	--	--	--	--	--
Stettler and others (1973)	--	--	--	X	--	--	X	--	--	X
Turner (1969)	X	--	--	--	X	--	X	--	X	--
Turner (1970a)	--	--	--	X	--	--	X	--	X	X
Turner (1971a)	X	--	--	X	--	--	X	--	--	X
Turner (1971b)	--	--	X	--	--	--	--	--	--	--
Turner (1972)	--	--	--	X	--	--	X	--	X	--
Turner and Cadogan (1974)	X	--	--	X	--	--	X	--	X	--
Turner and Cadogan (1975)	--	--	--	X	--	--	X	--	--	--
Turner, Miller, and Grasty (1966)	--	--	--	--	X	--	X	--	--	--
Turner and others (1971)	--	--	--	X	--	--	X	--	X	X
York and Berger (1970)	--	X	--	--	--	X	--	--	--	--